

**University of Eastern Piedmont
The Department of Health Science
PhD Program in Medical Sciences and Biotechnology
XXX Cycle**

**Phage display selection and development of
monoclonal antibodies against Protein Disulfide
Isomerase, a novel tumor associated antigen and
potential target for cancer immunotherapy**

PhD candidate: Tarasiuk Olga

**Tutor: Prof. Claudio Santoro
Coordinator: Prof. Marisa Gariglio**

Acknowledgements

With all appreciations and gratitude I would like to thank Prof. Claudio Santoro for giving me the opportunity to work in the laboratory of Applied Biology at the University of Eastern Piedmont. It was a great pleasure for me and I've appreciated the support and knowledge received to foster my professional grow.

Moreover, I would like to say my deepest words of thankfulness to Dr. Diego Cotella and Dr. Marco Corazzari for helping, teaching and supporting me through all the way to my PhD. I would have not be able to complete my PhD without them.

I also want to say my words of thankfulness to Dr. Silvia Zucchelli, Dr. Maria Felicia Soluri, Mara Gagliardi, Miriam Galasso, Marta Borchiellini, Gabriella Forestieri, Andrea Chiesa, Dr. Szilvia Bako, Dr. Laura Patrucco, Feba Varughese and all the people who were working in the lab. They were involved in my work, giving helpful suggestions and support.

My special thanks to Prof. Daniele Sblattero and all researchers at the Department of Life Sciences, University of Trieste for their key collaboration. A separate thank to Dr. Frank Antony for sharing knowledge and unpublished results.

To all my beloved ones, from the deepest of my heart I want to thank for support and understanding during these years of PhD.

Table of Contents

Chapter 1	1
1. Introduction	1
1.1. Ovarian cancer	1
1.2. Symptoms of ovarian cancer	2
1.3. Classification of ovarian cancer	2
1.4. Ovarian cancer treatment	3
2. Biomarkers-based personalized therapy	4
2.1. Biomarkers	4
2.2. Ovarian cancer biomarkers	5
2.3. Ovarian cancer ascites for biomarkers identification	5
3. Cancer and immunotherapy	6
3.1. Cancer triggers immune reaction	6
3.2. Autoantibodies	7
3.3. Tumor associated antigens (TAA)	7
4. TAA identification techniques	7
4.1. Serological proteome analysis (SERPA)	7
4.2. Screening of Expression library	8
4.3. Display systems	9
4.4. Phage Display	9
4.5. Publication: Phage display technology for human monoclonal antibodies	10
4.6. Phage Microarray	26
5. Monoclonal antibody therapy	27
5.1. Monoclonal antibodies (mAbs) mechanism of action	27
5.2. Complement dependent cytotoxicity (CDC)	27
5.3. Antibody-dependent cell-mediated cytotoxicity (ADCC)	28
5.4. CDC and ADCC interaction	29
Chapter 2	31
6. Project description	31
6.1. Objectives of the project	31
6.2. Project summary	31
Chapter 3	35
7. Results Part I: Publication	35
8. Results Part II	55
8.1. Introduction to results	55
8.2. Tumor associated antigen identification	56
8.2.1. Ovarian cancer patient ascites antibodies identification	56
8.2.2. SERPA tumor associated antigens identification	58
8.2.3. ELISA assay PDI specificity of ovarian cancer patient ascites antibodies	59
8.2.4. CDC assay	59
8.2.5. OVCA-3 surface PDI staining	60
8.3. Recombinant antibodies production	61
8.3.1. Phage display antibodies selection	61
8.3.2. Antibody production	64
8.3.3. ELISA assay	65
8.3.4. Epitope mapping	66
8.3.5. Immunofluorescent staining	69
8.3.6. PDI surface staining analyzed by FACS	72

8.3.7. Immunoprecipitation.....	73
8.3.8. Competition assay.....	73
8.3.9. CDC assay	75
Chapter 4	78
9. Discussion.....	78
9.1. Tumor associated antigen identification.....	78
9.2. Protein Disulfide Isomerase (PDI)	81
9.3. Recombinant antibodies production	83
9.4. Antibodies characterization in standard laboratory assays	84
10. Conclusions	85
Chapter 5	86
11. Material and methods	86
11.1. Section 1: Abbreviations.....	86
11.2. Section 2: Solutions and buffers	86
11.3. Section 3: Standard protocols.....	88
11.4. Section 4: Methods	90
11.4.1. Patient samples and cell lines	90
11.4.2. Identification of autoantibodies in ascites	91
11.4.3. PDI antigen identification	92
11.4.4. Antibody selection	94
11.4.5. Clones sequencing analysis	95
11.4.6. Recombinant antibodies production	95
11.4.7. Antibodies characterization by standard laboratory assays	96
11.4.8. Epitope mapping	98
11.4.9. CDC assay	99
12. References	100

List of figures

Fig.1. Ovarian cancer types.

Fig. 2. Scheme of the Open Reading Frame (ORF) - filtering approach. Random fragments are cloned upstream of a β -lactamase gene. Clones containing fragments that are ORFs allow the synthesis of a fusion protein that confer ampicillin resistance to transformed bacteria. After selection on ampicillin, the β -lactamase gene can be removed by passage through bacteria expressing Cre recombinase. The selected ORF can then be displayed on phage.

Fig.3. Different types of microarray. (A) Three types of microarray coating, namely antibody, peptide or protein coating. (B) Second step of microarray where studies interactors are added: proteins, cells or lysate for antibody microarray; proteins, antibodies or lysate for peptide microarray; and proteins or antibodies for protein microarray.

Fig.4. CDC scheme. Complement component C1 recognizes the Fc portion of IgG's and becomes activated, cleaves C4 into C4a and C4b and C2 into C2a and C2b. C4b and C2a together form the C3 convertase, which enzymatically cleaves C3 into C3a and C3b. C3b is incorporated into the classical C3 convertase to form C5 convertase, which cleaves C5 into C5a and C5b. C5b also gets deposited on the target cell surface. Complement proteins C6–C9 form the terminal complex, membrane attack complex (MAC), that forms a transmembrane channel, which causes osmotic lysis of the target cell.

Fig.5. ADCC scheme. Activation of NK cells is performed through transmembrane activating and inhibitory receptors. Activated NK cells lead to degranulation and cytokine secretion. Perforin and granzymes uptake by target cells and TNF family death receptor signaling causes target cell apoptosis. IFN γ released by NK cells activate nearby immune cells to promote antigen presentation and adaptive immune responses. Macrophages, neutrophils and eosinophils can mediate ADCC.

Fig.6. Schematic presentation of ovarian cancer antigens identification using two approaches. 1. Antibodies were purified from ovarian cancer, non-cancerous and other cancer ascites; 2. IF staining of OVCAR-3 cells surface using purified antibodies; 3. ORF library phage display selection; 4. Selected in phage display clones screened with ascites antibodies in microarray assay; 5. Validation of antibodies specificity to selected clones in ELISA assay; 6. Analyze of correlation of patients survival with antibodies; 7. Performing cell surface ELISA to show that ovarian cancer ascites contain antibodies against ovarian cancer cell surface proteins; 8. Identification the most abundant antibody in ovarian cancer ascites by SERPA; 9. Analyzing PDI specificity of ovarian cancer antibodies in ELISA assay; 10. Representing killing capabilities of anti-PDI antibodies in CDC assay; 11. Representing PDI protein on ovarian cancer cells surface by IF staining.

Fig.7. Schematic representation of recombinant antibodies production and its analysis: 1. Selection scFv's specific to PDI protein in phage display selection; 2. Confirmation of PDI specificity of selected clones in phage ELISA; 3. Sequencing of selected clones and correction of occurred TAG mutations; 4. Cloning of scFv's into pcDNA3.1/Hygro(+) vector, transfection CHO cells, selection of best antibodies producing clone and antibody production; 5. Identification of epitopes for each antibody; 6. Analyze of antibodies functionality in main laboratory assays, namely immunofluorescent assay (7), immunoprecipitation assay (8), ELISA assay (9), Competition assay (10), CDC assay (11).

Fig.8. Scheme of anti-PDIA1 autoantibodies identification by SERPA. OVCAR-3 cell lysate was separated by 2D-gel electrophoresis, transferred to membrane and incubated with ascites of ovarian cancer patients. Spots, where antibodies showed binding were isolated and analyzed by mass spectrometry for protein identification.

Fig.9. Characterization of ascitic fluid based on immune response. (A) Immunofluorescent staining of cell surface of ovarian cancer cells previously incubated by ovarian cancer ascites of patient #46. (B)

Immunofluorescent staining of cell surface of ovarian cancer cells previously incubated by non-cancerous ascites of patient #1206. (C) anti-Folate staining of ovarian cancer cell surface.

Fig.10. Ascites antibodies in Cell Surface ELISA and CDC assay. (A) Cell Surface Elisa. (B) Complement dependent cytotoxicity Assay. (C) Comparative analysis of CDC assay versus cell surface ELISA of all ovarian cancer ascites.

Fig.11.Serological Proteome Analysis. Recognition of OVCAR-3 cell lysate proteins separated by 2D-gellectoforesis and transferred to membrane by ovarian cancer (left panel) and non-cancerous (right panel) patient ascites and identification PDI as the most abundant antibody binding protein by MS (under panel).

Fig. 12. ELISA assay and Overall patient Survival analysis. Affinity purified antibodies of ovarian cancer, other cancer and non- cancerous ascites reactivity to recombinant PDIA1 in ELISA assay (left panel). Analysis of overall survival of ovarian cancer patients, which ascites showed Positive (above threshold) and Negative (bellow threshold) response to PDI in ELISA assay (right panel).

Fig.13. Anti-PDIA1 mediated complement dependent cytotoxicity. Affinity purified anti-PDI antibodies from ovarian cancer patient ascites, commercial anti-PDI and anti-Folate (used as positive control) antibodies activation of CDC. Affinity purified and commercial anti-PDI antibodies were cross-inhibited by incubation with PDI protein to represent it specificity.

Fig.14. PDI surface staining on not permeabilised OVCAR-3 cells. (A) Membrane surface staining (anti-Folate receptor staining). (B) Surface PDIA1 staining. (C) merge between A and B.

Fig.15. Clones specific for PDI identified during phage selection. 193 different colonies manually picked during phage display selection arranged in them reactivity to PDI protein. 36% of all colonies showed a strong reactivity signal in ELISA assay

Fig.16. Phage ELISA for selected clones A8, H7, D9, D2, H12 and B10. Phage clones were tested for it reactivity to GST-PDI folded, HIS-PDI folded, HIS-PDI denatured, GST and HIS-TG2 proteins (used as a control proteins to show that scFv's were selected against PDI protein and not to its tag, which were GST and 6xHIS).

Fig.17. Finger printing analyze. B10, H12, H7 clones restricted by HaeIII and BastNI restriction enzymes that represent different cut patrons for each antibody confirming that antibodies are different from each other.

Fig.18. Schematic representation of H12, H7 and B10 antibodies (minibodies) production. Plasmid pDAN5 was extracted from selected phage clones. scFv's were digested from pDAN plasmid and cloned into pcDNA3.1/Hygro vector. This vector was analyzed for its correct sequence and transfected into CHO cells. Transfected CHO cells were grown under Hygromycin selection for two days. Cells that developed resistance to Hygromycin were grown in 96 well plates in concertation 1 cell/well for monoclonal selection. Best antibody producing cells were selected based on WB and ELISA results and were expanded. Supernatant of it was collected and used to purify antibodies.

Fig.19. Minibodies production. (A) Scheme of selected scFv's cloning into pcDNA3.1/Hygro(+) vector that already contain fused Fc fragment that can be of different species. (1). (B) Produced antibodies were visualized in Western Blotting by anti-human and anti-SV5 antibodies. Produced antibodies were visualized and quantified in SDS-PAGE gel.

Fig.20. ELISA assay. ELISA wells were coated with 1µg/well recombinant HIS-PDI. Recombinant antibodies were used in different concentration to represent it reactivity to PDI.

Fig.21. Antibodies affinity. Saturating value of each antibody in ELISA assay was considered as maximum binding of antibody and was normalized till 1.0.

Fig.22. pTrcHIS B vector map

Fig.23. Different length PDI constructs. Schematic representation of different PDI constructs produced as separate proteins for epitope mapping. Domain A, B, B', linker, A', C correspond to domains as describes by Gruber *et.al.*

Fig.24. Epitope mapping using ELISA assay. ELISA wells were coated with 1µg/well of each PDI fragment (1-8 numbers correspond to the fragments in Fig.23). Recombinant antibodies shows different patron of epitope recognition.

Fig.25. WB epitope mapping of H12 antibody. H12 antibody recognizes PDI, constructs 1, 4 and less strongly constructs 2 and 8, that correspond to result in epitope mapping ELISA. Constructs correspond to it predicted weight.

Fig.26. Epitope sites for H12, H7 and B10 antibodies. Representation of PDI protein sites that are suggested to be recombinant antibodies epitopes. H12 antibody might recognize epitope located in between half of B' domain and part of the linker. H7 antibody recognizes epitope in a fragment restricted to B', linker, A' domain. B10 antibody has a complex conformational epitope and can recognize only full correctly folded PDI protein.

Fig.27. Immunofluorescent staining of intracellular PDI. OVCAR-3 cell line were permeabilised and stained with recombinant antibodies H12, H7 and B10. Transmission field represents position of the cells in slide. Merge between recombinant antibodies staining and transmission field shows that PDI staining is present in cytoplasm.

Fig.28. Immunofluorescent co-staining of intracellular PDI. OVCAR-3 cell line were permeabilised and stained with recombinant antibodies H12, H7 and B10 (bleu) in parallel with commercial anti-PDI antibodies (red). Merge between commercial anti-PDI and recombinant antibodies staining shows that staining correspond each other, what confirms specificity of recombinant antibodies to PDI protein.

Fig.29. Immunofluorescent staining of surface PDI in OVCAR-3 cells. Membrane staining performed by *Triticum vulgare* FITC conjugate (that recognizes glycoproteins and on not permeabilised cells gives membrane staining) is represented in green. Recombinant antibodies PDI staining is represented in bleu. Merge between membrane and PDI staining represent that PDI is located on cell surface.

Fig.30. Surface PDI staining in OVCAR-3 cells. FACS analysis of PDI present of the surface of not permeabilised OVCAR-3 cells using H12, H7 and B10 antibodies (green graphic). Negative control (black filled graphic) is anti-human CY5 antibody staining

Fig.31. Immunoprecipitation assay. IP of endogenous PDI in OVCAR-3 cell lysate. Preliminary cell lysate was incubated with protein A beads to remove proteins that might bind protein A not specifically. Afterwards equal amount of cell lysate was incubated with H12, H7, B10 and commercial anti-PDI antibodies. Antibody-protein complex was pulled down with protein A beads. Negative control (-C) was incubated only with protein A beads. A small fraction of cell lysate (correspond to approximately 6%) was loaded to represent total amount of endogenous PDI in cell lysate.

Fig.32. Schematic representation of competition experiments. Recombinant antibodies H12, H7 and B10 were mixed with HIS-PDI. In parallel the same antibodies were also mixed with HIS-TG2 protein. Incubation took 1-2 hour on rotation at RT. Afterwards these antibodies were used for surface IF staining of PDI protein on not permeabilised OVCAR-3 cells and in ELISA assay on the wells pre-coated with PDI protein.

Fig.33. Immunofluorescent staining of surface PDI in OVCAR-3 cells. (A) H12, H7, B10 staining of cell membrane PDI after being preincubated with HIS-TG2 (in bleu). (B) H12, H7, B10 staining of cell membrane PDI after being preincubated with HIS-PDI (in bleu). Membrane staining performed by *Triticum vulgare* FITC conjugate (that recognize glycoproteins and on not permeabilised cells gives membrane staining) is represented in green.

Fig.34. Competition ELISA. ELISA wells were pre-coated with 1µg/well PDI protein overnight at 4°C. H12, H7 and B10 antibodies used in ELISA assay were preinhibited with 0µg, 0,5µg, and 1µg of HIS-PDI or HIS-TG2.

Fig.35. Cell surface ELISA assay. Not permeabilised IGROV ovarian cancer cells were incubated with recombinant antibodies H12, B10 and H7 by each of it separately or in combination of three antibodies together B10+H7+H12. cMOV18 anti-Folate antibody was used a positive control

Fig.36. CDC assay. H12, B10 and H7 used in concentration 2µg/ml. Positive control anti-Folate receptor antibodies (cMOV18/19) used in concentration 2µg/ml each. Normal human serum (NHS) represents a negative control, cells that were incubated only with NHS.

Fig.37. Domains organization of PDI. (A) Models of human PDI and yeast PDI. (B) Ribbon diagram based on the crystal structure of yeast PDI showing the active-site cysteines in green space-filling representation. Colors of the domains are the same as in (A).

List of tables

Tab.1. Cancer of the ovary classified by FIGO in 2006.

Tab.2. Specific for PDI clones selected as result of plasmid sequencing.

Tab.3. Clones selected for TAG mutagenesis and further antibody production.

Summary

Epithelial ovarian cancer is the fifth most common cancer in women worldwide. Each year thousands of women are dying from it. Mostly asymptomatic during its development, EOC is diagnosed at late stages when metastasis occurs and treatment is mostly difficult. Despite huge efforts to identify novel molecular targets for diagnosis and cure, the treatment of ovarian cancer is still limited to cytoreductive surgery followed by chemotherapy. It's obviously that new therapeutic approaches have to be developed instantly.

Identification of effective biomarkers for early diagnosis, prognosis and response to treatment is still a challenge in the field of ovarian cancer research. By relying on auto-antibodies present in ovarian cancer patients' ascitic fluids we aimed to identify tumor specific antigens for diagnostic and therapeutic purposes. To achieve this goal were performed two approaches.

In the first approach systematic and in-depth profiling of ovarian cancer ascites was presented. Ascitic fluids were ranked by their antibody response against cellular antigens in ovarian cancer. Further, human cDNA ORF filtered phage display library was screened with antibodies purified from ovarian cancer ascites in order to identify tumor specific antigens. Phage libraries of open reading frame fragments, created from mRNA derived from various tissues, were used. Here, cDNAs are expressed as fusion proteins with one of the phage coat proteins and exposed on the surface of the phage thus allowing the selection with antibodies present in ascites collected from ovarian cancer patients. Phage display selected peptides were further screened for their immunoreactivity by protein microarray analysis. Further, microarray identified antigens were validated by indirect ELISA. Subsequently, correlation of autoantibodies signatures with known tumor expression of corresponding antigens, prognostic value and patient survival outcome were examined.

In the second approach potential ovarian cancer antigens were identified with SERPA and MS techniques, using ascites of ovarian cancer patient as antibodies source. Specificity of antibodies for identified target protein was confirmed by performing ELISA assay. Candidate antigen was used to correlate antibody level to clinical outcomes and to evaluate their potential CDC mediated activities. Subsequently, recombinant antibodies that target identified antigen were engineered and produced as potential immunotherapy for ovarian cancer.

Il cancro ovarico epiteliale è il quinto tumore più comune nelle donne in tutto il mondo. Ogni anno migliaia di donne muoiono. Essendo asintomatico durante il suo sviluppo, l'EOC viene diagnosticato in fasi avanzate quando si verificano metastasi e il trattamento risulta essere più difficile. Nonostante gli enormi sforzi per identificare nuovi bersagli molecolari per la diagnosi e la cura, il trattamento del cancro ovarico è ancora limitato alla chirurgia citoreducente seguita dalla chemioterapia. È ovvio che i nuovi approcci terapeutici devono essere sviluppati immediatamente.

L'identificazione di biomarcatori efficaci per la diagnosi precoce, la prognosi e la risposta al trattamento è ancora una sfida nel campo della ricerca sul cancro ovarico. Facendo affidamento sugli autoanticorpi presenti nei liquidi ascitici dei pazienti affetti da tumore ovarico, abbiamo mirato a identificare un antigene specifico del tumore a scopi diagnostici e terapeutici. Per raggiungere questo obiettivo sono stati eseguiti due approcci.

Nel primo approccio è stato delineato in maniera approfondita e sistematica il profilo dell'ascite del cancro ovarico. I fluidi ascitici sono stati classificati in base alla loro risposta anticorpale contro gli antigeni cellulari nel cancro ovarico. Inoltre, la libreria di visualizzazione dei fagi filtrati del cDNA ORF umano è stata analizzata con anticorpi purificati da ascite del cancro ovarico per identificare antigeni tumorali specifici. Sono state utilizzate librerie di fagi di frammenti di quadro di lettura aperti, creati da mRNA derivati da vari tessuti. Qui, i cDNA sono espressi come proteine di fusione con una delle proteine del phage coat ed esposte sulla superficie del fago consentendo così la selezione con anticorpi presenti negli asciti raccolti da pazienti con carcinoma ovarico. I peptidi selezionati per la visualizzazione dei fagi sono stati ulteriormente analizzati per la loro immunoreattività mediante analisi di microarray di proteine. Inoltre, gli antigeni identificati con microarray sono stati convalidati mediante ELISA indiretto. Successivamente, è stata esaminata la correlazione di autoanticorpi aventi profilo di espressione tumorale conosciuta nota di antigeni corrispondenti, come valore prognostico ed esito di sopravvivenza del paziente.

Nel secondo approccio, i potenziali antigeni del cancro ovarico sono stati identificati con le tecniche SERPA e MS, utilizzando l'ascite del paziente oncologico come fonte di anticorpi. La specificità degli anticorpi per la proteina bersaglio identificata è stata confermata eseguendo il test ELISA. L'antigene candidato è stato usato per correlare il livello degli anticorpi ai risultati clinici e per valutare le loro potenziali attività mediate dal CDC. Successivamente, sono stati progettati e prodotti anticorpi ricombinanti mirati verso l'antigene identificato, come potenziale approccio immunoterapico per il trattamento del cancro ovarico.

Chapter 1

1. Introduction

1.1. Ovarian cancer

Ovarian cancer (OC) is the leading cause of mortality among gynecological malignant cancers. It is the fifth most common cancer in women worldwide. Each year, almost 22,000 women are diagnosed with ovarian cancer and more than 14,000 women die from it. Treatment of patients in the late stages of cancer development, when metastasis already occurred, is difficult and gives low probability for survival (2). Unfortunately only 25% of patients are diagnosed at the early stage of cancer development, when cancer is still limited to the ovaries and can be treated by surgery and chemotherapy, which are effective for 80% of patients. About 70% of ovarian cancer cases are diagnosed at late stage and therefore are poorly treatable. Only 30% of them have a relative survival of 5 years (3).

Ovarian cancer can be divided in three types. The most diffuse one is the epithelial ovarian cancer (EOC) that originates from ovary outer surface cells and it accounts for 85% to 90% of all ovarian cancer cases, known as carcinomas. The other types of OCs originate either from germ cells or from stromal cells (Fig.1) (4).

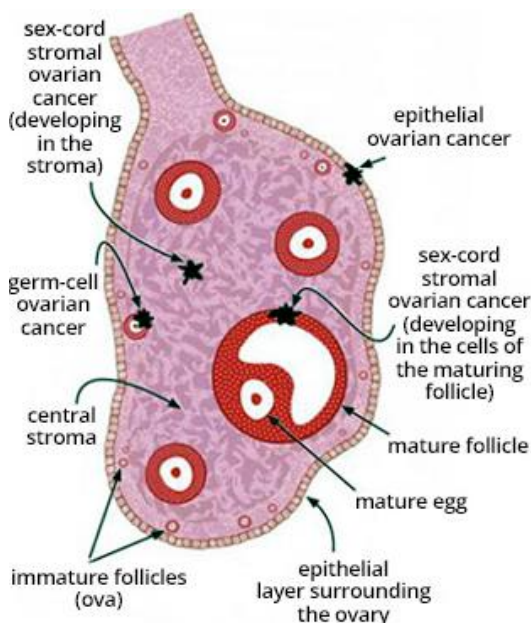


Fig.1. Ovarian cancer types (5).

OC patients are mostly in the age of 60 years. There is a genetic predisposition to OC since the frequency of patients is higher in families with a history of ovarian or breast cancers. Women who have inherited mutations in BRCA1 or BRCA2 genes have a substantially higher risk to develop ovarian cancer, and at a median age of diagnosis around 40. Inherited mutations in mismatch repair genes (BRCA1 or BRCA2) or in ARID1 gene have been reported to be associated with higher risk to develop OCs (6).

Nulliparity is a risk factor of ovarian cancer while oral contraception, pregnancy and lactation are associated with a reduced risk. It has been suggested that stimulation of the epithelium of the ovarian surface, which occurs in the nulliparous state as a result of uninterrupted ovulation, may predispose the epithelium to malignant transformation (7).

1.2. Symptoms of ovarian cancer

Ovarian cancer often grows as a complex cystic mass in pelvis. Unfortunately, symptoms are often misled as due to gastrointestinal or abdominal diseases which delays the correct diagnosis at late stages of cancer development. Main symptoms present in the patients are abdominal or pelvic pain (34,7%), increased abdominal girth (31,9%), vaginal bleeding (19,4%), change in bowel habits (16,7%). Other symptoms can be the frequency of urinary stimulus , abdominal pressure, weight gain or loss, decrease of appetite (8). In later stages ovarian cancer can have metastases, which are mostly spread in the peritoneal cavity. Moreover, metastases can be spread by lymphatic vessels to the nodes or to parenchymal organs by blood vessels. On late stages tumor mass can block lymphatic vessels in the abdomen and limit outflow of ascitic fluid (9).

1.3. Classification of ovarian cancer

OC staging is defined by the Gynecology Oncology Committee of FIGO and is accepted in 2006 Stages are numbered from I to IV depending on cancer spreading and metastasis in the organism. In Table 1 are shown the different characteristics for each stage (6).

FIGO Stage	Description
I	Growth limited to the ovaries
IA	Growth limited to one ovary; no ascites present containing malignant cells. No tumor on the external surface; capsule intact
IB	Growth limited to both ovaries; no ascites present containing malignant cells. No tumor on the external surfaces; capsules intact
IC ^a	Tumor either Stage IA or IB, but with tumor on surface of one or both ovaries, or with capsule ruptured, or with ascites present containing malignant cells, or with positive peritoneal washings
II	Growth involving one or both ovaries with pelvic extension
IIA	Extension and/or metastases to the uterus and/or tubes
IIB	Extension to other pelvic tissues
IIC ^a	Tumor either Stage IIA or IIB, but with tumor on surface of one or both ovaries, or with capsule(s) ruptured, or with ascites present containing malignant cells, or with positive peritoneal washings
III	Tumor involving one or both ovaries with histologically confirmed peritoneal implants outside the pelvis and/or positive regional lymph nodes. Superficial liver metastases equals Stage III. Tumor is limited to the true pelvis, but with histologically proven malignant extension to small bowel or omentum
IIIA	Tumor grossly limited to the true pelvis, with negative nodes, but with histologically confirmed microscopic seeding of abdominal peritoneal surfaces, or histologic proven extension to small bowel or mesentery
IIIB	Tumor of one or both ovaries with histologically confirmed implants, peritoneal metastasis of abdominal peritoneal surfaces, none exceeding 2 cm in diameter; nodes are negative
IIIC	Peritoneal metastasis beyond the pelvis >2 cm in diameter and/or positive regional lymph nodes
IV	Growth involving one or both ovaries with distant metastases. If pleural effusion is present, there must be positive cytology to allot a case to Stage IV. Parenchymal liver metastasis equals Stage IV

^a In order to evaluate the impact on prognosis of the different criteria for allotting cases to Stage IC or IIC, it would be of value to know if rupture of the capsule was spontaneous, or caused by the surgeon; and if the source of malignant cells detected was peritoneal washings, or ascites.

Tab.1. Cancer of the ovary classified by FIGO in 2006.

1.4. Ovarian cancer treatment

Despite progressive development of medical treatment in the last decades, the main treatment methodologies for ovarian cancer remain chemotherapy and surgery. Chemotherapy is given mostly to the patients that are already have metastasized cancer. Established chemotherapy is based on platinum compounds, such as cisplatin or carboplatin, or taxanes such as paclitaxel (Taxol®) or docetaxel (Taxotere®) (10). Carboplatin and paclitaxel are applied mostly in early-stage disease, are supplied in cycles between 3-6 times and can be used in combinations. Carboplatin is the most active medicine in ovarian cancer. Intraperitoneal chemotherapy with high local drug concentration has improved survival of the patients after surgery, but it is burdened by side effects such as nausea, tiredness, loss of weight and hair, skin and mucous layer lesions, anemia, immunodeficiency, bleeding and kidney damage. Moreover, chemotherapy is very damaging for organisms, as it targets also normal dividing cells and 50% of treated patients will have disease relapse (9), (11).

Surgical removing of cancer is one of the main treatment approaches but it depends on the stage of cancer. Debulking surgery is often performed with extensive tissue removal including fallopian tube, omentum, bladder and/or spleen.

One possible treatment in EOCs is hormone therapy. Luteinizing-hormone-releasing hormone (LHRH) agonists, such as goserelin (Zoladex®) and leuprolide (Lupron®), can be used to repress estrogen production. Other drugs include Tamoxifen, a selective estrogen-receptor modulator (SERM), aromatase inhibitors, such as letrozole (Femara®), anastrozole (Arimidex®), and exemestane (Aromasin®), that block the synthesis of estrogen.

Radiation therapy is another therapeutic option. The currently formats have devastating side effects, such as nausea, diarrhea, skin damage, tiredness (4), but new strategies have been developed based on site specific implantable radioactive devices (reff)..

Thus, there is a cogent need for new more effective therapies as those based on immunotherapy approaches. Increasing evidences support the protective role of the immune system against cancers and the clinical successes of monoclonal antibodies-based immunotherapy (12). In particular, the development of biomarker-driven anticancer-antibodies is considered promising for more personalized cancer therapy. To this respect a number of technologies allow the detection of biomarkers that have the potential to predict response of cancers to particular targeted therapy (13), (14).

2. Biomarkers-based personalized therapy

2.1. Biomarkers

Biomarkers are biochemical or molecular alterations of cellular character that increase in organism as result of normal or pathogenic biological processes or pharmacological responses to a therapeutic intervention and can be detected in tissues, cells or biological fluids. Biomarkers are widely applied in studding cardiovascular, infections, immunological, genetic diseases and cancer (15, 16).

Biomarkers can be DNA, mRNA, proteins or metabolites originated during cellular processes such as apoptosis, angiogenesis or proliferation. They can be produced by sick cells or by other cells of the organism as a reaction to disease or inflammation process. Biomarkers can be described as diagnostic, prognostic or predictive. Diagnostic biomarkers are those used to identify a disease. Prognostic biomarkers are applied once disease is already identified and is necessary to predict probable development or regression of it. Often these biomarkers can represent survival rate of patients. Predictive biomarkers are those that can predict sensitivity of patient to a therapy before treatment is started. Ideal biomarker has to be quickly and easily measurable in biological fluids of patient, represent high analytical sensitivity and specificity, have a long half-life time in the biological fluid and be exclusively correlated to one biological process in the organism (17).

Biomarker-based personalized cancer therapy is a relatively new direction in cancer treatment, which intends to design therapy based on tumor genotypes and patient genetic profiles. Personalized medicine aims to classify cancer based on molecular characteristics, genetic abnormality, mutations and signaling pathway activation of which need to be targeted during treatment. Understanding molecular carcinogenesis will help to treat patients with preferentially targeted substances based on specific molecular profiles found in individual tumor tissues. Development of biomarker-based personalized medicine opens new opportunities for goal oriented treatment but is quit challenging. One of the hardest complications is to translate cancer mutations into related progression of the cancer over time. In spite of this knowledge gap, these recent advances in identifying biomarkers using

modern technologies is continuing to make great developments which hold enormous promise for advancing cancer treatment (18).

2.2. Ovarian cancer biomarkers

Diagnostic of ovarian cancer can be performed using computed tomography (CT) scans, magnetic resonance imaging (MRI) scans, ultrasound studies, laparoscopy, colonoscopy, tissue biopsy. Nowadays only two tests are used for ovarian cancer screening, transvaginal ultrasound (TVUS) and the CA-125 blood test. TVUS test makes possible to look at the uterus, fallopian tubes, and ovaries using sound waves. It can detect tumor formation but it can't actually tell if a mass is cancer or benign. As result of screening, most of the masses found are not cancer (4).

CA-125 protein is an accepted ovarian cancer biomarker. Increased serum levels are related to cancer. CA-125 is a tumor associated protein expressed as a membrane bound protein. CA-125 is mucin-type O-linked glycoprotein and it has been suggested to play a role in cell-mediated immune response. In cancer cells it is shown to suppress anti-tumor immune response. Patients with CA-125 level in blood higher than 35 units/ml are considered for the further analysis with potential chance for cancer development. It has been shown that in 99% of healthy women CA-125 is not elevated and remains less than 35. Patient that has ovarian cancer shows CA-125 concentration in blood of hundreds and thousands units/ml. It has been shown that 85% of ovarian cancer patients are having high CA-125 concentration while less than 1% of healthy woman have elevated CA-125. However, specificity of CA-125 as ovarian cancer biomarker is not so accurate and it can show elevation due to the other cancer types or some infectious diseases and give false positive results. Only 50% of patients in the I stage of ovarian cancer development are having elevated CA-125. Nowadays CA-125 is considered to be the only preclinical serum marker to analyze the risk of ovarian cancer developing in diagnostic and an early detection to guide treatment in women known to have ovarian cancer (2).

Some other biomarkers that can give useful information during antiangiogenic therapies of cancer, can be in situ tissue biomarkers, such as microvessel density (MVD), vascular endothelial growth factor (VEGF) and VEGF receptor (VEGFR), neuropilin-1, phosphatidylinositol-glycan biosynthesis class F (PIGF), basic fibroblast growth factor (bFGF), intercellular adhesion molecule 1 (ICAM-1), thrombospondin-1 and p53. However, these biomarkers have some practical limitations as it requires numerous biopsies from primary cancer and metastatic sites to represent dynamic changes before and after treatment. Use of circulating biomarker proteins is less laborious and does not require traumatization of cancer tissue. Certain studies evaluated the level of VEGF in circulating forms but also as urinary biomarkers. It has been shown that low baseline serum VEGF-A levels is correlated with increased response to bevacizumab treatment and improved survival in patients with OC (19). Other known biomarkers are chorionic gonadotropin (hCG), alpha-fetoprotein (AFP), lactate dehydrogenase (LDH). Increased inhibin and hormones such as estrogen and testosterone can be also detected (4).

2.3. Ovarian cancer ascites for biomarkers identification

New biomarkers for ovarian cancer with higher sensitivity need to be discovered for early diagnosis, prognosis, or monitoring of ovarian cancer. With the significant development of MS and proteomic technologies, protein biomarker identification became an important goal of proteome analysis in different diseases.

Analyzing body fluids for biomarkers identification is becoming more usual than tissue biopsy. Study body fluids gives advantages as samples are easy to collect and proceed, it has low invasiveness and minimum cost. Human body fluids used for proteome analyzing can be human plasma, urine, cerebrospinal fluid, saliva, bronchoalveolar lavage fluid, ascites

Human plasma proteins originate from a variety of tissue and blood cells as a result of secretion or leakage. It has been shown that proteins present in plasma represent physiological or pathological states of the human body and can be used for disease diagnosis and prognosis. Plasma/serum sample preparation is important process as serum protein composition is different from plasma and can be crucial for proteome analysis. Plasma is rich for protein but also very complex fluid where proteins can interact with each other or be bound to other carrier proteins, which make it analyzing very challenging.

OCs at advanced stage are characterized by fast growth of intraperitoneal tumors and accumulation of ascites fluid in the peritoneal cavity. Ascites are due to high secretion by malignant cells of proteins that include growth factors and cytokines that promote neovascularization and increased capillary permeability. (20). As result, ascites fluid represents the local microenvironment of ovarian cancer that contains various cell types, malignant cell, the secretome of ovarian cancer, survival factors, cytokines, chemokines, growth factors, associated with invasion and metastasis. Matte et. al. (21) describe the cytokines profile in 10 ovarian cancer patient ascites. They showed increased expression of several factors including angiogenin, angiopoietin, GRO, ICAM-1, IL-6, IL-6R, IL-8, IL10, leptin, MCP-1, MIF, NAP-2, osteoprotegerin (OPG), RANTES, TIMP-2, and urokinase plasminogen activator receptor (uPAR) . Some of them were associated with shorter progression-free survival. It has been also described that ascites of cancer patients contain different cell population that are playing a role in tumor microenvironment and interact with each other through soluble mediators. Some of the cell populations present in ascites of ovarian cancer patients are cancer-associated fibroblasts (CAFs), infiltrating macrophages/monocytes, bone marrow-derived mesenchymal stem cells (MSCs), and cytotoxic or Treg, tumor-infiltrating CD8⁺ T cells (22). Analyzing the exact protein content of human ascites can present critical information about ovarian tumor growth, progression, outcome and treatment response, disease surveillance, and potentially early detection. Due to it ascites are an excellent medium for potential biomarkers identification (23-25).

3. Cancer and immunotherapy

3.1. Cancer triggers immune reaction

Several studies demonstrated that immunotherapy might represent a novel valuable therapeutic approach through which T lymphocytes are activated to specifically kill cancer cells. The immune system has a key role in the recognition of self- and non-self- antigens to protect multicellular organism against pathogens. The combination of a variety of T cell receptors (TCRs) together with antibodies from adaptive immunity makes it an extraordinary precise system for the recognition of non-self-antigens.

Cellular transformation resulting in cancer development and progression involves an uncontrolled cell proliferation typically paralleled by a continuous accumulation of gene mutations. Sometimes, mutations in protein-coding genes might result in the generation of a mutant protein, recognized by the immune system as non-self-proteins. This process is mediated by the processing of mutant proteins by APC cells (antigen-presenting cells) and the exposure of these neo-antigens through the MHC-I and -II system. Antigens are than recognized by T cells through their TCRs molecules and, together with

other co-stimulating signals, result in T cell activation (26). Importantly, it has also been shown that non-mutated self-antigens can also stimulate the immune system toward self-proteins on cancer cells. Although the precise molecular mechanism(s) responsible for this autoantibodies production is not completely clear, one hypothesis relay on the potential exposure/secretion of proteins normally confined to intracellular compartments and, thus, invisible to the immune surveillance (27), (26).

3.2. Autoantibodies

Autoantibodies produced by organisms against autologous tumor-associated antigens have been detected in different cancer types and can be potentially used as biomarkers for early cancer diagnosis. Most autoantibodies found in the sera of these patients target cellular proteins due to their unusual modifications, abnormal localization, or expression. Therefore, the identification and functional characterization of these immunological ‘reporters’ might also help to uncover the early molecular events during carcinogenesis (28). Antibodies raised against tumor associated antigens (TAA) might therefore represent good candidates in cancer diagnosis due to: i) their early production during carcinogenesis; ii) a single antigen can stimulate the production of TAA by B lymphocytes; iii) their relative long half-life (approximately 21 days in patients’ sera); low-invasive method to obtain biological samples to test; both cheap and low complex analysis of samples. (29).

3.3. Tumor associated antigens (TAA)

Tumor associated antigens can be divided in five groups: the first group is represented by proteins which are only expressed in cancer cells, therefore named tumor specific antigens. These antigens are proteins overexpressed in cancer cells and often are shared among a cohort of patients affected by the same malignancy. A second antigens group comprises antigens that can be expressed in both cancer and normal tissue differentiated cells. These antigens are called tumor associated antigens. The third group is represented by antigens derived by tumor-specific mutations, named tumor-specific antigens (30). These proteins arise from mutations occurring during the uncontrolled cancer cells proliferation, when atypical posttranslational modification, such as phosphorylation, can give rise to tumor-associated antigens (31). It has been shown that TAA are key proteins in triggering immune system activation to target cancer cells (32). However, although most TAA are patient-specific, a number of them are shared by many patients and can then be used in clinic (33).

4. TAA identification techniques

4.1. Serological proteome analysis (SERPA)

There are several methodologies and approaches to identify new tumor associated antigens, although the identification of antigens triggering the strongest immune response is still a complicated matter. Techniques used to identify new potential antigens can be divided into groups such as serological analysis techniques (SERPA, SEREX, AMIDA), interaction studies (surface plasmon resonance, phage display), array technologies (proteins-, antibodies-, oligonucleotides-, tissue microarrays), proteomic analysis (mass spectrometry, 2D-gel electrophoresis, flow cytometry, liquid chromatography), and gene analyzing technologies (WES, SAGE).

Serological proteome analysis (SERPA) is a method that allows the identification of a whole antigens profile using the antibodies repertoire present in the serological fluids of a single patients (34). This technique is also known as Proteomex or Spear (Serological and Proteomic Evaluation of antibody responses). This technique combines 2D-gel electrophoresis (2D-GE) and Western Blotting (WB) procedures. Cancer proteins are separated by 2D-gel electrophoresis, transferred onto a membrane and

incubated with patient sera. Spots on the membrane indicate antibodies-antigens binding and mass spectrometry can be used to identify the target proteins. An important advantage of this technology is that, although proteins undergo denaturation during 2D-GE analysis, allowing the identification of linear epitopes, post-translational modifications such as glycosylation, sumoylation, acetylation, phosphorylation, and others that could be part of epitopes possibly triggering the immune response, are maintained during sample processing (35), (36). However, limitations arise from the inherent limitations of 2D-GE technique. Those are the potential loss of small (<15 kDa), very large (>200 kDa), extremely acidic (pI < 3) or basic (pI > 10), and highly hydrophobic proteins as well as the inability to detect TAA with conformational epitopes due to the denaturing conditions. The group of Francesco Novelli has successfully demonstrated the efficacy of this technique in the prediction of early stages of pancreatic ductal adenocarcinoma (PDAC) by detecting autoantibodies against Ezrin (37).

4.2. Screening of Expression Libraries

The approach based on the screening of cDNA expression libraries has been a powerful technique for TAA discovery and identification. This methodology provides a direct physical association between the protein under analysis and the gene encoding these proteins. Expression libraries can be screened for several purposes (38-41) but those based on the phage-display of filtered ORFs are particularly suitable for screening with antibodies.

Figure 2 schematically illustrates the key points of ORF filtering as described by Zacchi *et.al.* (38). Briefly, cDNA fragments are cloned upstream the β -lactamase gene and the bacteria transformed by in frame constructs can be selected for ampicillin resistance. ORF filtered library is then Cre-lox recombined to replace β -lactamase gene with the phage gene encoding the pIII coat protein.

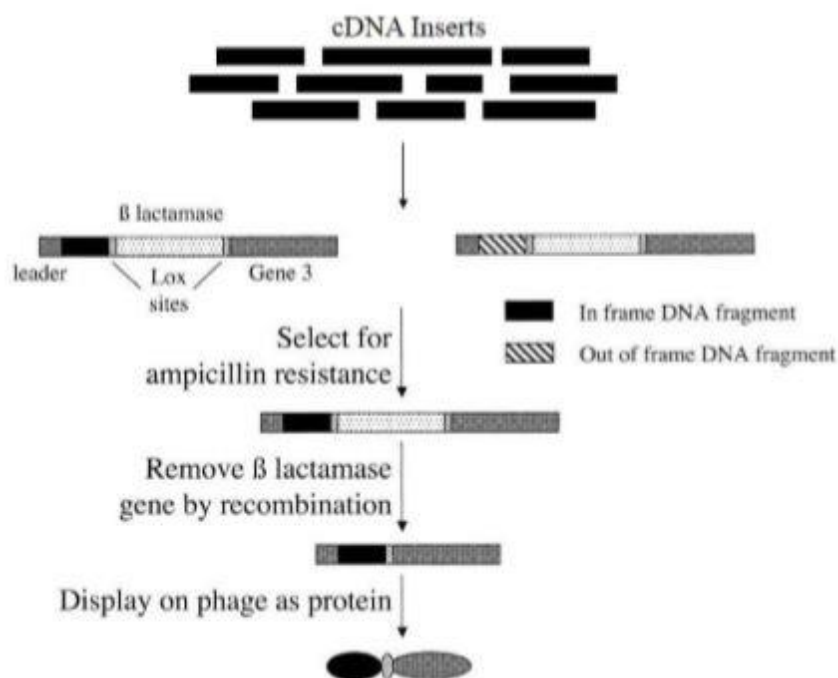


Fig. 2. Scheme of the Open Reading Frame(ORF)-filtering approach. Random fragments are cloned upstream of a β -lactamase gene. Clones containing fragments that are ORFs allow the synthesis of a fusion protein that confer ampicillin resistance to transformed bacteria. After selection on ampicillin, the β -lactamase gene can be removed by passage through bacteria expressing Cre recombinase. The selected ORF can then be displayed on phage (38).

4.3. Display systems

The concept of expression library can be readily applied to the display systems. Display technology refers to a collection of methods for creating libraries of modularly coded biomolecules that can be screened for desired properties in a high-throughput format on a global scale. It allows to analyses large-scale of protein–protein/protein– substrate interactions. Main advantages of this system are, that the selected protein can be immediately characterized and identified by a simple DNA sequencing reaction; and the gene encoding protein of interest can be manipulated with all the tools provided by molecular biology and genetic engineering techniques. Thus, allowing isolation and identification of specific proteins and related genes from a background of billions of unreactive clones (39).

Major formats include: i) Peptide-on- DNA/RNA display. These are cell-free display systems where DNA or RNA are capable to bind its own coded peptide. Thus, permitting a screening of a large pool of complexes and identify the interactors by isolation and sequencing of nucleotide sequences of either DNA or RNA. ii) Phage display: it is one of the most commonly used display system. Here the gene of interest is cloned into the coding sequence of viral coat proteins and expressed as fusion with a surface protein of the phage; ii) Cell based display: here the cDNA library encoding various proteins is recombinant expressed in cultured cells and selected for binding to a specific ligand on the cell surface. Yeast two hybrid system is the most popular among this category due to the high efficiency of transformation.

4.4. Phage Display

Phage display is technique applied for high-throughput screening of protein–protein, protein–peptide, and protein–DNA interactions that make a use of filamentous bacteriophages, that couple phenotype to genotype. Phagemids are Ff-phage-derived vectors containing origin of replication of a plasmid, selection marker, intergenic region, a gene encoding for phage coat protein, multiple cloning site, promoter and a DNA segment encoding a signal peptide. Proteins, peptides or polypeptides are exposed on the surface of filamentous M13 derived bacteriophage. This system allows the selection and isolation of novel interactors for its binding property to a given protein from a collection of billions of phages.

Depending on the particular application, phage display system makes a use of Ff filamentous phage, Lambda or T7. The most used one is Ff filamentous phage family (M13 and its close relatives fd and fl) due to it robust and highly flexible platform for display. Generally, the DNA fragments are cloned upstream to the gene encoding the pIII or pVIII coating proteins and are present as a single copy. The major differences between type III and type VIII phagemids are the length of foreign protein, the copy number of the displayed foreign proteins in the progeny phages and the influence of infection of progeny phages. Type VIII phagemid is used for small protein of interest and can produce hundreds or thousands of new copies. On the other hand, type III phagemids are used for large proteins and produce 5 copies of fusion proteins.

Phagemids can be converted to filamentous phage particles by co-infection with the helper phages. Firstly the phagemid, encoding for protein of interest, must infect *Escherichia coli* strain. Inside *E.coli*, the single-stranded DNA (ssDNA) of phagemid particles can be converted into replicative form of the phagemids by the host RNA and DNA polymerases and topoisomerase. Phage replicative origin is activated only when *E.coli* is co-infected with helper phage. Consequently phages will be produced and released from bacteria.

4.5. Publication: Phage display technology for human monoclonal antibodies

Dal Ferro Marco¹, Rizzo Serena¹, Rizzo Emanuela¹, Marano Francesca¹, Luisi Immacolata¹, Tarasiuk Olga¹ and Daniele Sblattero¹ *

TITEL

Phage display technology for human monoclonal antibodies

AUTHORS AFFILIATIONS

1 University of Trieste, Department of Life Sciences, Via L. Giorgieri 5, 34127 Trieste, Italy

2 University of Eastern Piedmont; Department of Health Sciences and IRCAD, Novara, Italy

* Corresponding author.

Prof. Daniele Sblattero
Department of Life Science,
University of Trieste, Via L. Giorgieri 5,
34127 Trieste Italy,
Telephone +39 040 5588681 FAX: +39 040 558 2134
E-mail: dsblattero@units.it

i. Running Head

Making and selection of phage display antibody libraries

ii. Abstract

During the last 20 years *in vitro* technologies opened powerful routes to combine the generation of large libraries together with fast selection and screening procedures to identify lead candidates. One of the most successful method is based on the use of filamentous phages. Functional Antibodies (Abs) fragments can be displayed on the surface of phages by fusing the coding sequence of the antibody variable (V) regions to the phage minor coat protein pIII. By creating large libraries, antibodies with affinities comparable to those obtained using traditional hybridoma technology can be isolated by a series of cycles of selection on the antigen of interest. In this system, antibody genes can be recovered simultaneously with selection and can be easily further engineered, for example by increasing their affinity to levels unobtainable in the immune system, or by modulating their specificity and their effector functions (by recloning into a full-length immunoglobulin scaffold). This chapter describes the basic protocols for antibody library construction and selection of binder with desired specificity.

iii. Key Words: phage display; antigens; monoclonal antibody, high-throughput; scFv

1. Introduction

Traditional methods to generate monoclonal antibodies rely on the immunization of laboratory animals and the subsequent immortalization and selection of specific hybridoma cells. The process is laborious, requires costly animal houses and its efficacy depends on the ability of the immune system to mount a humoral productive response to the potential antigens. The advent of recombinant DNA technology has brought in the field new potentialities allowing to recapitulate *in vitro* the complete process of antibody production and selection, by-passing immunization, animal handling and the laborious process of clone isolation. The great advantage of *in vitro* methods is the possibility of coupling together the cloning of functional antibody fragments, their selection and finally the isolation of the positive

antibodies coding genes. *In vitro* methods allow to identify antibodies with high throughput potential, speed and flexibility: antibodies can be selected and their affinities and specificities can be precisely tailored according to the needs. Phage (1, 2) and yeast display (3, 4) are the commonest methods for this purpose.

In 1985, G.P. Smith (5) first introduced the concept of displaying exogenous proteins on the surface of M13 phages, showing the potentials of building phage libraries displaying large repertoires of different proteins. Antibody display libraries have been the most successful application of this concept (6). The basic idea behind the display technology is that once a large library of antibodies is created, those with desirable properties can be selected. A phage displaying a specific antibody on its surface can be isolated for its binding property to a target ligand starting from a collection of billions of phages displaying different antibodies. Since the phage displayed protein gene is present in the phage genome, the selection of a virus allows the concomitant recovery of the corresponding antibody gene. Once isolated genetic details are easily identified by DNA sequencing and the sequence could be used for subsequent applications (see figure 1). [Fig.1 near here]

To carry out this procedure a few essential steps are required.

First, a library containing the antibody DNA sequences is created. Antibody diversity is restricted to the variable regions (VH and VL) and these gene fragments are inserted into a specific vector in frame with the sequence encoding the phage protein pIII. Once assembled, the phage particle will expose the functional antibody fragment fused to the amino terminus of the minor coat protein III. In the creation of an antibody library several different choices can be made: a) which form of antibody fragment to use; b) the source of V regions repertoire. In general, successful approaches have employed either the single chain fragment variables (scFv) (7) format, consisting in a VL and VH regions linked by a flexible linker, or the Fab (Fragment antigen-binding) format, in which VH-CH1 and VL-CL associate non-covalently (8).

Natural V region repertoires can be recovered by RT-PCR amplification starting from lymphocytes which may or may not have undergone antigen stimulation. Such V genes are amplified using primers which recognise the 5' end of the V genes and the 3' end of the J genes (9). These naïve libraries turned out to be robust sources of antibodies potentially against any target (10–12), including those poorly antigenic in animals. As an alternative, synthetic antibody libraries have been created by introducing diversity artificially using oligonucleotides into frameworks with desirable properties (13–15). To generate diversity, completely degenerate oligonucleotides were used (16), although recently it has been found that diversity restricted to only few amino acids can provide antibodies with similar high affinities (17).

Before proceeding to selection the clonal diversity of the library, either naïve or synthetic, needs to be assessed. Next generation sequencing is now routinely used to measure diversity and to validate the design of displayed libraries (18).

Once a library is created, the enrichment of antigen specific phage antibodies is carried out by 'phage panning', using immobilized (19) or labeled antigens (20).

[Fig 2 near here].

In this process, the antigen of interest is directly immobilized on a solid support, such as microplate wells or is coupled to magnetic beads. The phage particles are then added to allow the binding of phages displaying appropriate antibody. After extensive washing to remove all non-specifically bound material, phages displaying specific antibodies are retained while low affinity or unspecific phages are washed away. The selection procedure is repeated two to five rounds usually decreasing antigen concentration and increasing stringency of washing steps, leading to the isolation of phages expressing the desired

antibodies (i.e. those that bind the antigen of interest). Bound phages are then eluted from the target antigen and used to infect bacteria for binding analysis. The possibility to perform successive rounds of selection allow the isolation of binders present in very low number in a population of billions of different phages. A typical selection round is illustrated in figure 2.

At the end, specific antibodies for a given antigen are identified through an ELISA screening within several random clones. At this point, as antibody genes are directly identified by sequencing they can be subjected to downstream genetic engineering, for instance to increase affinity (through the generation of mutated antibodies secondary libraries) and/or to build full-length immunoglobulin with the desired effector functions.

2. Materials

2.1 Construction of Antibody Libraries

1. Bacterial strain used is *Escherichia coli* DH5 α F' [*F'*/*endA1 hsd17(rK_mKb) supE44 thi-1 recA1gyrA (Nalr) relA1 _ (lacZYA-argF) U169 deoR (F80dlacD-(lacZ)M15)*].

2. Ficoll-Paque PLUS (GE Healthcare).

3. Plasmid DNA is prepared using a commercial Miniprep kit, following the instructions of the manufacturer.

4. Stock solutions of antibiotics are prepared by dissolving kanamycin at 50 mg/mL in water and ampicillin at 100 mg/mL in water. Kanamycin and ampicillin stocks are filtered with 0.22 μ m filter device and stored at -20°C . Repeated freeze and thaw of ampicillin is avoided, and aliquots are prepared for single use.

5. 2xTY (2x Tryptone Yeast) liquid broth is prepared adding 16 g bacto-tryptone, 10 g bacto-yeast and 5 g NaCl to 1 L of ddH₂O. Final pH 7.0. Agar plates are prepared by adding 1.5% bacto-agar to 2xTY broth. Make up to 1 L with distilled water, autoclave and allow to cool to 55°C . At this temperature antibiotics and glucose can be added, prior to pouring into plates.

6. Glycerol molecular biology grade, (60% v/v), autoclaved.

7. All restriction endonucleases, T4 DNA ligase and buffers are purchased from New England Biolabs. All cloning steps are performed according to the manufacturer suggestions and to standard molecular biology procedures.

8. Commercial Gel Extraction Kit and PCR Clean-Up Kit are used for purification of DNA from agarose gel and restriction reaction mixtures, respectively, following the instructions of the manufacturer.

9. Commercial DNA clean and concentrator kit is used to purified and concentrate the ligation mixture, following the instructions of the manufacturer (see Note 1).

10. High-efficiency Electrocompetent Cells for Phage Display are used for transformations. 25 μ L aliquot is used for transformation of 1-2 μ L of purified DNA, using 1 mm gap cuvette (see Note 2).

2.2 Phage Production and Titration

1. Helper phage M13KO7.

2. Solution for precipitation of phages: 20% (w/v) polyethylene glycol (PEG) 6000 and 2.5 M NaCl. The solution is filtered through a 0.22 μ m filter before use, store at room temperature.

3. PBS: 8 g NaCl, 0.2 g KCl, 1.44 g Na₂HPO₄ and 0.24 g KH₂PO₄ in 1 L H₂O, final pH 7.4.

4. 20% glucose: filtered with 0.22 μm filter device and stored at room temperature.
5. 2xTYAG (2xTY Ampicillin Glucose): add 100 $\mu\text{g}/\text{mL}$ ampicillin and 1% of glucose to 2xTY liquid broth.
6. 2xTYAK (2xTY Ampicillin Kanamycin): add 100 $\mu\text{g}/\text{mL}$ ampicillin and 50 $\mu\text{g}/\text{mL}$ kanamycin to 2xTY liquid broth.

2.3 Phage selection to immobilized Antigen

1. Immuno MaxiSorp Tubes.
2. Antigen of interest dissolved in either carbonate buffer (pH 9.6) or PBS at a concentration of 1-100 $\mu\text{g}/\text{mL}$.
3. Carbonate buffer: mix 0.1 M Na_2CO_3 and 0.1 M NaHCO_3 until pH 9.6. 0.1 M Na_2CO_3 , 10.6 g $\text{Na}_2\text{CO}_3/\text{liter H}_2\text{O}$; 0.1 M NaHCO_3 8.4 g $\text{NaHCO}_3/\text{L H}_2\text{O}$.
4. PBS-Tween-20: add 1 ml of Tween-20 per liter of PBS.
5. 2% MPBS: 2 g non-fat milk powder /100 mL PBS.
6. 4% MPBS: 4 g non-fat milk powder /100 mL PBS.
7. 100 mM triethylamine (TEA): 140 μL triethylamine/10 mL H_2O . Prepare fresh; pH 12.

2.4 Immunoprecipitation with magnetic beads

1. Biotinylated antigen, 100-500 nM, best done using a commercial kit.
2. Streptavidin-coupled Dynabeads M-280 (Invitrogen).
3. Small magnets designed for fitting of 1.5-2 mL tubes.
4. 100 mM triethylamine: 140 μL triethylamine/10 mL H_2O . Prepare fresh; pH 12.
5. 1 mM DTT (1,4-Dithiothreitol).

2.5 Phage ELISA

1. Antigen: 1-100 $\mu\text{g}/\text{mL}$ dissolved in either carbonate buffer or PBS.
2. For antigen immobilization done by absorption to MaxiSorp 96-well plates
3. Anti-phage mAb horseradish peroxidase (HRP)-conjugated used at a final dilution of 1:5000 (GE Healthcare).
4. TMB (3,3',5,5'-tetramethylbenzidine) ready-to-use, pre-mixed solution for colorimetric HRP-based ELISA detection.
5. 2 N sulfuric acid: 55.6 mL 97% sulfuric acid dilute up to 1 Liter H_2O .

2.6 Soluble ELISA

1. Antigen: 1-100 $\mu\text{g}/\text{mL}$ dissolved in either carbonate buffer or PBS.
2. MaxiSorp 96-well plates for antigen immobilization by absorption.
3. Monoclonal antibody anti-immunoaffinity tag (e.g., 9E10 anti-myc, anti HIS6, anti V5) for detection of soluble scFv.

4. Horseradish peroxidase (HRP)-conjugated anti-mouse IgG.
5. 3,3',5,5'-tetramethylbenzidine ready-to-use, pre-mixed solution for colorimetric HRP-based ELISA detection.
6. 2 N sulfuric acid: 55.6 mL 97% sulfuric acid dilute up to 1 L H₂O.

3. Methods

3.1 V genes amplification from peripheral blood lymphocytes

A library with the maximum antibody diversity could be generated by amplifying naturally rearranged V genes. There are two requirements: the availability of peripheral blood lymphocytes (PBLs) from several non-immunized donors and a set of PCR primers able to amplify all known VH, Vk, and Vλ gene sequences (9, 21).

1. Samples of human PBLs are purified by density gradient centrifugation on Ficoll Paque PLUS and are used as starting material (see Note 3).
2. Total RNA is prepared by using a commercial kit. The quality of the RNA preparation must be checked on an appropriate gel.
3. cDNA is synthesized using Reverse Transcriptase and random hexamer primers starting with 1 μg of total RNA in a final volume of 20 μL following instructions provided.
4. VH genes are amplified by PCRs and a reaction should be carried out for each individual VH-Back primer (as described in (9)) in order to amplify even rarely occurring VH genes. VH back primers are paired with an IgM constant-region primer.

Reactions are performed using 1 μL of cDNA as template, with a High-Fidelity DNA Polymerase, in a volume of 50 μl. Cycling parameters are 98°C for 10 sec (denaturation), 65°C for 30 sec (annealing) and 72°C for 30 sec (extension) for 31 cycles. All 50 μL are loaded on a 1.5% agarose gel and purified using a purification kit.

5. Vλ and Vk genes are similarly amplified (using individual VL-back primers with the mix of VL-for primers) from random primed cDNA with the same cycling parameters. All 50 μL are loaded on a 1.5% agarose gel and purified using a purification kit.

6. Pull through PCR of amplified V regions. V regions amplified from cDNA are re-amplified to increase the amount available for cloning as well as to add extra DNA sequences (e.g. restrictions sites) at each end. As the starting template is a PCR fragment this amplification tends to be extremely efficient. VH (and VL) purified genes are pooled equally and re-amplified using external primers (see fig 1B) in 50 μL reaction volume using 5 ng of purified VH (other parameters as above). All 50 μL are loaded on a 1.5% agarose gel and purified.

7. The scFv library is generated by mixing equal amounts (5-50 ng) of VH and VL genes and performing a two-step overlapping PCR, essentially as described in (22): 8 cycles of PCR without primers followed by 25 cycles in the presence of external primers. Cycling parameters are 98°C for 10 sec (denaturation), 60°C for 30 sec (annealing) and 72°C for 30 sec (extension). At least 5 assembly reaction of 50 μl should be set up and product purified on a 1.5% agarose gel.

3.2 Ligation and electroporation of ScFv library

In general, the diversity of a library is limited by the amount of vector/insert used and by the transformation efficiency of bacteria. The largest libraries require hundreds of electroporations to generate the required diversity (see Note 4).

1. Both phagemid cloning vector pDAN5 (12) and purified scFv fragments are sequentially digested, with BssHIII restriction endonuclease for 2 h at 50°C and then with NheI for 4 h at 37°C. Efficient digestion with both enzymes is crucial to avoid self-ligation of the vector. Vector is loaded on an agarose gel and gel purified using a purification kit. scFv inserts are purified using clean up kit.
2. Ligation reaction is prepared as follow: double-digested and purified vector 2–5 µg, double digested and purified scFv 1-2.5 µg (phagemid:insert molar ratio of 1:3); T4 DNA ligase; 1X DNA ligase buffer. Incubate reactions at 2 h at 22°C and then at 16°C overnight (see Note 5).
3. Clean up and concentrate ligation using a commercial kit.
4. Elute the DNA in ultrapure H₂O.
5. The ligation mix is electroporated into Electrocompetent Cells. The number of total electroporation should be determined calculating the number of transformants obtained with a single electroporation. (see Note 6).
6. Transformations are pooled and plated on 2xTYAG 15 cm plates and grow O/N at 25-28°C to obtain a primary library. Make dilutions to estimate library diversity.
7. The next day colonies are scraped up in 2xTY 20% glycerol and frozen down in 1 mL aliquots and some small working aliquots of 100 µL.

3.3 Rescuing phagemid particles from libraries

Growth of phagemid libraries requires the use of helper phage, which provides all the other proteins needed to produce the phage particles. The helper phage has a disabled or weaker packaging signal than that of the phagemid vector and provides all the proteins required for phagemid replication, ssDNA production and packaging. The different clones of the library have very different effects on bacterial growth rates, therefore library amplification should be minimized to prevent bias towards the least toxic clones.

1. The starting culture should contain at least ten times more clones than the original library diversity but should not exceed OD 600_{nm} 0.05. For most rescues, the inoculum is therefore 30-300 µL of the glycerol stock (or concentrated solution of bacteria scraped from plate). The inoculum should be placed in an appropriate volume of 2xTYAG in a sterile flask 5-10 times bigger than the culture volume.
2. Grow with shaking (250 rpm) for 1.5-2.5 h at 37°C, to an OD 600_{nm} of 0.5. Check the OD regularly so not to overgrow the cells (once reached this OD, cells are into the mid-log phase and they express the F-pilus for infection) (see Note 7).
3. When an OD 600_{nm} of 0.5 is reached, add a 20-fold excess of helper phage (consider culture concentration as 5x10⁸ cells/mL). Leave at 37°C for 45 min, standing with occasional shaking.
4. Spin the cells for 15 min at 4,000 g. When bacteria need to be kept vital, they should be spun no greater than 4,000 g. When they are to be removed to collect supernatant, higher g forces can be used.
5. Discard the supernatant.
6. Dissolve the bacterial pellet in a volume 5 times greater than the initial culture volume of 2xTYAK. Grow shaking (250 rpm) overnight at 28°C, using enough flasks to ensure that the flask volume is 5 times greater than the culture volume.
7. The following day bacteria are centrifuged at 7,000-10,000 rpm for 25 min at 4° C. The supernatant, containing phages, is collected and subjected to PEG precipitation.

3.4 PEG precipitation of phagemid particles

The concentration of phage or phagemid particles in the supernatant of culture medium is usually 10^{11-12} per mL. It is often useful to remove bacterial debris and concentrate phages. This is best done by PEG precipitation. The addition of polyethylene glycol (average molecular weight 6000) to a final concentration of 1-4% (w/v) results in the precipitation of essentially all phage particles. Particles are dissolved in PBS and re-centrifuged to remove bacteria, prior to a second PEG precipitation and filter sterilization, if desired.

1. Add 1/5 volume of PEG/NaCl solution to the cleared supernatant (e.g. 20 mL to 80 mL), mix well and leave for 30-60 min on ice. Successful precipitation can usually be seen after few minutes as haziness.
2. Spin down at 4500 g for 15 min at 4°C; discard supernatant. The pellet should be white. If it is brown, this is usually due to contamination with bacteria, and the PEG precipitation should be repeated.
3. Dissolve phage pellet in 1/10 original volume with PBS.
4. Spin in microcentrifuge (10 min, max speed) to remove the remaining bacteria, a small brown pellet could be visible. Transfer supernatant to a new tube.
5. Steps 1-4 can be repeated for added purity (double PEG precipitation), and especially if the first PEG precipitate is brown, and should always be done for prolonged storage of phage preparations. In this case add 1/5 PEG solution to the supernatant; leave on ice for 10-20 minutes; haziness should be seen immediately. Spin phage down (5 min, max speed), remove supernatant carefully and dissolve the pellet in PBS 1/50 of the original volume with a 1 mL filter-tip. Remove bacteria again by spinning (2 min, max speed).
6. The phages are now ready for selection. The standard titer after double precipitation should be about $2-10 \times 10^{13}$ phages/mL. Although phages can be stored at 4°C without much loss of titer the displayed antibodies will proteolytically be removed by contaminating proteases, so they should be used within few days (see Note 8).

3.5 Phage titration into *E. coli*

Phagemid concentration should be titrated both before the selection as well as after (i.e. eluted phages). *E. coli* expressing F-pili are infected by phagemid and after appropriate dilution plated into 2xTY agar plates with the appropriate antibiotic. Only those cells which have been infected, thus acquiring the antibiotic resistance, will form colonies after O/N growth.

1. Make serial 10- to 100-fold dilutions of the phagemid solution in 2xTY medium to final volume of 1 mL; (i.e. 10 μ L into 990 μ L (10^{-2}); 10 μ L of this into 990 μ L (10^{-4}) etc). For accurate titrations make 10-fold rather than 100-fold dilutions steps around the relevant dilutions. Use new sterile tips for pipetting each titration step, otherwise the titration is inaccurate. For phagemid stocks after PEG precipitation (10^{12-13} phages/mL) go down to 10^{10} ; for phagemid eluates (10^{6-8} phages/mL at round 1-2 of selections) go down to 10^6 .
2. Add 10 μ L of the diluted phages to 1 mL of exponentially growing *E. coli* (OD_{600nm}=0.5). Incubate without shaking at 37°C for 45 min.
3. Plate 100 μ L of each dilution onto 2xTYAG plates and incubate O/N at 28°C.
4. As a control, uninfected *E. coli* should be plated and grown on a separate plate with ampicillin. Colonies grown on this plate indicate a possible contamination, indicating inadequate sterile techniques.

5. Next day, count the number of colonies and calculate the phage titer. Titer is expressed as number of phages/ μL .

3.6 Selection of phage antibodies to an antigen immobilized on plastic surfaces

While many different plastic surfaces are suitable for selections, Immuno MaxiSorp Tubes have become the standard. They have a high capacity (600 ng/cm^2) and have yielded many specific antibodies from several different antibody libraries. Surfaces can be coated with antigen in a variety of ways, the most common is direct adsorption to a plastic surface where it is non-covalently associated via electrostatic and van-der-Waals interactions. Usually antigen is coated at $1\text{-}10 \text{ }\mu\text{g/mL}$ and conditions which work for ELISA are likely to work for selection. Non-fat powdered milk is the standard blocking reagent. Tween 20 $0.1\text{-}0.5\%$ can also be added to all incubation to reduce non-specific or polyreactive binders. After antigen coating the phagemid library is incubated in direct contact with plastic surface. Washes are then performed and in principle non-binding phages are washed away while specific phages will be retained and later rescued by infection. In practice, this cannot be carried out in a single cycle, but requires several rounds of binding, washing, elution and amplification. In general, two to four cycles are usually required.

1. Add 1 mL antigen, (usually concentrated $10 \text{ }\mu\text{g/mL}$) to a 75 mm x 12 mm Immuno Tube. Leave O/N at 4°C (or 1 h at 37°C). Next day, wash 3x with PBS (simply pour solution in and pour out again immediately).
2. Block the immunotube by adding 2% MPBS to the rim. Seal the tube with parafilm and leave for 30 min-2 h at room temperature. Meanwhile, preblock PEG-concentrated phage ($1\text{-}5 \times 10^{12}$ phages) in a final volume of 1 mL with 2% MPBS (see Note 9).
3. Wash the immunotube 2x with PBS-Tween-20 and 2x with PBS and transfer phage-mix (step 2) to immunotube and cover tube with parafilm. Incubate for 30 min on a rotator and then for 1.5 h standing at room temperature.
4. Wash tubes 10 times with PBS-Tween-20, then 10 times with PBS (see Note 10). Each washing step is performed by pouring buffer in and out immediately (see Note 11).
5. Elute phages from tube by adding 1 mL 100 mM triethylamine. Cover tube with fresh parafilm (this prevents cross contamination) and rotate the tube for 10 min on an under and over turntable. Do not increase elution time as phage viability decreases.
6. Transfer the solution into an Eppendorf tube with 0.5 mL of 1.0 M Tris-HCl, pH 7.4 and mix by inversion. It is necessary to neutralize the phage eluate immediately after elution.
7. Transfer phage mix into ice or store at 4°C .
8. Titrate the phage in DH5 α F' cells to determine the output.
9. Re-infect the selected phages in DH5 α F' cells and harvest phages (see 3.3).
10. Start a new round of selection.
11. An alternative method to elute selected phages from the immunotube includes adding 1 mL of bacteria at OD 600_{nm} 0.5 (see Note 12) and leave the tube at 37°C for 30 to 45 min with occasional shaking. In this case bacteria are plated directly on 2 cm x 15 cm 2xTY agar plates added with ampicillin and incubated O/N at 28°C .

3.7 Selection of phage antibodies using biotinylated antigen and streptavidin-paramagnetic beads

An alternative to select antibodies bound to plastic plates is to select the antibodies in solution. This solves problems related to antigens that change conformation when directly

coated onto solid surfaces. Furthermore, affinity selections are more straightforward with this method allowing a precise control of the interaction between the phage particle and the antigen that takes place in solution. The antigen is labeled by biotinylation (using kits which are sold by many companies) and incubated with the phage antibody library, after both have been appropriately blocked. Once interaction between the two has occurred the complex can be retrieved by using magnetic beads coated with streptavidin. Specificity is achieved by washing the beads several times. Phages are eluted from the beads with either acid or alkaline solution.

1. Phage preparation (corresponding to 10^{12} phages) is saturated to a final concentration of 2% MPBS in 500 μ L volume. 100 μ L of streptavidin-magnetic beads are added to select streptavidin binding phage. Solution is equilibrated on rotator at room temperature for 60 min.
2. Remove the streptavidin binding phage by drawing the beads to one side using a magnet and remove the supernatant.
3. Add biotinylated antigen (100-500 nM) to the equilibrated phage mix.
4. Incubate on rotator at room temperature for 30 min-1 h.
5. While incubating the phage wash 100-200 μ L streptavidin-magnetic beads with PBS and resuspend in 2% MPBS on rotator at room temperature for 30 min – 1 h.
6. Draw equilibrated beads to one side with magnet, remove buffer and resuspend beads with phage-antigen mix and incubate on rotator at room temperature for 15 min (see Note 13).
7. Place tubes in magnetic rack and wait until all beads are bound to the magnetic site (30 sec). Wash the beads from the cap by tipping the rack upside down and back again.
8. Leave tubes in the rack for 1-2 min then aspirate the supernatant carefully, leaving the beads on the side of the tube.
9. Wash the beads carefully 6 times with 0.75 mL PBS-Tween-20.
10. Wash the beads 4 times with 0.75 mL PBS.
11. Elute phage from beads with 500 μ L 100 mM TEA for 10 min maximum.
12. Transfer the solution to an Eppendorf tube containing 250 μ L Tris-HCl, pH 7.4 and mix by inversion. It is necessary to neutralize the phage eluate immediately after elution.
13. Use an aliquot of the selected phages to re-infect in DH5 α F' cells for another round of selection, repeating all steps above.
14. Store the remaining beads or eluate at 4°C as a backup.
15. Bound phages could be eluted by mixing the beads with 1 mL of *E. coli* DH5 α F', at OD_{600nm} 0.5, at 37° C, for 45 min, with occasional shaking (see Note 12). In this case bacteria are plated on 2x15 cm 2XTY agar plates added with ampicillin and grown O/N at 28° C.

3.8 Library amplification after selection.

1. In the case of Immuno Tube selection mix 5 mL of DH5 α F' cell with 0.5 mL of phage eluate (see Note 14) in a 50 mL tube. The eluate must be diluted at least 10-fold (for toxicity reasons) if TEA has been used for elution.
2. For soluble biotinylated antigen selections mix 1 mL of *E. coli* with 100-200 μ L of phage eluate (see Note 14).

3. Incubate at 37°C for 30 min with occasional shaking.
4. Plate out samples on 2x15 cm 2xTYAG plates. For later rounds of selection, one plate is sufficient, as diversity is reduced.
5. Grow the plates O/N at 28°C. Growth at higher temperatures may lead to loss of some antibody clones.
6. After overnight growth add 2 mL into 2x15 cm plates and scrape the bacteria off using a sterile spreader.
7. Transfer the cells into a tube and make a homogeneous suspension by pipetting up and down with a sterile pipette.
8. Add sterile glycerol to 20% final concentration and immediately store at -80 °C samples into a Cryotube in at least three aliquots.
9. Rescue phages from library according to protocol 3.3

3.9 Growing phage clones in microtiter plates for ELISA testing

After two or three rounds of selection, individual colonies from the selection are tested for antigen binding by ELISA. A microtiter-well system can be used for individual phage preparation. The principle involving growth, helper phage infection, and phage production is the same as that for the library, but it is applied to single clones in the 96-well plate format. Care must be taken to prevent cross-contamination between wells; both growth and ELISA controls should be included on the master plates.

1. Put 100 µL of 2xTYAG into each well of a round-bottomed 96-well plate. Inoculate a single colony in each well by touching the top of a colony with an autoclaved toothpick or sterile plastic tip. Grow with shaking (250 rpm) overnight at 30°C (see Note 15). There is no need for specific holder designed for microtiter plates, this could be inserted within a plastic box cushioned with foam, tightly taped and placed as far as possible from the ventilator to avoid evaporation (see Note 16).
2. Next day, use a 96-well sterile transfer device or pipet to inoculate 2 µL per well from this plate to a round-bottomed 96-well containing 120 µL 2xTYAG per well. Grow to OD_{600nm} 0.5 (around 2.5 hours), at 37 °C, shaking.
3. To each well add 50 µL 2xTYAG containing 1x10⁹ pfu helper phage. The ratio of phage to bacterium should be about 20:1. Stand 45 min at 37°C.
4. After the incubation, spin at 1,700 rpm (faster will crack the plates) for 20 min; then remove the supernatant with a multichannel pipette or suction device.
5. Resuspend the bacterial pellet in 120 µL 2xTYAK. Glucose is omitted in this step. Grow overnight 28°C, shaking.
6. Next day, spin at 1,700 rpm for 10 min and use 50 µL supernatant per well for phage ELISA.

3.10 Phage ELISA

1. Coat plate with 100 µL per well of protein antigen used for selections. Coating antigen is usually prepared in PBS (occasionally in carbonate buffer). Leave O/N at 4°C or at 37°C for 2 h. This is dependent upon the specific antigen and should be tested if possible (see Note 17).

2. Discard the antigen solution, rinse wells twice with PBS and block with 120 μL per well of 2% MPBS, for at least 45 min at room temperature.
3. Wash wells twice with PBS.
4. Add 50 μL 4% MPBS and 50 μL culture supernatant containing the phage antibodies to the appropriate wells, mix carefully. Leave approximately 1.5 h at room temperature with mild shaking.
5. Discard solution, wash out wells 3x with PBS-Tween-20 and 3x with PBS.
6. Add 100 μL diluted HRP-conjugated mouse anti-phage mAb. Use the dilution indicated by the manufacturer. Incubate for 1 h at room temperature.
7. Discard solution and wash wells 3x with PBS-Tween-20 and 3x with PBS.
8. Dispense 100 μL TMB solution per well, leave at room temperature in the dark for 5 to 20 min (sometimes longer).
9. Quench by adding 42 μL stop solution 2 N H_2SO_4 .
10. Read at 450 nm.

3.11 Growing soluble fragments in microtiter plates

An alternative to using phagemids for ELISAs is to use antibody soluble fragments. The phagemid vector usually carries an amber stop codon between the gene coding for the scFv and the genIII, therefore the gene coding for the scFv fragment is transcribed and soluble fragments are produced. The antibody leaks into the supernatant that could be directly used as primary antibody source.

1. Put 100 μL of 2xTYAG into each well of a 96-well round-bottomed plate. Inoculate a single colony in each well by touching the top of a colony with an autoclaved toothpick or sterile plastic tip. Grow with shaking (250 rpm) overnight at 30°C (see Note 15). There is no need for specific holder designed for microtiter plates, this could be inserted within a plastic box cushioned with foam, tightly taped and placed as far as possible from the ventilator to avoid evaporation (see Note 16).
2. Next day, use a 96-well sterile transfer device or pipette to inoculate 2 μL per well from this plate to a 96-well round-bottomed plate containing 100 μL 2xTYA, 0.1% glucose per well. Grow at 37°C, shaking, until OD 600_{nm} is approximately 0.6 (about 2-3 h).
3. Add 50 μL 2xTYA, 1.5 mM IPTG (final concentration 0.5 mM IPTG). Continue shaking at 25-28°C O/N.
4. Next day, spin at 1,700 rpm for 10 min and use 50 μL supernatant in ELISA.

3.12 Soluble fragment ELISA in microtiter plates

Soluble scFv can be tested for antigen binding activity on ELISA plates coated directly with antigens. Detection is done by a sandwich assay involving anti-tag antibody and a secondary enzyme-conjugated antibody.

1. Coat plate with 100 μL per well of protein antigen used for selections. Coating antigen is prepared in PBS (occasionally in carbonate buffer). Leave overnight at 4°C or at 37°C for 1 h. This is dependent upon the particular antigen and it should be tested if possible.
2. Discard the antigen solution and rinse wells twice with PBS and block with 120 μL per well of 2% MPBS, for at least 45 min at room temperature.

3. Wash wells twice with PBS.
4. Add 50 μ L 4% MPBS to all wells and then add 50 μ L culture supernatant containing soluble antibody fragment to the appropriate wells. Leave 1.5 h at room temperature with mild shaking.
5. Discard solution, wash out wells 3x with PBS-Tween-20 and 3x with PBS.
6. Pipette 100 μ L of anti-tag antibody, at the appropriate dilution, in 2% MPBS into each well. Incubate at room temperature for 1 h.
7. Discard antibody, wash out wells with 3x with PBS-Tween-20 and 3x with PBS.
8. Add 100 μ L of diluted anti-mouse-HRP (horseradish peroxidase), or anti-mouse-AP (alkaline phosphatase), labeled secondary antibody to each well. Incubate for 1 h at room temperature.
9. Discard 2nd antibody, and wash wells 3x with PBS-Tween-20 and 3x with PBS.
10. To develop with TMB: dispense 100 μ L TMB solution per well, leave at room temperature in the dark for 10-30 min (sometimes longer). Quench by adding 42 μ L stop solution 2 N H_2SO_4 .
11. Read at 450 nm.

3.13 PCR amplification and fingerprinting of selected clones

After positive clones have been identified, it is important to determine how many different antibodies have been selected.

A simple and fast method involves the use of PCR to amplify the scFv regions and then to digest the DNA samples with a frequently cutting restriction enzyme, such as BstNI or HaeIII. The digested DNA fragments are separated on an agarose gel and the various clones are characterized by their own DNA fragment patterns.

1. Make up a PCR-Mastermix with 20 μ L per clone. Use forward and back primers mapping external to the 5' and 3' end of the scFv insert.
2. Aliquot 20 μ L of the Mastermix into 0.5 mL tubes, or into 96-well PCR microplates.
3. Add 0.5-1 μ L of culture taken from the master plate into PCR reaction (excess bacteria in the PCR reaction can cause inhibition)
4. Heat to 95°C for 10 min using the PCR-block. This is needed to break open the bacteria and release the template DNA. Perform 30 cycles of denaturation, annealing and elongation steps using the temperature and incubation times indicated on the DNA Taq Polymerase datasheet (see Note 18).
5. Check 2 μ L of the PCR reaction on a 1.5% agarose-gel. This will indicate how many clones lack the insert.
6. Make up a fingerprinting-Mastermix and add 15 μ L to each PCR tube.

Mastermix is as follow: BstNI buffer (10x) 3 μ L, Water 11.6 μ L, BstNI (10U/ \square L) 0.2 \square L.

7. Digest samples at 60°C for 2-3 h.
8. Load on a 3% agarose gel, run and compare the banding patterns of individual clones on a UV transilluminator.

4. Notes

1. Electroporation of pure DNA strongly increase transformation efficiency: we recommend to clean and concentrate the ligation mixture using the DNA Clean & Concentrator™-5 kit from Zymo Research. This kit allows to purify and concentrate up to 5 ug of ligation mixture in a final volume of 6 ul of water.
2. Electrocompetent cells can be produced in-house or purchased from several manufacturers. The use of high-efficiency cells (above 5×10^9 transformants per μg of DNA) is recommended to obtain high number of transformants. To generate large libraries we suggest the use of TG1 Electrocompetent Cells from Lucigen (above 10^{10} transformants per μg of DNA), following the instructions of the manufacturer.
3. Blood samples should be processed as soon as these are taken from the donor. Prolonged storage on ice or at 4°C results in the isolation of degraded RNA.
4. Large libraries are constructed by maximizing the efficiency of all reactions and protocols. Small decrease in the performances of protocols at any of these steps will easily lead to the production of libraries 10- to 100-fold smaller than expected. Optimized steps must include RNA extraction, PCR amplification, restriction enzymes digestion, ligation, and purification. For an efficient ligation, DNA fragments and vector must be fully cut, with no or little degradation; most of the vectors are re-ligated after a partial cutting.
5. The ligation should be done using high-concentration T4 DNA ligase enzyme O/N. Overnight ligations give best results compared with few hours at room temperature. Cleanup of the large-scale ligation and resuspension in water is essential, as high concentration of DNA is required without presence of any salts in solution, since the presence of contaminants lead to a dramatic decrease in the electroporation transformation efficiency.
6. To obtain high transformation efficiency, work as quickly as possible throughout the whole protocol, cells must be kept in a cold environment.
7. During the infection of F' bacteria with phagemid, it is important to ensure that the bacteria are expressing the pilus. At the time of infection, bacteria should be in log-phase growth, with an $\text{OD}_{600\text{nm}}$ around 0.5. This value could not be simply obtained by diluting bacteria grown to saturation (i.e. $\text{OD}_{600\text{nm}}$ 2.0). Bacteria should always be kept at 37°C before infection, as the pilus is lost after 2-3 min at room temperature. It is therefore strongly suggested to prepare in advance all reagents before removing the bacteria from the shaker, and to perform all steps quickly, without allowing the temperature to decrease.
8. For selection steps, it is strongly suggested to use freshly prepared phages, and to store them at 4°C for no longer than one day. Alternatively, phages could be purified by CsCl gradient centrifugation: in this case they are stable for years if stored at -80°C .
9. This blocking step is suggested to reduce background binding and should be performed in all selection rounds.
10. Sometimes, antigen 'stickiness' is a problem, in which case polyreactive clones may be selected from the repertoire. In that case inclusion of Tween-20 (0.05-0.1%) in all incubation steps (in selection itself, in all washes and blocking steps) may help to remove these binders, reduce the background, and favor the specific ones.
11. According to most experimental protocols, the stringency of the washing steps should increase with the selection rounds. We use the following procedure: tubes are washed 15 times with PBS-Tween-20 (0.05-0.1%) and 15 times with PBS, to remove unbound phages, for the first round of selection. For the second round, 10 washes with PBS-Tween-20 (0.05-0.1%) are followed by 10 min washing in rotation with PBS, followed by 10 more PBS washes.

12. It is important that bacterial culture has the correct OD_{600nm} for the elution step at the end of the selection. It is therefore necessary to start bacterial growth early enough so that at the end of the experiment (about 3 hours) bacteria are in log-phase growth with an OD_{600nm} in the 0.3- 0.6 range. It is suggested to grow bacteria in several tubes (only 1 mL is required for a single elution) inoculating different starting amounts of bacteria, and choose the tube with the OD_{600nm} closest to 0.5 for the final elution step.
13. Incubation with slow and constant rotation is required, since the beads quickly form deposits on the bottom of the tube.
14. It is advisable to use no more than half of the selected phages for amplification, since in the event of an error, one can always return and repeat the amplification.
15. This plate will be the “master plate” with the primary selected clones that are not infected by helper phage. Care should be taken to avoid contamination or mislabeling of the plate.
16. Growth conditions in microtiter plates (speed, temperature and position of the plate in the incubator) should be tested during the first time growth.
17. The antigen can be recovered after coating for further use if needed. In this case overnight incubation at 4°C is recommended.
18. The PCR reactions performed on the positive selected clones have the purpose to check the full-length of the scFv. Therefore, a High-Fidelity DNA Taq Polymerase is not required and whatever Polymerase can be used.

5. References

1. Marks, J. D., Hoogenboom, H. R., Bonnert, T. P., McCafferty, J., Griffiths, A. D., and Winter, G. (1991) By-passing immunization. Human antibodies from V-gene libraries displayed on phage. *J Mol Biol.* **222**, 581–597
2. Scott, J. K., and Smith, G. P. (1990) Searching for peptide ligands with an epitope library. *Science (80-).* **249**, 386–390
3. Boder, E. T., Midelfort, K. S., and Wittrup, K. D. (2000) Directed evolution of antibody fragments with monovalent femtomolar antigen-binding affinity. *Proc. Natl. Acad. Sci. U.S.A.* **97**, 10701–10705
4. Boder, E. T., and Wittrup, K. D. (1997) Yeast surface display for screening combinatorial polypeptide libraries. *Nat. Biotechnol.* **15**, 553–557
5. Smith, G. P. (1985) Filamentous fusion phage: novel expression vectors that display cloned antigens on the virion surface. *Science (80-).* **228**, 1315–1317
6. Bradbury, A., Velappan, N., Verzillo, V., Ovecka, M., Chasteen, L., Sblattero, D., Marzari, R., Lou, J., Siegel, R., and Pavlik, P. (2003) Antibodies in proteomics I: generating antibodies. *Trends Biotechnol.* **21**, 275–281
7. McCafferty, J., Griffiths, A. D., Winter, G., and Chiswell, D. J. (1990) Phage antibodies: filamentous phage displaying antibody variable domains. *Nature.* **348**, 552–554
8. Hoogenboom, H. R., Griffiths, A. D., Johnson, K. S., Chiswell, D. J., Hudson, P., and Winter, G. (1991) Multi-subunit proteins on the surface of filamentous phage: methodologies for displaying antibody (Fab) heavy and light chains. *Nucleic Acids Res.* **19**, 4133–4137
9. Sblattero, D., and Bradbury, A. (1998) A definitive set of oligonucleotide primers for amplifying human V regions. *Immunotechnology.* **3**, 271–278
10. Marks, J. D., Griffiths, A. D., Malmqvist, M., Clackson, T., Bye, J. M., and Winter, G. (1992) By-passing immunization: building high affinity human antibodies by chain shuffling. *BioTechnology.* **10**, 779–783
11. Vaughan, T. J., Williams, A. J., Pritchard, K., Osbourn, J. K., Pope, A. R., Earnshaw, J. C., McCafferty, J., Hodits, R. A., Wilton, J., and Johnson, K. S. (1996) Human antibodies with sub-nanomolar affinities isolated from a large non-immunized phage display library [see comments]. *Nat Biotechnol.* **14**, 309–314
12. Sblattero, D., and Bradbury, A. (2000) Exploiting recombination in single bacteria to make large phage antibody libraries. *Nat Biotechnol.* **18**, 75–80.
13. Hoogenboom, H. R., and Winter, G. (1992) By-passing immunisation. Human antibodies from synthetic

- repertoires of germline VH gene segments rearranged in vitro. *J Mol Biol.* **227**, 381–388
14. Prassler, J., Thiel, S., Pracht, C., Polzer, A., Peters, S., Bauer, M., Nörenberg, S., Stark, Y., Kölln, J., Popp, A., Urlinger, S., and Enzelberger, M. (2011) HuCAL PLATINUM, a Synthetic Fab Library Optimized for Sequence Diversity and Superior Performance in Mammalian Expression Systems. *J. Mol. Biol.* **413**, 261–278
 15. Weber, M., Bujak, E., Putelli, A., Villa, A., Matasci, M., Gualandi, L., Hemmerle, T., Wulhfard, S., and Neri, D. (2014) A highly functional synthetic phage display library containing over 40 billion human antibody clones. *PLoS One.* 10.1371/journal.pone.0100000
 16. Krebs, B., Rauchenberger, R., Reiffert, S., Rothe, C., Tesar, M., Thomassen, E., Cao, M., Dreier, T., Fischer, D., Hoss, A., Inge, L., Knappik, A., Marget, M., Pack, P., Meng, X. Q., Schier, R., Sohlmann, P., Winter, J., Wolle, J., and Kretzschmar, T. (2001) High-throughput generation and engineering of recombinant human antibodies. *J Immunol Methods.* **254**, 67–84.
 17. Fellouse, F. A., Esaki, K., Birtalan, S., Raptis, D., Cancasci, V. J., Koide, A., Jhurani, P., Vasser, M., Wiesmann, C., Kossiakoff, A. A., Koide, S., and Sidhu, S. S. (2007) High-throughput generation of synthetic antibodies from highly functional minimalist phage-displayed libraries. *J Mol Biol.* **373**, 924–940
 18. Rouet, R., Jackson, K. J. L., Langley, D. B., and Christ, D. (2018) Next-generation sequencing of antibody display repertoires. *Front. Immunol.* 10.3389/fimmu.2018.00118
 19. Bradbury, A., Velappan, N., Verzillo, V., Ovecka, M., Chasteen, L., Sblattero, D., Marzari, R., Lou, J., Siegel, R., and Pavlik, P. (2003) Antibodies in proteomics II: screening, high-throughput characterization and downstream applications. *Trends Biotechnol.* **21**, 312–317
 20. Di Niro, R., Sulic, A. M., Mignone, F., D'Angelo, S., Bordoni, R., Iacono, M., Marzari, R., Gaiotto, T., Lavric, M., Bradbury, A. R., Biancone, L., Zevin-Sonkin, D., De Bellis, G., Santoro, C., and Sblattero, D. (2010) Rapid interactome profiling by massive sequencing. *Nucleic Acids Res.* **38**, e110
 21. Lim, T. S., Mollova, S., Rubelt, F., Sievert, V., Dubel, S., Lehrach, H., and Konthur, Z. (2010) V-gene amplification revisited - An optimised procedure for amplification of rearranged human antibody genes of different isotypes. *N Biotechnol.* **27**, 108–117
 22. Krebber, A., Bornhauser, S., Burmester, J., Honegger, A., Willuda, J., H.R., B., and Pluckthun, A. (1997) Reliable cloning of functional antibody variable domains from hybridomas and spleen cell repertoires employing a reengineered phage display system. *J. Immunol. Methods.* **201**, 35–55

FIGURES

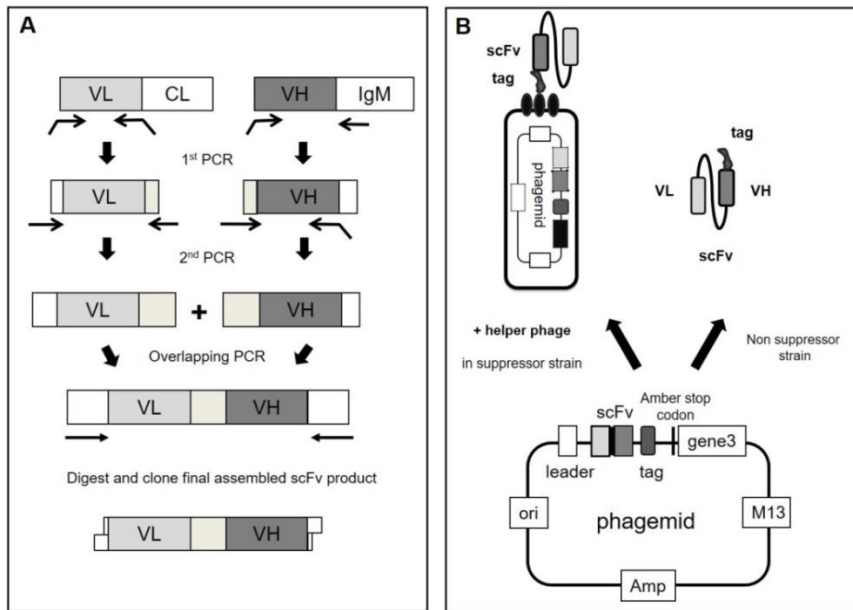


FIG. 1 A) PCR assembly of V genes into a scFv format. B) Schematic of a phagemid display vector with phage or soluble scFv production scheme.

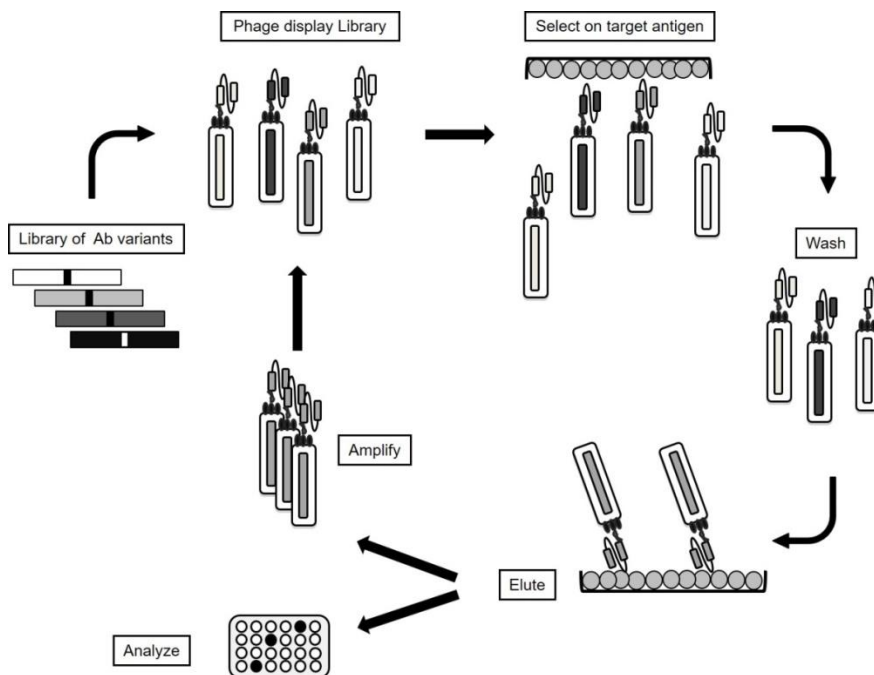


FIG. 2 Phage display selection cycle. Up to five rounds of selection over a specific target are performed; in each round, unreactive clones are removed, and reactive clones are amplified. Positive clones are successively isolated and identified by DNA sequencing.

4.6. Protein Microarray

Protein arrays provide a powerful tool to examine interactions between proteins (including antibodies), peptides, DNA/RNA or chemical compounds on a large scale. Protein arrays contain between 500 up to a million different proteins immobilized in an orderly manner to a solid surface (40). In the field of oncology, protein arrays are potent tools for the identification of cancer biomarkers, in particular auto-antibody/antigen markers. The identification of tumor associated antigens (TAAs) recognized by patient's serum antibodies represents an exciting approach to identify novel diagnostic cancer biomarkers and to contribute towards a better understanding of the pathogenetic mechanisms.

There are three general types of protein array (Fig 3):

- i) Functional protein microarrays, constructed by immobilizing large sets of purified proteins or an entire proteome are screened for a wide range of biochemical functions, such as protein-protein, protein-DNA, protein-small molecule interactions and enzyme activity, and to detect antibodies and demonstrate their specificity. It comprises protein/peptide/antigen microarrays.
- ii) Analytical microarray, where primarily antibodies, antibody mimics, affinity reagents, but may also be nucleic acid aptamers arrayed and used to evaluate the presence and concentrations of proteins in a complex mixture such as plasma/serum or tissue extracts. It comprises antibody microarrays.
- iii) Reverse-phase microarrays employ the complex samples such as tissue lysates are printed on the surface (the bait) to capture antibodies (the prey). In the case of lysates from cancer tissue or cell lines as source of the bait, proteins require liquid phase fractionation, incorporating isoelectric focusing and reverse-phase liquid chromatography (LC), prior to printing onto an array support. It comprises lysate microarrays.

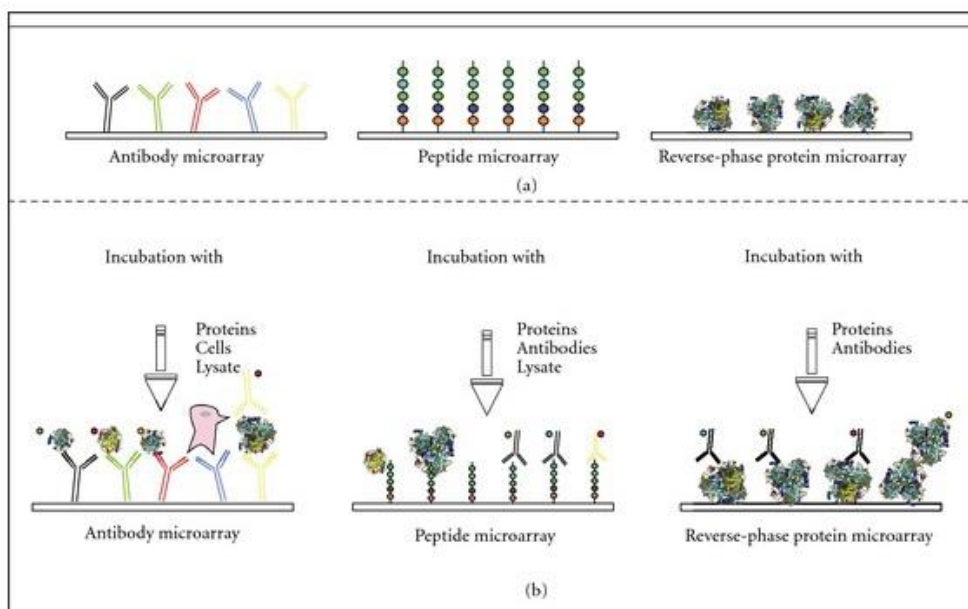


Fig.3. Different types of microarray. (A) Three types of microarray coating, namely antibody, peptide or protein coating. (B) Second step of microarray where studies interactors are added: proteins, cells or lysate for antibody microarray; proteins, antibodies or lysate for peptide microarray; and proteins or antibodies for protein microarray (41).

5. Monoclonal antibody therapy

5.1. Monoclonal antibodies (mAbs) mechanism of action

Monoclonal antibodies (mAb) immunotherapy in cancer has been studied for more than a decade, however it shows mixed results. Some mAb can induce tumor cell killing directly by influencing tumor cell signaling, while others trigger opsonization of tumor cells by complement activation (42).

Monoclonal antibodies can regulate cancer grow by three mechanism of action. It can decrease cancer proliferation by activation of signaling pathway that stop or reduce cancer grow. Other monoclonal antibodies can prevent binding of cancer-grow molecules with their receptors and, therefore, decreasing cancer cell proliferation. For example, antibodies that target vascular endothelial growth factor (VEGF) inhibit it binding to specific receptor. Other mechanism of action is targeting immune cells by monoclonal antibodies. They can block for example CTL-4 antigen, which role is to inhibit immune effector cells, and this way increase adaptive immune response to cancer cells. Bispecific mAbs is other strategy to use antibodies that enhance immune effector cells. It recognizes tumor cells and immune effector cells and provokes immune recognition of the cancer. Monoclonal antibodies can activate antibody-dependent cell-mediated cytotoxicity (ADCC) by natural killer (NK) cells or complement dependent cytotoxicity (16).

5.2. Complement dependent cytotoxicity

The complement system is a fundamental part of innate immunity as a reaction to infection present in organism and removal of apoptotic cells. In this process antibody–antigen complex activates a cascade of proteolytic enzymes that ultimately results in the formation of a terminal lytic complex that is inserted into a cell membrane, resulting in lysis and cell death (43). Cancer cells that strongly differ from normal cells can trigger complement system activation. Complement system contains over 30 proteins synthesized by liver or different cell types, like macrophages, fibroblasts and endothelial cells circulating in blood plasma and present in it inactive form. Once foreign or damaged material is detected in the body, protease receives a signal and release cytokines, which activate cascade of complement proteins.

There exist three CDC activation pathways. Classical complement pathway is activated due to the antigen—antibody interaction. Alternative pathway can be activated by C3 hydrolysis, foreign material, pathogens, or damaged cells. The mannose-binding lectin pathway can be activated by C3 hydrolysis or antigens and do not require antibody. When antibody (including mAb) bound to an antigen on the cell surface it starts cascade of proteins activation. Firstly complement component C1 recognizes the Fc portion of IgG's and becomes activated, cleaves C4 into C4a and C4b and C2 into C2a and C2b. C4b and C2a together form the C3 convertase (C4b2a), which enzymatically cleaves complement component C3 into C3a and C3b. C3a has a weak anaphylatoxin activity, which trigger degranulation of mast cells and recruit immune effector cells to the site of complement activation. This opsonization stimulates phagocytosis and cytotoxic killing, thereby “complementing” adaptive immunity. C3b is also incorporated into the classical C3 convertase to form C5 convertase (C4b2a3b), which cleaves C5 into C5a and C5b. Similar to C3a, C5a acts as a strong anaphylatoxin and binds immune cells expressing the C5a receptor (C5aR), inducing inflammation and phagocytosis. Like C3b, C5b also gets deposited on the target cell surface. Upon C5b deposition, subsequent complement proteins C6–C9 form the terminal complex, membrane attack complex (MAC). MAC forms a transmembrane channel, which causes osmotic lysis of the target cell, as represented in Fig.4. Finally pathogen is phagocytized by Kupffer cells and other macrophage cell (42), (44).

It has been shown that malignant ascites contain diverse cell populations including tumor cells, mesothelial cells, fibroblasts, macrophages, white blood cells and red blood cells. Studies showed that cellular composition in OC ascitic fluids consist of $\approx 37\%$ lymphocytes, $\approx 29\%$ mesothelial cells, $\approx 32\%$ macrophages and $<0.1\%$ adenocarcinoma cells (45). Different studies have reported the presence of complement-dependent hemolytic activity in OC ascites (46).

These findings suggest that ascites can be appropriate samples to discover and study new OC-related TAAs. Discovering these TAAs would help in better understanding the cancer biology and could supply new targets for personalized treatment.

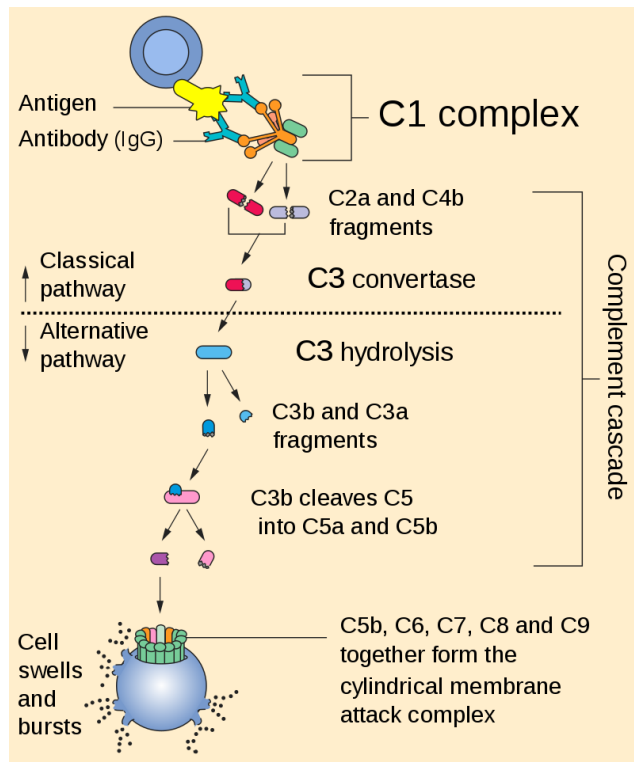


Fig.4. CDC scheme. Complement component C1 recognizes the Fc portion of IgG's and becomes activated, cleaves C4 into C4a and C4b and C2 into C2a and C2b. C4b and C2a together form the C3 convertase, which enzymatically cleaves C3 into C3a and C3b. C3b is incorporated into the classical C3 convertase to form C5 convertase, which cleaves C5 into C5a and C5b. C5b also gets deposited on the target cell surface. Complement proteins C6–C9 form the terminal complex, membrane attack complex (MAC), that forms a transmembrane channel, which causes osmotic lysis of the target cell (47).

5.3. Antibody-dependent cell-mediated cytotoxicity (ADCC)

The antibody-dependent cell-mediated cytotoxicity (ADCC) is a cell-mediated immune defense triggered by the binding of antibodies to cell antigens. ADCC effector cells are the natural killer (NK) cells, macrophages, neutrophils and eosinophils.

Natural killer (NK) cells play an important role in activating immune response as result of monoclonal antibodies cancer immunotherapy. In opposite to B and T cells, NK cells do not undergo somatic gene rearrangements to produce highly specific receptors that recognize target cells. NK cells contain large amounts of cytotoxic granules containing perforin, granzymes and mRNA for $IFN\gamma$ translation. Activation of NK cells is performed through transmembrane activating and inhibitory receptors. When stress-induced ligands bind to receptor, followed by phosphorylation, down-stream kinases are activated, leading to NK cell degranulation and cytokine secretion. Inhibitory receptors recruit phosphatases and deactivate signaling kinases, resulting in NK cell inhibition. NK cell activity is

tightly regulated through the balance between inhibitory and activating signals transduced by these receptors.

Antibody-dependent NK-mediated tumor killing is performed through several different pathways, namely: (1) exocytosis of cytotoxic granules; (2) TNF family death receptors signaling; (3) pro-inflammatory cytokine release, such as IFN γ . Perforin and granzymes uptake by target cells and TNF family death receptor signaling causes target cell apoptosis. IFN γ released by NK cells activate nearby immune cells to promote antigen presentation and adaptive immune responses, as represented in Fig.5. (48).

An important receptor in NK cells activation is Fc γ RIIIA and Fc γ RIIC, which can bind to the Fc portion of monoclonal antibody and send a signals to activate NK cells (42). NK cells also express killer immunoglobulin-like receptors (KIRs). It is a family of receptors which regulate the function and activity of NK cells by interacting with ligands on cancer cells. Mutations and polymorphisms in KIR and Fc γ Rs receptors can control NK cell and be an escape mechanism of cancer (48).

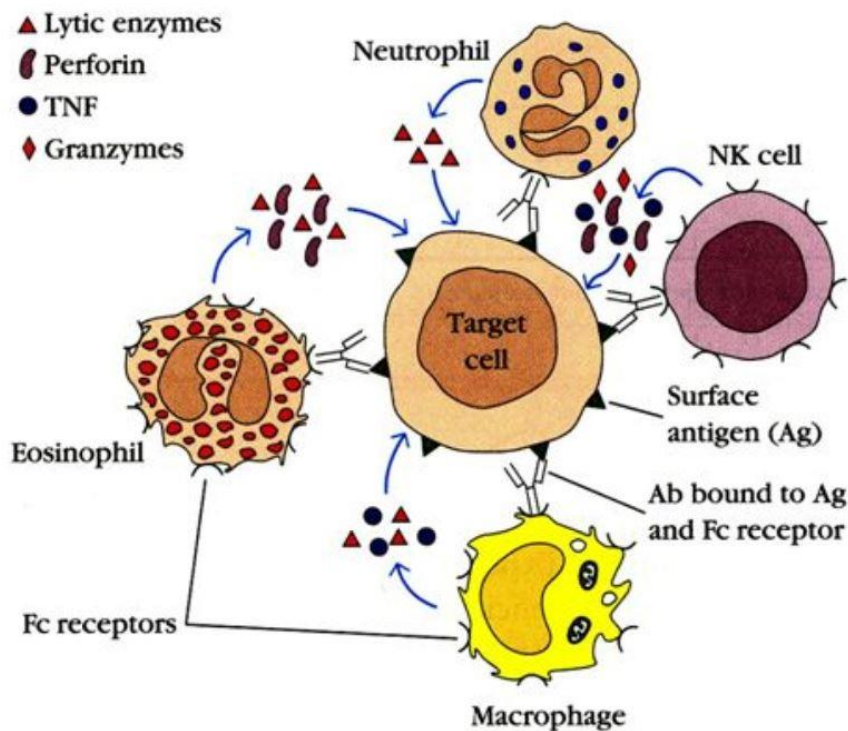


Fig.5. ADCC scheme. Activation of NK cells is performed through transmembrane activating and inhibitory receptors. Activated NK cells lead to degranulation and cytokine secretion. Perforin and granzymes uptake by target cells and TNF family death receptor signaling causes target cell apoptosis. IFN γ released by NK cells activate nearby immune cells to promote antigen presentation and adaptive immune responses. Macrophages, neutrophils and eosinophils can mediate ADCC.

5.4. CDC and ADCC interaction

CDC and ADCC are related processes and can influence each other. The mechanism of mAb activity possibly is depending on the antibody self, and could even differ from patient to patient. Many aspects could influence whether mechanism of action develop direction to CDC or ADCC. Immune complex concentration plays an important role in it. It has been shown that CDC activity and tumor cell lysis directly associated with antigen expression. As more mAb target antigens on the cell surface of cancer cells as stronger activation of CDC will occur (49). In contrary, ADCC activation is not dependent on

antigen expression and might act synergistically with CDC, especially in tumor environments with low antigen expression (50).

It has also been suggested that mechanism of action can depend on tumor situation. For example some studies suggest that CDC is more effective in the vascular system, while ADCC in tissues outside the vascular compartment including the tumor microenvironment. The tumor microenvironment may differ depends on the tumor location and influence sensitivity to mAb therapy.

Nowadays studies indicating that tumor lysis during mAb therapy can lead to cross-presentation of tumor antigens, trigger active anti-tumor immunity, and that complement components might contribute to this process. Several complement fragments improve release of pro-inflammatory mediators, increase lymphocyte activation and as result improve the anti-tumor immune response by recruiting antigen-presenting cells to the tumor microenvironment. These observations conform to the traditional view of complement as pro-inflammatory component and project complement as a positive regulator of anti-tumor immunity (51), (52), (42) .

Chapter 2

6. Project description

6.1. Objectives of the project

Epithelial ovarian cancer (EOC) is the fifth most common cancer in women worldwide. Each year thousands of women are dying from it. Mostly asymptomatic during its development, EOC is diagnosed at late stages when metastasis have grown and treatment is mostly difficult (2). Despite huge efforts to identify novel molecular targets for diagnosis and cure, the treatment of ovarian cancer is still limited to cytoreductive surgery followed by chemotherapy. It's obviously that new therapeutic approaches have to be developed instantly. One of the promising alternative and rational therapeutic approaches is immunotherapy. Nowadays there are more evidences supporting a protective role of the immune system against cancers and clinical success of immunotherapy using monoclonal antibodies (12).

Different studies analyzed ascites of ovarian cancer patients and suggested it to be suitable sample to study ovarian cancer antigens. Ascites are fluids that have direct contact with ovarian cancer showed to contain secretome of ovarian cancer cells and proteins from ovarian cancer cell lysis. Moreover ascites of ovarian cancer patient showed to have a high titer of antibodies and soluble molecules of complement system suggesting that antibodies present in ascites activate local complement dependent cytotoxicity cascade. Circulating antibodies directed against self-antigens are a hallmark of several cancers. The detection of antibody response to tumor-associated antigens (TAA) has already proven its usefulness.

The aim of the project was to profile ovarian cancer antibody repertoire in ascites of ovarian cancer patients in order to identify potential TAAs for diagnostic and therapeutic purposes. To achieve this goal I performed two approaches. Firstly, I screened a human cDNA ORF filtered phage display library with antibodies purified from OC ascites in order to identify tumor specific antigens. In the second approach OC ascites were used to identify TAAs by serological proteome analysis (SERPA). Ascitic fluids were collected from various disease conditions based on the reactivity on ovarian carcinoma cell lines. Candidate antigens were used to correlate antibody levels to clinical outcomes and to evaluate their potential CDC mediated activities. Here, I report the identification of candidate proteins with the potential to drive the development of monoclonal antibodies for cancer immunotherapy.

6.2. Project summary

In the first part of the project, I present a systematic and in-depth profiling of ovarian cancer ascites. For it, I ranked ascitic fluid for its reactivity by characterizing them for their antibody response against cellular antigens in ovarian cancer. To show that ovarian cancer patient ascites have a high titer of antibodies, ovarian cancer cells OVCAR-3 were incubated with these ascites. Antibodies present in ascites bound to cell membrane and were visualized in immunofluorescent staining. As result ovarian cancer ascites showed abundant antibody binding to some proteins present on the cell surface of ovarian cancer cells OVCAR-3. The most reactive ascites were chosen for further investigation. To this extent, I utilized a protein expression platform that combines cDNA phage display library selection and proteins microarray approach. Phage libraries of open reading frame fragments created from

mRNA derived from various tissues were used. Here, cDNAs are expressed as fusion proteins with one of the phage coat proteins and exposed on the surface of the phage thus allowing the selection with antibody present in ascites collected from ovarian cancer patients. Successive rounds of biopanning allowed the patient antibodies to select their own ideal binding peptide and isolation of these less abundant interacting proteins from a library with large diversity. Phage display selected peptides were further screened for their immunoreactivity by protein microarray analysis. Further, microarray identified antigens were validated by indirect ELISA. Subsequently, correlates of autoantibody signatures with known tumor expression of corresponding antigens, prognostic value and patient survival outcome were examined.

In the second part of the project potential ovarian cancer antigens were identified with other approach, using SERPA and MS techniques. To understand which ovarian cancer cell surface proteins trigger so abundant antibody production in patient organisms I performed SERPA analysis using ascites of ovarian cancer patient as antibodies source. Using MS, PDIA1 protein was identified to have the highest antibodies binding. Further, purified from ovarian cancer ascites antibodies were used to perform ELISA assay, where reactivity of antibody pool of ovarian cancer, non-cancerous and other cancer ascites against PDI was analyzed. As result ovarian cancer ascites antibodies showed significant higher binding to PDIA1 protein compare to non-cancerous or other cancer ascites. Accordingly, analyzing overall survival of these patients we identified that patient who were having higher anti-PDIA1 antibodies titer, were having a higher survival rate. Moreover, affinity purified from ovarian cancer ascites anti-PDI antibodies were used in CDC assay and showed to be able to activate complement killing of ovarian cancer cells. Fig. 6 gives a schematic representation of the flow of both approaches applied in this project.

Based on these results I was able to hypothesis that PDIA1 is a potential target for immune system of ovarian cancer patient. Subsequently, the second aim of the project was to develop recombinant anti-PDIA1 antibodies for potential immunotherapy. For it, anti-PDIA1 scFv's were selected using unique antibodies scFv's phage display library, developed by Department of Life Science from University of Trieste. The selecting specificity of this library has already been documented by other studies (53), (54). After selection, reactive to PDIA1 scFv's were tested for it specificity in phage ELISA assay. Once selected scFv's confirmed its specificity, they were cloned into human Fc encoding pcDNA3.1/Hygro(+) vector. Antibody coding vectors were transfected into CHO cells. CHO cell that showed best transfection and antibody production was isolated by monoclonal selection and expanded. CHO cells were growing and secreting antibodies into supernatant. After that, antibodies purified from supernatant were characterized for it reactivity and functionality in different laboratory assays, namely in ELISA, IF, IP, WB, FACS. CDC assay was performed to test antibodies killing capability. Epitope mapping was performed to identify antibodies binding site on PDIA1 protein. Fig.7 represents important steps in the antibody production approach.

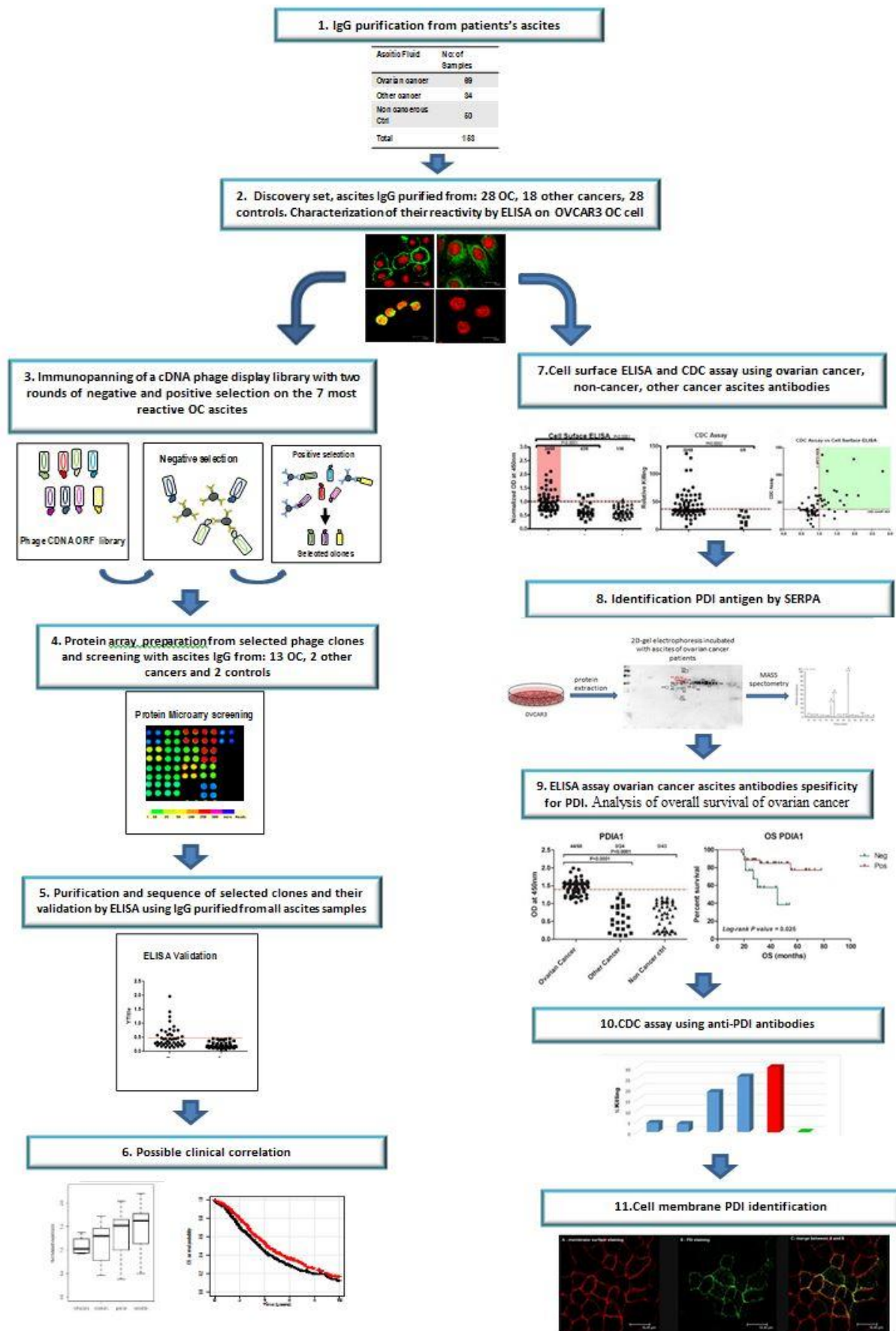


Fig.6. Schematic presentation of ovarian cancer antigens identification using two approaches.

1. Antibodies were purified from ovarian cancer, non-cancerous and other cancer ascites; 2. IF staining of OVCAR-3 cells surface using purified antibodies; 3. ORF library phage display selection; 4. Selected in phage display clones screened with ascites antibodies in microarray assay; 5. Validation of antibodies specificity to selected clones in ELISA assay; 6. Analyze of correlation of patients survival with antibodies; 7. Performing cell surface ELISA to show that ovarian cancer ascites contain antibodies against ovarian cancer cell surface proteins; 8. Identification the most abundant antibody in ovarian cancer ascites by SERPA; 9. Analyzing PDI specificity of ovarian cancer antibodies in ELISA assay; 10. Representing killing capabilities of anti-PDI antibodies in CDC assay; 11. Representing PDI protein on ovarian cancer cells surface by IF staining.

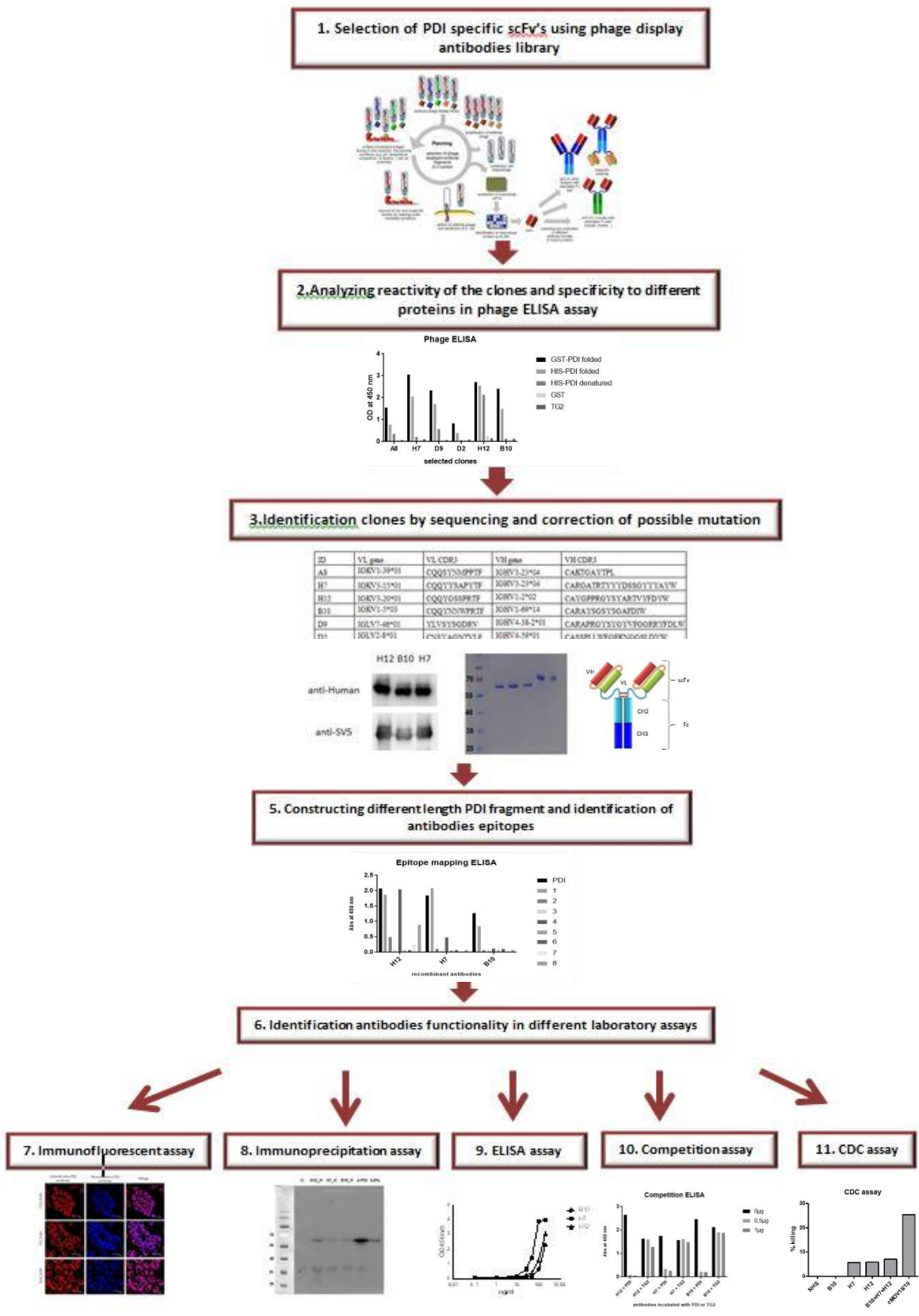


Fig.7. Schematic representation of recombinant antibodies production and its analysis: 1. Selection of scFv's specific to PDI protein in phage display selection; 2. Confirmation of PDI specificity of selected clones in phage ELISA; 3. Sequencing of selected clones and correction of occurred TAG mutations; 4. Cloning of scFv's into pcDNA3.1/Hygro(+) vector, transfection of CHO cells, selection of best antibodies producing clones and antibody production; 5. Identification of epitope for each antibody; 6. Analyze of antibodies functionality in main laboratory assays, namely immunofluorescent assay (7), immunoprecipitation assay (8), ELISA assay (9), competition assay (10), CDC assay (11).

Chapter 3

7. Results Part I: Publication

Antony Frank¹, Deantonio Cecilia¹, Cotella Diego¹, Soluri Maria Felicia¹, Tarasiuk Olja¹, Mezzanzanica Delia², Adorni Fulvio³, Piazza Silvano⁴, Ciani Yari⁴, Santoro Claudio¹, Macor Paolo⁵, Sblattero Daniele⁵

TITLE

High-throughput profiling of antibody repertoire in ovarian cancer ascitic fluid

AUTHORS AFFILIATIONS

¹Department of Health Sciences, and Interdisciplinary Research Center of Autoimmune Diseases (IRCAD) Università del Piemonte Orientale, Via Solaroli 17, Novara 28100, Italy

² Department of Experimental Oncology and Molecular Medicine, Fondazione IRCCS Istituto Nazionale dei Tumori, Milan, ITALY

³ Institute of Biomedical Technologies, National Research Council, Segrate, Milan, Italy.

⁴ Laboratorio Nazionale del Consorzio Interuniversitario per le Biotecnologie (LNCIB), Area Science Park Trieste, Italy;

⁵ Department of Life Science, University of Trieste, Via L. Giorgieri 5, 34127 Trieste Italy

RUNNING TITLE

Autoantibodies repertoire profiling in ovarian cancer ascites

KEYWORDS

Ovarian cancer, biomarker, tumor-associated antigen, ascite, protein microarray

FINANCIAL SUPPORT:

This work was supported by Regione Piemonte (*IMMONC Piattaforme Innovative*) and Cariplo Foundation (Milan). FA is a recipient of an international PhD fellowship in Innovative Biomedical Technologies (IBT) funded by Cariplo Foundation, YC is supported by AIRC/FIRC 2015.

For correspondence:

Prof. Daniele Sblattero
Università degli studi di Trieste
Dipartimento Scienze della Vita
Via L. Giorgieri 5
34127 Trieste
tel +39 0321 5588681
email dsblattero@units.it

ABSTRACT

Purpose: Identification of effective biomarkers for early diagnosis, prognosis and response to treatment is still a challenge in the field of ovarian cancer (OC) research. By relying on

auto-antibodies present in OC patients' ascitic fluids we aimed to identify a tumor specific antigenic signature.

Experimental Design: We initially used a discovery set of IgGs purified from 7 OC patients' ascites to select tumor specific antigens from a phage display cDNA library. After biopanning seven hundred proteins were expressed as fusion protein and used in protein array to enabled large scale immunoscreening with independent sets of cancer and non-cancerous control ascitic samples. Final selected antigens were validated by ELISA.

Results The initial screening with our discovery set allowed the identification of eight antigenic clones: CREB3, MRPL46, EXOSC10, BCOR, HMGN2, HIP1R, OLFM4 and KIAA1755. All antigens were further validated by ELISA in a study involving ascites' IgGs from 153 patients (69 OC, 34 other cancers and 50 non-cancerous conditions). CREB3 resulted in highest sensitivity (86.95%) and specificity of (98%). Notably, we were able to identify an association between the autoantibody titer with response to first line tumor treatment (platinum-based chemotherapy). A stronger association was found by combing three antigens (BCOR, CREB3 and MRLP46) in a single antibody signature.

Conclusions: Measurement, in ascites, of an autoantibody response to multiple tumor-associated antigens may aid in the identification of new prognostic signature in OC patients. The utility of this antigenic panel may also extend beyond its diagnostic value pointing the attention to new possible relevant targets.

Introduction

Ovarian cancer (OC) is the major cause of death from gynecologic cancers mainly because of late diagnosis and development of chemoresistance (1). Most OC patients present with advanced stage disease due to the lack of specific symptoms, adequate diagnostic tools and screening strategies (2, 3). Standard treatment for advanced stage OC is tumor-debulking surgery followed by adjuvant platinum-based chemotherapy. Despite a good response rate to front-line treatment the majority of these patients eventually develop an incurable state of platinum-resistant disease with a five-year survival rate still below 40% (4). Several new drugs have now become available for patients with OC. However, it is difficult to determine the effectiveness of a given treatment due to a lack of efficient biomarkers for patients' selection, prognosis and overall outcome (5). Cancer antigen-125 (CA-125) is the most extensively investigated OC biomarker (6) but it has a limited ability to detect the disease at early stage being mainly used for patients' monitoring during follow up procedures (7). A number of other different biomarkers present in serum, plasma and urine (such as HE4, Mesothelin, Prostatein, Kallikriens, Osteopontin) have been identified. None of them have met the clinical standards when each marker is considered individually (2) while combination of multiple markers as a panel along CA125 have been demonstrated to improve diagnostic performances (8). Finding additional biomarkers is therefore needed not only for diagnosis but also for prognosis and response to treatment (9). By applying recent approaches in the field of biomarkers discovery it has been possible to perform the so called "seromic profiling" (10) allowing the identification of tumor associated antigens recognized by patient's antibody directed against aberrantly expressed, mutated or post-translationally modified proteins. By using peptide/protein array (11), two dimensional gel electrophoresis (12), and phage display technology (13), dozens of proteins have been identified as target of patient's immune response in different tumors. Body fluids have been shown to be excellent media for biomarker discovery. Accumulation of ascitic fluid in the peritoneal cavity is one important feature of OC and its accessibility over the course of treatment makes it an excellent alternative source for biomarker discovery and translational research (14, 15). Malignant ascites typically comprises variable proportions of suspended cells that include tumor cells, mesothelial cells, fibroblasts, macrophages, white blood cells, red blood cells and debris, depending on the pathogenesis. In addition to the suspended cells, ascitic fluid contains proteins secreted or leaked from tumor tissue, soluble growth factors that have been associated with invasion and metastasis, factors of the complement system, chemokines and, above all, antibodies. Ascitic fluids have received very little attention being nevertheless an invaluable resource for prognostic and predictive biomarkers identification, pharmacodynamic information, as well as for molecular profiling of OC. Although some proteomics studies have been performed describing thousands of proteins present only few of them showed limited

correlation with clinical features of the disease (16–19). In this study, we present a systematic and in-depth profiling of OC ascites antibody signature. We first showed that ascites contains antibodies targeting proteins expressed in OC cells. Then, by a high-throughput protein expression and screening platform that combines phage display and proteins microarray, we profiled ascitic fluids antibody response and identified eight new autoantibody-binding antigens. This tumor autoantibody signature is associated and correlated with response to chemotherapy.

Materials and Methods

Patient samples and cell lines

Ascites were collected from 153 female patients with various disease conditions including OC (n=69), non-ovarian tumors (n=34), and non-cancerous diseases (n=50) (summarized in Table 1). Ascites from OC patients were collected at the Fondazione IRCCS Istituto Nazionale dei Tumori, Milan, while ascites from non-ovarian tumors and from non-oncological diseases were collected at the University of Torino. Approvals by the ethical committees of each institute and informed consent were obtained from all the participants. Ascites were centrifuged at 11,000 rpm at 4°C for 5 minutes and supernatants aliquots were stored at -80°C until processed. Immunoglobulins (IgG) were affinity purified using Protein A-agarose (Roche) according to the manufacturer's instructions (Supplementary Figure 1, step 1). Human ovarian adenocarcinoma cell line OVCAR-3 (ATCC® HTB-161™) was grown in RPMI 1640 media containing 10% fetal calf serum and 1% penicillin/streptomycin. Cells were maintained at 37°C in a humidified atmosphere containing CO₂. Cells were routinely tested for Mycoplasma contamination and identity by STR profile.

Characterization of ascitic fluid based on autoantibody response

Affinity purified IgGs obtained from patients' ascites were characterized for their reactivity using OVCAR-3 OC cell line as described below (supplementary Figure 1, step 2).

Western blotting of OVCAR-3 cell extracts. Proteins from OVCAR-3 cells were extracted under denaturing conditions using 8M Urea, resolved by SDS-PAGE and transferred to nitrocellulose. Membranes were saturated for 1 hr with 4% milk in PBS-Tween 20 buffer (MPBST), then incubated for 90 min with IgGs purified from ascites as the source of primary antibodies, diluted 1:50 in 2% MPBST. Immun-reactive bands were detected after incubation with an alkaline phosphatase-conjugated secondary antibody and developed with the chromogenic substrates NBT/BCIP (Roche).

Immunofluorescence. OVCAR-3 cells were grown on glass coverslips until 80% confluency and subjected to immunofluorescence staining afterward. Images were obtained with a Leica DMIRE2 confocal fluorescence microscope (Leica Microsystems) equipped with the software Leica Confocal Software v.2.61. For intracellular staining cells were washed twice with PBS, fixed with 4% paraformaldehyde (in PBS, 4% sucrose) and permeabilized with 0.2% Triton X-100. Fixed cells were blocked with 2% BSA and incubated for 2 hrs at 37°C with a 1:10 dilution of IgGs purified from ascites. Slides were then incubated with an anti human Cy5-conjugated secondary antibody (Jackson Immuno Research) diluted 1:200 and cell nuclei were counterstained with propidium iodide. For surface staining cells growing on coverslips were washed with serum-free RPMI medium and incubated for 2 hrs with the IgG purified from ascites, diluted 1:10 in blocking buffer (5% BSA in serum free RPMI medium). All incubation steps were carried out at 4°C to prevent the cellular uptake of antibodies. After washing bound IgGs were revealed by incubation with the secondary antibody. The washed cells were fixed, permeabilized and counterstained as described above.

Whole-cell ELISA. OVCAR-3 cells were seeded in 96-wells culture plates (10⁴cells/well) and left adhere overnight. Cells were washed with blocking buffer, fixed with methanol and incubated at 4°C for 90 min with the ascites' IgGs diluted 1:50 in blocking buffer, followed by 1 hr incubation at 4°C with a peroxidase-conjugated secondary antibody (Dako). Immunocomplexes were revealed with TMB and the plates read at 450 nm. Experiments were performed in triplicate. Positivity cutoff value for each antigen was calculated as cumulative mean of the OD₄₅₀ value obtained with ascites' IgG from non-cancerous control plus 2 standard deviation (SD).

Cell lysate ELISA. Confluent OVCAR-3 cells grown on 100mm dishes were washed with ice-cold PBS and lysed with a non-denaturing extraction buffer (100 mM Tris, 150 mM NaCl, 1 mM EGTA, 1 mM EDTA, 1% Igepal CA-630, protease inhibitors, pH=7.4). Cells lysates were incubated on ice for 15-30 min then briefly sonicated, soluble material was recovered after centrifugation at 13,000 rpm for 10 min at 4°C and protein concentration was determined by the BCA assay. To perform cell lysate ELISA assays, microtiter plates were coated overnight with 3.2 µg OVCAR-3 cell extract then blocked with 2% BSA in PBST (0.05%) for 1hr at 30°C. Plates were incubated for 90 min at 30°C with the IgGs purified from ascites diluted 1:50. Immunocomplexes were detected as described above.

Construction and selection of ORF cDNA phage display library

The human ORF cDNA phage display library was prepared from mRNA derived from different tissues as described in Di Niro *et al* (20). The biopanning of the library was performed with negative and positive selections using healthy control sera followed by independent selections using 7 different ascites from patients diagnosed with OC representing stage II-IV, that have already been identified as the most reactive based on the initial immunological assays (Supplementary Figure 1, step 3). Two successive rounds of selection using immunoglobulins purified from ascites, captured on protein G-coated magnetic beads (Dynabeads), were performed as described in Di Niro *et al* (21). ORF cDNA fragments from the second round of selection were subcloned from the phagemid DNA into a modified pGEX4T (GE-Healthcare) expression vector to yield GST-fusion products with C-terminal Flag tag, and transformed in the host bacteria *E.coli*.

BL21 (DE3) RIPL cells for enhanced protein production. Approximately seven hundred individual clones were randomly picked (96 clones from each of the seven selections), and recombinant GST fusion protein production was carried out by auto-inducing medium ZYM₅₀₅₂ in 96 wells format as described by Studier *et al* (22). Cells were grown under constant air supply using a custom-built air-well sparging minifermenter system (23). Proteins were affinity-purified using glutathione magnetic beads (Promega) and analyzed for their quantity and quality by Coomassie staining and Western blot with anti-tag antibodies (anti-GST and anti-FLAG antibodies).

Protein microarrays and ORF sequencing

GST-fusion proteins were printed onto nitrocellulose-coated slides (Whatman) using a BioOdyssey Calligrapher miniarrayer (Biorad). The arrayed slides were processed as described in D'Angelo *et al* (24). The slides blocked with 3% milk in PBST were incubated individually with affinity-purified antibodies from 17 ascites (including OC, other cancer and non-cancerous patients, Supplementary Figure 1, step 4) as the source of primary antibodies at a dilution of 1:200 in binding buffer (2% milk in PBST). Bound antibodies were detected by incubation with a Cy5-conjugated anti-human IgG secondary antibody diluted 1:200 for 1 hr. Fluorescent signals were measured with a ScanArray Gx[®] (PerkinElmer) and analyzed with the ScanArray Expression Software (PerkinElmer). Arrays were normalized with a 2-step protocol. Background response was evaluated using the signal generated for each tested ascite sample against a reference GST protein and a set of serial dilutions of purified IgG printed on each array was used to generate a calibration curve of arbitrary IgG units. Positive proteins were identified by comparing the frequency of reactive ascitic samples. The proteins with a significant difference in reactivity between OC patients and non-cancerous controls were identified as putative candidates for further analysis. The most immun-reactive clones screened by microarray analysis were amplified by PCR using pGEX sense (GGGCTGGCAAGCCACGTTTGGTG) and anti-sense primers (GGTGAAAACCTCTGACACATGCAGCTCCCGG). Purified PCR-amplification products were sequenced in ABI PRISM[®] 3100 Genetic Analyzer (Applied Biosystem) using Applied Biosystems, BigDye Terminator v1.1 Cycle Sequencing Kit (Applied Biosystems).

Indirect ELISA

Recombinant GST-proteins were diluted in PBS to 10µg/ml and 100µl were coated in ELISA wells (Nunc) overnight (O/N) at 4°C. Wells were washed with PBS and 200µl of blocking solution (2% BSA in PBST) were added to each well, for 1h at RT. Affinity purified and normalized ascite IgG from 153 patients diluted 1: 50 in blocking buffer was used as primary antibodies and incubated for 90 min at 30°C (Supplementary Figure 1, step 5). Extensive washes were performed with PBST and PBS to remove the unbound primary antibodies. Secondary antibody was a goat anti-human-IgG HRP conjugated (Jackson) diluted 1:3,000 in blocking solution, for 1 h at 30°C. After extensive washing, immunocomplexes were revealed with TMB and the plate read at 450 nm. A cut-off value for positivity for each antigen was calculated independently as the mean OD₄₅₀ value obtained with non-cancerous ascites IgG samples plus 2 standard deviations (SD).

Statistical analysis

The ELISA data were analyzed to test for differences in the presence of antibodies directed towards the identified antigens between the three groups of patients. Chi-square or Fisher's exact test, depending on the expected value of each cell in the cross-tabulation, were first performed to infer statistical significance in the overall comparison between OC patients, other cancer patients and non-cancerous controls, and then when separately comparing OC vs. other tumors or vs. healthy subjects. ROC analyses were performed to evaluate the performances, including the AUCs estimates with their 95% confidence limits, of each antigen in correctly classifying the disease condition. All the tests were two-sided and the level of statistical significance level was set as $\alpha=0.05$. All of the analyses, performed using Statistical Software Packages SPSS (IBM Corp. Released 2013. IBM SPSS Statistics for Windows, Version 22.0. Armonk, NY: IBM Corp).

Survival analysis on internal dataset.

The clinical impact of antibody titer on patients' response to treatment was assessed by the Mann-Whitney test, stratifying patients in three groups based on their response to treatment (resistant, partial sensitive and sensitive, for relapse occurring during treatment, within 6 months, between 6 and 12 months and after 12 months from the end of treatment, respectively). All analyses were performed in R/Bioconductor environment. For all analyses, differences were considered significant at P values < 0.05 (Supplementary Figure 1, step 6).

Survival analysis on external dataset.

The prognostic value of the levels of expression of the genes of interest was analyzed in a dataset comprising more than 2950 OC patients from 23 studies with curated and documented clinical metadata (25). The curated Ovarian Data package provides data for gene expression analysis in patients with OC and we selected samples for which Overall survival (OS) information were available. Patients were classified according to the normalized mean expression of the genes of interest as low or high, a Mantel-Haenszel test was applied and the Kaplan-Meier survival curves were obtained and compared with the log-rank test (Supplementary Figure 1, step 6). All analyses were performed in R/Bioconductor environment using survival package.

Results

Project strategy

To identify antigens responsible for an auto-antibody response detectable in OC ascites, we applied the research pipeline described in Supplementary Fig. 1. A discovery set of affinity purified IgGs from 7 OC ascites, selected on the bases of their reactivity on the OVCAR-3 OC cell line, was used as bait for a phage display cDNA library. The biomarkers were then identified by protein microarray; selected antigens were produced and purified as recombinant proteins and ELISA was performed with all samples of ascites' IgGs to validate protein antigenicity. Finally, correlations between antibody titer, gene expression profile and clinical data were explored.

Ascites from OC contain antibodies targeting tumor cell antigens

In this study, a total of 153 different ascitic fluids were collected from patients diagnosed with OC (N=69), other cancers (N=34) and non-cancerous diseases (N=50) (Table 1). IgGs from all samples were affinity purified and quantified (Supplementary Fig. 2), showing a comparable concentration range (1-8.5 $\mu\text{g}/\mu\text{l}$) within the three groups. To detect the presence of antibodies against tumor-associated antigens (TAA) in OC ascitic fluids, five purified IgGs samples were initially tested for their reactivity against an OC cell line lysate (OVCAR-3 cells) by Western blot analysis (Fig. 1A). Antibodies affinity-purified from distinct OC-derived ascites (Fig. 1A lanes a and b) generated a distinct recognition patterns with a high number of proteins recognized on OVCAR-3 cell lysate. Notably, in the same experimental conditions, antibodies from non-cancerous controls (Fig. 1A lanes c and d) fail to clearly detect proteins with comparable frequency and specificity. The same recognition pattern was further confirmed by immunofluorescence (IF) analysis on OVCAR-3 cells. Fig. 1B shows that IgG affinity-purified from OC patients' ascites, clearly stain cells in different subcellular compartments, including plasma membranes (panel a), cytoplasm (panel b), and nuclei (panel c). Tumor cells stained with antibodies from non-cancerous patient fail to produce any detectable signal (panel d). To confirm in a more quantitative way the presence of specific antibodies in OC-derived ascites, ELISA was performed using OVCAR-3 cells as source of TAA. Purified antibodies from OC (n=28), other cancers (n=18) or non-cancerous (n=28) ascitic fluids were incubated either with fixed whole-cells (Fig. 1C), or with total cell lysate cells (Fig. 1D), in order to detect antibodies to cellular antigens. As expected, ELISA results indicated the presence of a high titer of antibodies in OC ascites as compared to other cancer or non-cancerous controls (Fig. 1C and 1D) confirming data obtained by IF. Taken together, these results indicate the presence of a high-titer of antibodies for OC antigens in OC patient's ascites and that this reactivity was not observed in ascites from non-cancerous patients as well as from non-ovarian cancers.

Selection and identification of antigens by phage display and protein microarray

To identify the antigens recognized by the antibodies present in OC ascites' a "discovery set" of reactive IgGs was selected. Seven IgG samples purified from OC ascites with different clinical-pathological features and showing high reactivity on OVCAR-3 cell line, were identified (Supplementary table 1), and each sample was used as a bait in an independent selections of an ORF cDNA phage display library. Phage selection was performed over two consecutive cycles, each one preceded by a "pre-clearing step" done using antibodies from healthy donors in order to remove common or polyreactive clones. Following biopanning, positive clones were identified using protein microarray with selected DNA fragments coding proteins expressed as GST fusion proteins. One hundred clones from each of the seven selections were randomly picked, recombinant proteins were expressed and affinity purified yielding approximately 700 independent GST fusion proteins. Protein microarrays were created by spotting purified proteins onto nitrocellulose slides along with controls and calibrator IgGs. Array quality control was performed with anti GST antibody (Supplementary Fig. 3A) showing the correct printing and concentration range of more than 90% of selected antigens. Each array was then challenged individually with purified antibodies from 17 different ascites representing patients with: OC (n=13, including the 7 used for selection), other cancer (n=2) and non-cancerous conditions (n=2). Non-cancerous control antibodies were giving a limited number of positive staining spots (Supplementary Fig. 3C), while arrays exhibited significantly increased immune-recognition when incubated with IgG purified form OC ascites (Supplementary Fig. 3B). Following spot' signal quantification, 73 distinct clones were found to have increased immunogenicity towards one or more OC ascites IgG sample compared to non-cancerous ascites. Antigens were ranked according to the frequency of positive OC reactivity and a subset of eight clones were identified as specifically recognized by all 13 tested OC samples but not from controls (both other cancer and non-cancerous). These clones were recovered and proteins identified by DNA sequencing. A total of 8 different proteins were identified (Table 2): Cyclic AMP-responsive element-binding protein 3 (CREB3); Mitochondrial ribosomal protein L46 (MRPL46); Exosome component 10 (EXOSC10), BCL-6 corepressor (BCOR), High mobility group nucleosomal binding domain 2 (HMGN2), Huntingtin interacting protein 1 related (HIP1R); Olfactomedin 4 (OLFM4) and KIAA1755.

Validation of protein immunoreactivity by ELISA

To confirm the antigenicity of the selected proteins, purified antibodies from patients and controls cohorts were screened by ELISA. The eight proteins were produced in a larger quantity, purified by affinity chromatography and quality was assessed by coomassie staining (Supplementary Fig. 4A) and Western blot (Supplementary Fig. 4B,C). Preliminary set up experiments were performed to establish antigen coating concentration as well as antibody dilution. Finally, each antigen was tested by ELISA against the full set of 153 ascites' purified antibodies. As expected, ELISA reactivity towards the 8 antigens was not homogenous showing a wide range of immunorecognition (Fig. 2). In general, control ascites' antibodies showed no or very low reactivity towards all antigens providing a specificity higher than 94% for all proteins (see supplementary table 2 and 3). Samples from other cancers showed a large degree of variability in recognition while OC samples were highly reactive against all antigens tested. CREB3 with 60 positive sample out of 69 showed a sensitivity of 87%, MRPL46 and BCOR around 73% and EXOSC10 56%, with HMG2 being the least sensitive among the antigenic panel being detected by only 13 out of 69 OC samples (supplementary tables 2 and 3). When the antigens were used to identify differences in the three samples population, the analyses showed that for all the eight antigens there was a statistically significant difference in immunoreactivity between OC and non-cancerous control ascites. Interestingly three antigens, namely CREB3, MRPL46 and EXOSC10 were also able to significantly differentiate OC samples from other cancer, therefore confirming the isolation of antigens specific for OC ascites antibodies (Supplementary table 3).

Specific antibody titer correlates with chemotherapy response in OC patients

We then analyzed if the antibody titer to specific antigen correlated with clinical data. None of the clinical-pathological characteristics, except response to platinum-based therapy, correlated with the Abs titer. Patients were stratified according to the response to treatment, as platinum resistant' (28 patients) with disease progression within 6 months from the end of therapy; 'partially platinum sensitive' (16 patients) with progression between 6 and 12 months and 'platinum sensitive' (24 patients) with progression after 12 months.

The distribution of ELISA normalized signal values, obtained on individual antigens, was then compared within the three classes of chemotherapy responses. For all the eight antigens (Fig. 3C) (and supplementary Fig.5) there was no difference between the signals when the platinum 'resistant' and 'partially' platinum sensitive classes were compared (Fig. 3C). Notably for two antigens (BCOR, and MRPL46) the difference in antibody titer was statistically significant ($p < 0.05$) between 'resistant' and 'platinum sensitive' patients with the second having the higher specific antibody titer (Fig. 3A, C). Although not significant also CREB3 antigen showed a trend toward an increase in titer from resistant to sensitive classes. Furthermore, when these three antigens were combined in a single antibody signature (Fig. 3B), a stronger association between higher antibody titer and platinum sensitivity was observed with a p-value reaching 6×10^{-3} .

Antibody titer to OC antigens only partially correlate with increased gene expression

We analyzed a curated collection of 23 datasets including gene expression and clinical data from OC patients to assess the impact of the target antigens' gene expression on patients' OS (see supplementary table 4).

More than 1800 OC patients with a 10 year follow up were stratified for gene expression. We found that the correlation between the gene expression of the identified antigens and patients' survival was more complex than that seen with antibody titer and response to treatment. In fact, although anti BCOR antibody level has the most significant concordance between high titer and platinum sensitivity, we found no significant correlation between high BCOR gene expression and longer OS (Fig. 4A). On the other hand, for both CREB3 (Fig. 4B) and MRLP46 (Fig. 4C) higher gene expression significantly correlated with longer OS. Interestingly although the BCOR expression data alone were not showing a significant correlation with OS, when the three single gene expression data were combined into a novel gene signature (Fig 4D), as done for the antibody, the level of significance was higher reaching a p-value of 1.9×10^{-4} and identifying a novel prognostic gene signature.

Discussion

Effective detection and monitoring of OC by using biomarkers still holds great promise as an approach to reduce mortality from this disease. This study focuses, for the first time, on a systematic analysis to profile OC antibody repertoire in ascites. We have used a high-throughput proteomic based technological platform that combines the selection of a phage display cDNA library followed by protein microarray (20) and we identified a final set of 8 proteins whose recognition was peculiar in OC patients compared to controls.

Ascitic fluids are accessible and provide an ideal source of material to analyze both the cellular components as well as the secretome derived from tumor and not tumor cells. This unique material represent a still largely unexplored source for identification of possible diagnostic, prognostic and predictive biomarkers (26). By applying Mass spectrometry (MS)-based proteomic, the secretory components of ascites fluids were analyzed and some potential tumor biomarkers identified (17–19, 27). Although technology for proteins identification by MS is improving, it is still confined to few laboratories limiting the number of samples as well. On the contrary ascites antibodies represent a secretory component that could be analyzed by well-established technique as well as for a large number of samples. Furthermore, even in cancer, antibodies are usually detectable at early stage of the disease and, being relatively stable molecules, their presence is detectable for long time.

Our initial strategy was aimed to the identification of an antibody signature present in ascitic fluid from OC patients. Being a proximal fluid, ascites might reveal events in the early stage of OC and contain cancer-associated soluble factors, including autoantibodies, at concentration much higher than in serum. Ascites from various disease conditions were characterized for their antibody response against OC cellular antigen and, although not homogenous within OC patients, the titer of antibody response was considerably higher than that of non-ovarian cancer patients or that of patients with a non-cancerous condition. The 8 proteins that we then identified following selection of an ORF cDNA phage display library and protein array screening, produced a statistically significant difference in immunoreactivity when challenged with antibodies purified from ascites of OC patients compared to non-cancerous patients and, to a lesser extent also to other cancers. In fact, not surprisingly, some of the identified proteins have been previously associated with various cancer-related pathologies (28–32) suggesting that these antigens share common pathways in various disease conditions.

Although the first screening of antibodies isolated from OC patients' ascitic fluids performed on OC cells identified a complex pattern of recognition with immunofluorescence showing both intracellular (nuclear and cytoplasmic) and membrane staining, seven of the eight identified proteins resulted to be intracellular antigens. We cannot exclude that other autoantibodies directed against surface antigens or glycosylated antigens can be present in ascitic fluids from OC patients nevertheless autoantibody response to intracellular antigens is well known. A response to an intracellular antigen like p53, has been detectable in OC patients as a results of a spontaneous and early humoral immune response of the host against the accumulation of an antigenic mutated p53 protein in tumour cells. Beside serum these antibodies can be detected also in tissues, ascites, and other body fluids (33).

We are aware that from a diagnostic point of view, assays relying of detection of autoantibodies in serum rather than in ascites may be more useful for OC early detection. Indeed, the serum response of OC patients has been profiled to identify signatures of proteins useful for the detection of the disease. However, the added value of the selected auto-antibodies as markers for OC early detection beyond CA125, remained limited (11, 34)

Tumor autoantibodies in OC have been explored as biomarkers not only for early diagnosis, but also for prediction of prognosis, recurrence and developing of therapeutic approaches (35). The possibility to correlate the level of tumor autoantibodies with the clinical outcome of cancer patients might permit their possible stratification into prognostic categories helping in the selection of second-line therapeutic treatments following primary debulking surgery and platinum based first-line chemotherapy. The identification of patients most likely to respond to first-line treatment is still a clinical urgent need. In fact, after an initial response the majority of OC patients experience disease recurrence (1, 36, 37). We were able to show an association between the autoantibody titer with the response to first-line treatment. OC patients, sensitive to platinum treatment showed higher titer of autoantibodies to the identified tumor antigens. Our

data show a correlation between treatment response and a high immune response against BCOR, MRPL46 and CREB3 individually or combined. This can suggest a higher presence of this antigen in particular sub-groups of patients. However, the level of autoantibodies is the results of a complex and multistep activation of the immune system that not always directly correlates with the level of the gene expression of the target antigens. Therefore, not necessarily the level of gene expression of target antigens may correlate with patients' prognosis. In fact, while this was true for CREB3 and MRPL46, BCOR gene expression level alone failed to correlate with patients' prognosis. Nevertheless, as for the antibody titer, the combined signature of BCOR with CREB3 and MRPL46 gene expression levels had a greater prognostic impact than each of them individually.

The interest in relying on auto-antibodies against tumor-associated antigens as biomarkers for cancer diagnosis and prognosis, derives from the recognition that these antibodies are generally absent, or present in very low titers, in normal individuals and in non-cancerous conditions (8, 37). Persistence and stability of anti-TAA antibodies in the body fluids of cancer patients is an advantage over other potential markers, including the TAAs themselves, which are released by tumors but rapidly degraded or cleared (38). Furthermore, the widespread availability of methods and reagents to detect autoantibodies facilitates their characterization in cancer patients. In conclusion, the strategy proposed within this work, providing a systematic profiling of OC ascites by coupling phage display to high-throughput screening technologies, could be a new valuable tool to obtain selection of tumor associated antigens with potential diagnostic/prognostic relevance in any autoantibody/antigen-related pathology.

Authors' contribution

PM, DM, DC CS, DS designed the study and wrote the paper, MFS, FA, CD OT performed phage display selection and clone characterization, YC SP, FA performed statistical analysis, DM, PM collect and analyze patients and control sera. All authors analyzed the results and approved the final version of the manuscript

Figure

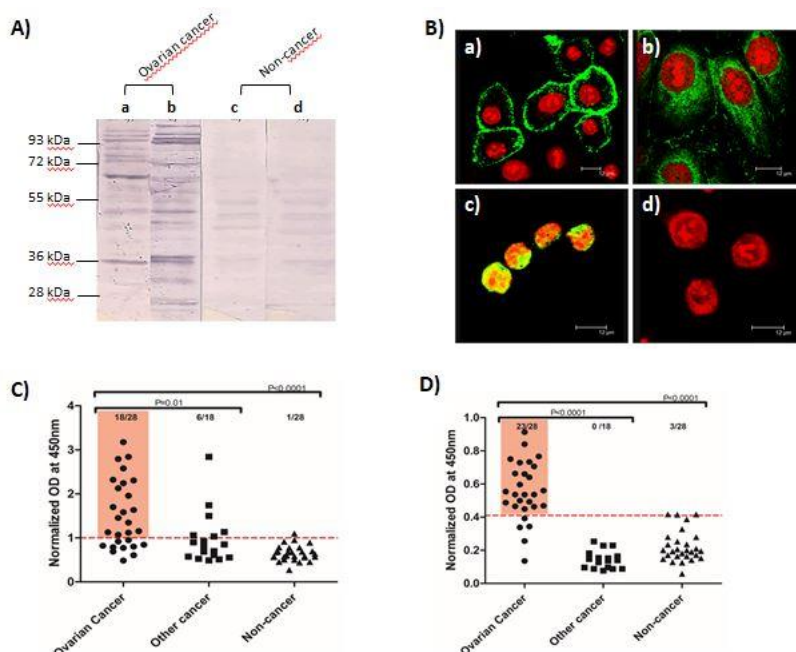


Fig 1. Ascitic fluid antibodies react to tumour cell

A) Western blot on OVCAR-3 cell lysate. Each lane contains equal amount of OVCAR-3 cell lysate incubated with Ig purified from: OC patients' ascites (a-b) or non cancerous controls (c and d). Immunoreactivity was detected with Alkaline phosphatase conjugated anti-human IgG secondary Ab. B) Immunofluorescence assay on OVCAR-3 cells with IgG purified form ascites. The cellular localization of TAA was detected with anti-human immunoglobulin conjugated to

Cy5 (in Green). Nuclei were stained with Propidium iodide (in red). (a) cell surface staining of live cells incubated with IgG from OC ascites; (b, c and d) staining of fixed and permeabilized cells incubated with IgG either from OC ascites (b and c) showing cytoplasmic (b) and nuclear (c) localization, respectively or incubated with IgG from non-cancerous ascites (d) failing to produce any signal of binding. C) OC whole cell ELISA. Fixed and permeabilized 80% confluent OVCAR-3 cells were incubated with 1:50 dilution of IgG purified from OC ascites; ascites from other cancers and non-cancerous controls. D) OC cell lysate ELISA. OVCAR-3 cell lysates were prepared in a non-denaturing condition, used to coat microtiter plates and incubated with 1: 50 dilutions of IgG purified from: OC ascites, ascites from other cancers and non-cancerous controls. Dotted red line represent cut-off level calculated as cumulative mean plus 2 standard deviation (SD) of the absorbance from non cancerous control wells. Orange shaded area identifies positive OC samples. Groups were compared by two tailed unpaired t-test and p values are reported. P-value<0.05 are considered significant.

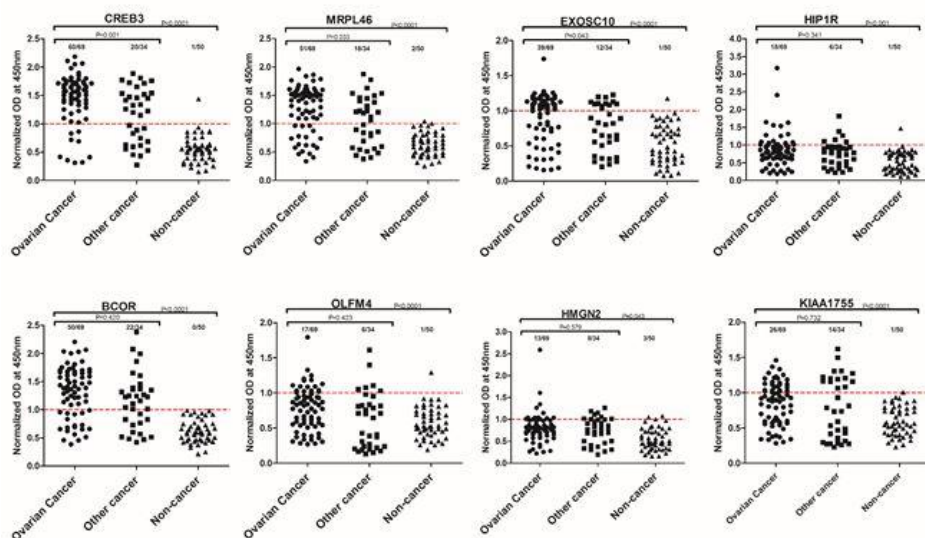


Fig 2. Validation of antigenic proteins recognition by ELISA.

Each antigen was challenged with 1: 50 dilutions of IgG purified from ascites of 153 patients diagnosed with: OC (n=69); other cancer (n=34) and non-cancerous disease (n=50). Cut-off value for each antigen was calculated independently as the mean OD₄₅₀ value obtained with non-cancerous ascites IgG samples plus 2 standard deviations (SD). Significance for ELISA data obtained for each antigen are reported. The prevalence of autoantibodies in OC patient is described by the P-value calculated using Fisher's exact test. Antigens with P-value<0.05 are considered significant.

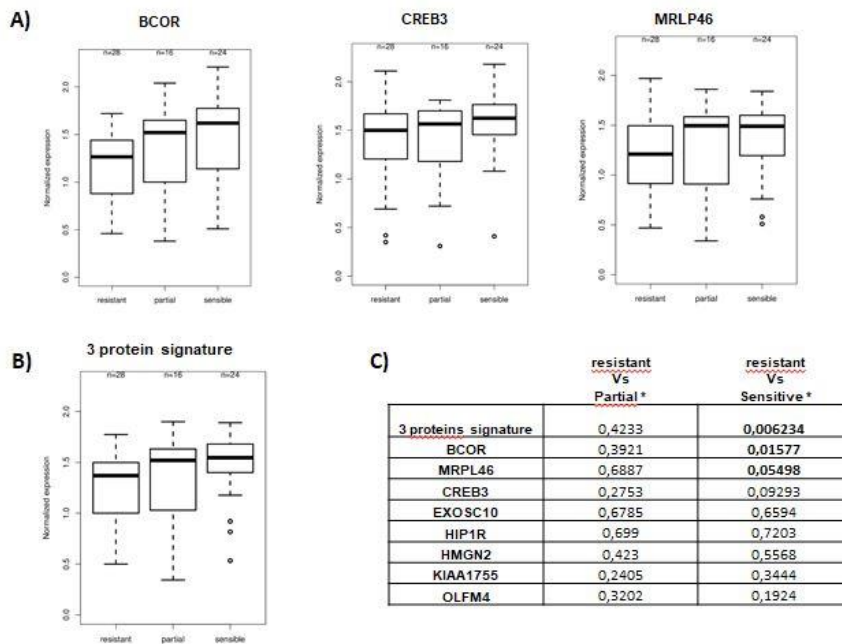


Fig 3. Antibody titer and correlation to clinical data

OC patients were stratified in three groups, according to the response to platinum-based treatment, as 'resistant' (28 patients); 'partially sensitive' (16 patients) and 'sensitive' (24 patients). A) level of ELISA signal (antibody titer) in the different patients' classes for BCOR CREB3 and MRPL46; B) level of ELISA signal (antibody titer) for the signature derived by the combinations of BCOR CREB3 and MRPL46 signals in the different patients' classes; C) P values referred to antibody titer comparison for reactivity against the 8 antigens or the three proteins signature between resistant and partially sensitive or resistant and sensitive patients (Mann-Whitney test).

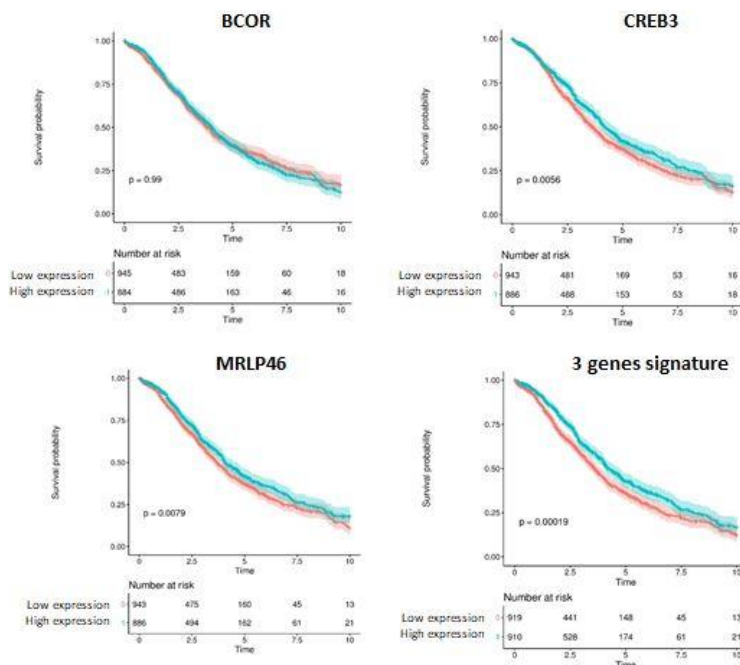


Fig 4. Gene expression and OS correlation

Kaplan-Meier analysis of overall survival of OC patients according to the normalized mean expression of the genes of interest categorized as low or high. Gene expression levels of BCOR, CREB3, MRPL46 and the combined gene signature of three antigens were measured in OC patients with 10 years follow up data. BCOR gene expression (A) shows no correlation with OS. CREB3 (B) and MRPL46 (C) higher gene expression significantly associated with longer

OS time. A much higher correlation was observed for combined signature of three gene expression data as a novel gene signature (D). Log-rank p values are reported.

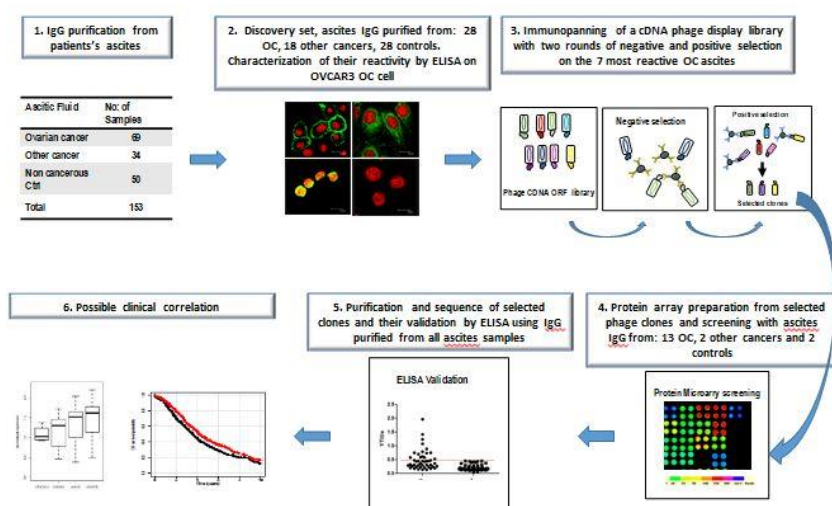
Sets of ascitic fluids	N°		%	
Ovarian cancer (69)	Age, years			
	mean, median	57, 60		
	range	32-85		
	Histology			
	Serous	47	68	
	Non-serous	22	32	
	Stage (FIGO)			
	II	2	3	
	III	45	65	
	IV	21	31	
	Missing Information	1	1	
	Grade			
	1, well differentiated	1	1	
	2, moderately differentiated	8	12	
	3, poorly differentiated	60	87	
	Amount of residual disease			
	NED	15	22	
	<1 cm, mRD	11	16	
	>1 cm, GRD	41	59	
	Missing information	2	3	
Response to Platinum treatment				
Sensitive	24	35		
Partially sensitive	16	23		
Resistant	28*	41		
Missing information	1	1		
Other cancers (34)	cancer of: lung, liver, colon, breast, gallbladder, pancreas, stomach rectum. Lymphoma. Mesothelioma			
Non-cancerous controls (50)	Cirrhosis caused by various pathologies. Pulmonary fibrosis. Cholestatic liver diseases. Pneumonia. Side effects from transplantations.			

Table 1: Characteristics of patients included into the study.

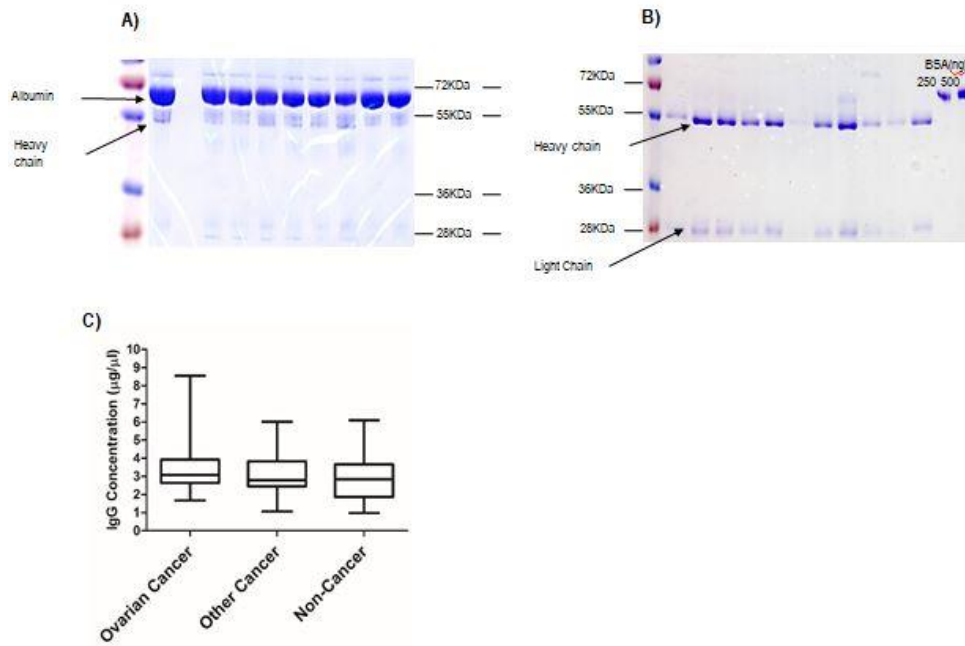
Protein Name	HUGO Name	protein length (aa)	Protein Function	References
Cyclic AMP-responsive element-binding protein 3	CREB3	395	Transcription factor	(39, 40)

39S ribosomal protein L46, mitochondrial	MRPL46	279	Structural constituent of ribosome	(41, 42)
Exosome component 10	EXOSC10	885	rRNA Processing	(41, 42)
BCL6 corepressor	BCOR	1755	Transcriptional corepressor	(30, 45)
Non-histone chromosomal protein HMG-17	HMGN2	90	nucleosomal DNA binding	(31, 46)
Huntingtin-interacting protein 1-related protein	HIP1R	1068	Component of clathrin-coated pits and vesicles,	(32, 47)
Olfactomedin-4	OLFM4	510	Cell adhesion	(48, 49)
Uncharacterized protein KIAA1755	KIAA1755	1200	unknown	

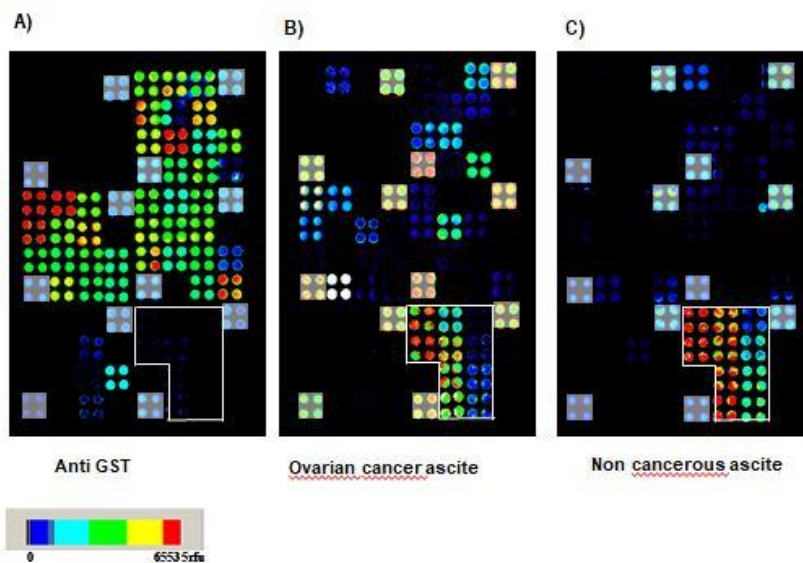
Table 2: Identified tumor associated antigens, their length and known main functions.



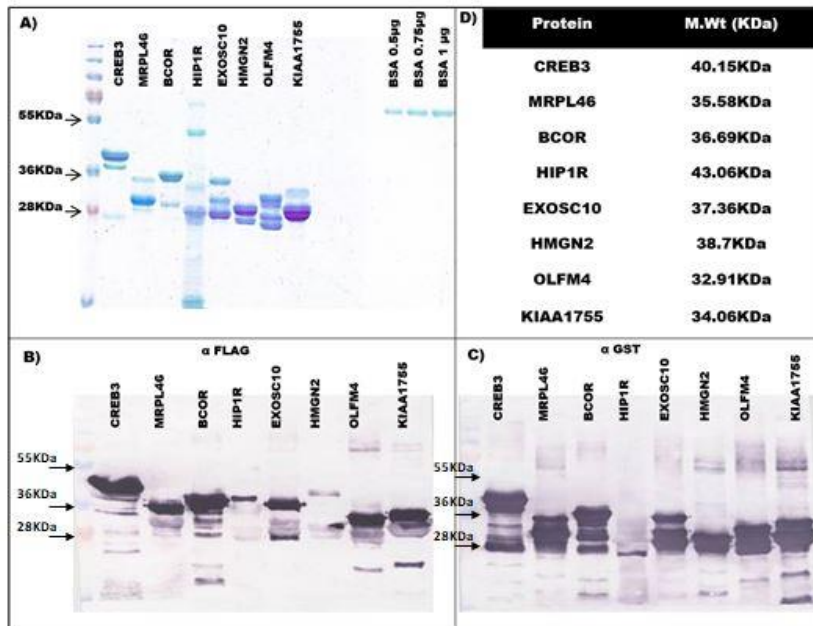
Supplementary figure 1 Workflow of the project: 1) Isolation of autoantibodies from patients' ascitic fluids. 2) Characterization of auto-antibodies reactivity on OVCAR-3 OC cell line by ELISA. 3) Rounds of negative/positive selection of an Open Reading Frame (ORF) fragments library displayed on filamentous phage: negative selection performed with IgG from healthy control sera; positive selection performed with ascites' IgGs. 4) Protein microarray approach for screening of phage-selected peptides expressed as fusion protein. 5) ELISA validation. 6) Novel putative antigens clinical correlation to antibody titer and gene expression.



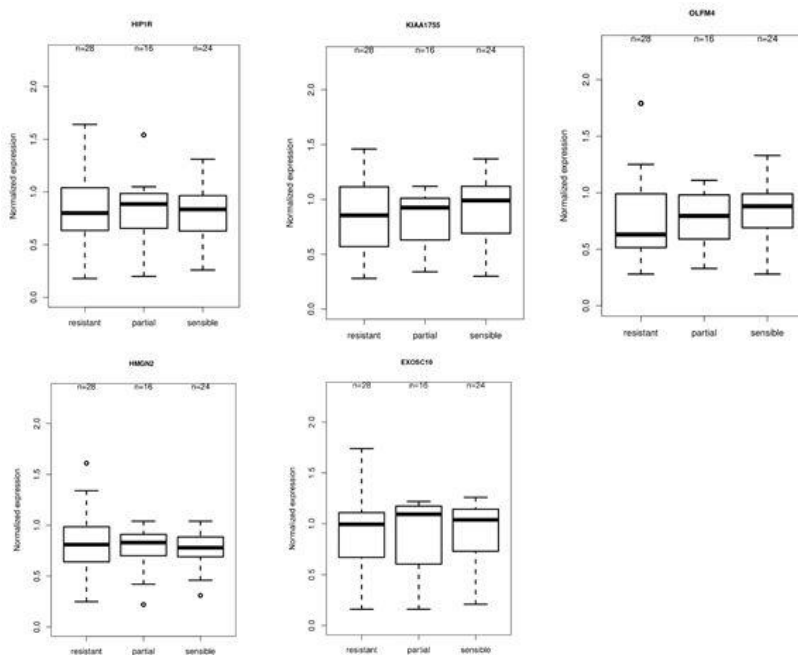
Supplementary figure 2: Affinity purification of immunoglobulins was performed from 153 ascites A) SDS-PAGE gel shows representative ascitic fluids prior to purification. B) SDS-PAGE gel shows the protein A agarose affinity purified immunoglobulins from ascites. C) The graph shows the distribution of values of Immunoglobulin concentration within the three groups of ascites.



Supplementary figure 3: Immune-screening by protein microarray. (A) Array challenged with α -GST as positive control for expression of full length recombinant proteins. (B) and (C) show fluorescent signal from representative arrays screened with 1:200 dilution of IgG purified from OC ascitic fluids and noncancerous controls, respectively. Each protein is spotted in 4 replicates, shaded area represents positive controls. On the bottom right corner in each array, the IgG calibrator (white box).



Supplementary figure 4: Expression and Purification of recognized Antigens: (A) Coomassie staining; (B,C) Western blot of all predicted antigens with anti-FLAG antibody (B), anti-GST antibody (C). Selected antigens with their corresponding molecular weight.



Supplementary figure 5: OC patients were stratified in three groups, depending on the response to treatment, as 'platinum resistant' (28 patients); 'partially platinum sensitive' (16 patients) and 'platinum sensitive' (24 patients). The graph shows correlation between the level of ELISA signal (antibody titer) in the different patients' classes towards 5 antigens with no significant difference within groups.

Ascite ID	Stage	Grade	Age at diagnosis	Cancer Cells in ascites	Histology	Sensitivity to platinum
TM08 15A	II	G2	51	Numerous	Non Serous	Sensitive
TM07 08A	II	G3	61	Rare/some	Serous	Sensitive
TM09 03A	III	G3	65	Numerous	Serous	Partially Sensitive
TM08 16A	III	G1	65	Rare/some	Serous	Sensitive
TM0707A	III	G3	69	Numerous	Serous	Resistant
TM0618A	III	G3	60	Numerous	Serous	Sensitive
TM0725A	IV	G2	43	Numerous	Non Serous	Resistant

Supplementary table 1: OC ascitic fluids collected from patients with different clinical pathological characteristics. Ascites were initially characterized for their immune-reactivity towards antigen present in OVCAR-3 OC cell line. Samples presenting the higher reactivity in both ELISA assays (whole cell or cell lysate) were chosen as bait for the phage library selection.

Ag	OC vs CTRL						OC vs OTC					
	Se	Sp	PPV	NPV	Acc	AUC (95%CI)	Se	Sp	PPV	NPV	Acc	AUC (95%CI)
CREB3	87.0	98.0	98.4	84.5	91.6	0.92 (0.87-0.98)	87.0	41.2	75.0	60.9	71.8	0.68 (0.56-0.81)
MRPL46	73.9	96.0	96.2	72.7	83.2	0.85 (0.78-0.92)	73.9	47.1	73.9	47.1	65.0	0.62 (0.49-0.75)
BCOR	72.5	100.0	100.0	72.5	84.0	0.86 (0.79-0.93)	72.5	35.3	69.4	38.7	60.2	0.58 (0.45-0.70)
HIP1R	26.1	98.0	94.7	49.0	56.3	0.62 (0.52-0.72)	26.1	82.4	75.0	35.4	44.7	0.54 (0.42-0.67)
EXOSC10	56.5	98.0	97.5	62.0	73.9	0.77 (0.69-0.86)	56.5	64.7	76.5	42.3	59.2	0.64 (0.52-0.76)
HMG2	18.8	94.0	81.3	45.6	50.4	0.56 (0.46-0.67)	18.8	76.5	61.9	31.7	37.9	0.47 (0.34-0.60)
OLFM4	24.6	98.0	94.4	48.5	55.5	0.61 (0.51-0.71)	24.6	82.4	73.9	35.0	43.7	0.53 (0.41-0.66)
KIAA1755	37.7	98.0	96.3	53.3	63.0	0.68 (0.58-0.77)	37.7	58.8	65.0	31.7	44.7	0.51 (0.38-0.64)

Supplementary Table 2: Classification performances by antigen. Se= Sensitivity, Sp= Specificity, PPV= Positive Predictive Value, NPV= Negative Predictive Value, Acc= Accuracy, AUC= Area Under the Curve, CI= Confidence Interval. OC= Ovarian Cancer, OTC= Other Cancer, CTRL=Controls

Antigen	Samples			Total (N=153)	Statistical significance		
	OC (N=69)	OTC (N=34)	CTRL		Overall	OC vs OTH	OC vs CTRL
CREB3	60 (87.0)	20 (58.8)	1 (2.0)	81 (52.9)	.000	.001	.000
MRPL46	51 (73.9)	18 (52.9)	2 (4.0)	71 (46.4)	.000	.033	.000

BCOR	50 (72.5)	22 (64.7)	0 (0.0)	72 (47.1)	.000	.420	.000
HIP1R	18 (26.1)	6 (17.6)	1 (2.0)	25 (16.3)	.002	.341	.001
EXOSC10	39 (56.5)	12 (35.3)	1 (2.0)	52 (34.0)	.000	.043	.000
HMG2	13 (18.8)	8 (23.5)	3 (6.0)	24 (15.7)	.059	.579	.043
OLFM4	17 (24.6)	6 (17.6)	1 (2.0)	24 (15.7)	.003	.423	.000
KIAA1755	26 (37.7)	14 (41.2)	1 (2.0)	41 (26.8)	.000	.732	.000

Supplementary table 3: Antigen presence and frequency, and overall and paired comparisons between groups of patients. The Antigen's significance to differentiate OC from OTH and HE was evaluated using Fisher's exact chi-square test. A P-value<0.05 are considered significant. OC= OC, OTH= Other Cancer, CTRL= controls.

	BCOR		CREB3		MRPL46		3 genes	
	LOW	HIGH	LOW	HIGH	LOW	HIGH	LOW	HIGH
Cpatients?	945	884	943	886	945	884	919	910
events	480	477	526	431	512	445	502	455
median	3,86	4,03	3,64	4,19	3,7	4,09	3,62	4,19
0.95LCL	3,62	3,74	3,3	3,98	3,42	3,95	3,3	3,99
0.95UCL	4,07	4,28	3,95	4,68	4,03	4,55	3,93	4,68

Supplementary table 4.

References

- Jayson, G. C., Kohn, E. C., Kitchener, H. C., and Ledermann, J. A. (2014) Ovarian cancer. *Lancet*. **384**, 1376–1388
- Das, P. M., and Bast, R. C. (2008) Early detection of ovarian cancer. *Biomark. Med.* **2**, 291–303
- Clarke-Pearson, D. L. (2009) Clinical practice. Screening for ovarian cancer. *N Engl J Med.* **361**, 170–177
- Vaughan, S., Coward, J. I., Jr, R. C. B., Berchuck, A., Berek, J. S., Brenton, J. D., Coukos, G., Crum, C. C., Drapkin, R., Etemadmoghadam, D., Friedlander, M., Gabra, H., Kaye, S. B., Lord, C. J., Lengyel, E., Levine, D. A., Mcneish, I. A., Stronach, E. A., Walczak, H., Bowtell, D. D., and Balkwill, F. R. (2011) Rethinking ovarian cancer: recommendations for improving outcomes. *Nat. Rev. cancer.* **11**, 719–25
- Coleman, R. L., Monk, B. J., Sood, A. K., and Herzog, T. J. (2013) Latest research and treatment of advanced-stage epithelial ovarian cancer. *Nat. Rev. Clin. Oncol.* **10**, 211–24
- Zurawski, V. R., Orjaseter, H., Andersen, A., and Jellum, E. (1988) Elevated serum CA 125 levels prior to diagnosis of ovarian neoplasia: Relevance for early detection of ovarian cancer. *Int. J. Cancer.* **42**, 677–680
- Skates, S. J., Horick, N., Yu, Y., Xu, F. J., Berchuck, A., Havrilesky, L. J., de Bruijn, H. W., van der Zee, A. G., Woolas, R. P., Jacobs, I. J., Zhang, Z., and Bast Jr., R. C. (2004) Preoperative sensitivity and specificity for early-stage ovarian cancer when combining cancer antigen CA-125II, CA 15-3, CA 72-4, and macrophage colony-stimulating factor using mixtures of multivariate normal distributions. *J Clin Oncol.* **22**, 4059–4066
- Moore, R. G., Brown, A. K., Miller, M. C., Skates, S., Allard, W. J., Verch, T., Steinhoff, M., Messerlian, G., DiSilvestro, P., Granai, C. O., and Bast Jr., R. C. (2008) The use of multiple novel tumor biomarkers for the detection of ovarian carcinoma in patients with a pelvic mass. *Gynecol Oncol.* **108**, 402–408
- Szajnik, M., Czystowska-Kuzmicz, M., Elishaev, E., and Whiteside, T. L. (2016) Biological markers of prognosis, response to therapy and outcome in ovarian carcinoma. *Expert Rev. Mol. Diagn.* **16**, 811–826
- Gnjatic, S., Ritter, E., Buchler, M. W., Giese, N. A., Brors, B., Frei, C., Murray, A., Halama, N., Zornig, I., Chen, Y. T., Andrews, C., Ritter, G., Old, L. J., Odunsi, K., and Jager, D. (2010) Seromic profiling of ovarian and pancreatic cancer. *Proc Natl Acad Sci U S A.* **107**, 5088–5093
- Stafford, P., Cichacz, Z., Woodbury, N. W., and Johnston, S. A. (2014) Immunosignature system for diagnosis of cancer. *Proc Natl Acad Sci U S A.* **111**, E3072–80
- Gagnon, A., Kim, J. H., Schorge, J. O., Ye, B., Liu, B., Hasselblatt, K., Welch, W. R., Bandera, C. A., and

- Mok, S. C. (2008) Use of a combination of approaches to identify and validate relevant tumor-associated antigens and their corresponding autoantibodies in ovarian cancer patients. *Clin Cancer Res.* **14**, 764–771
13. Chatterjee, M., Mohapatra, S., Ionan, A., Bawa, G., Ali-Fehmi, R., Wang, X., Nowak, J., Ye, B., Nahhas, F. A., Lu, K., Witkin, S. S., Fishman, D., Munkarah, A., Morris, R., Levin, N. K., Shirley, N. N., Tromp, G., Abrams, J., Draghici, S., and Tainsky, M. A. (2006) Diagnostic markers of ovarian cancer by high-throughput antigen cloning and detection on arrays. *Cancer Res.* **66**, 1181–1190
 14. Kipps, E., Tan, D. S., and Kaye, S. B. (2013) Meeting the challenge of ascites in ovarian cancer: new avenues for therapy and research. *Nat Rev Cancer.* **13**, 273–282
 15. Kuk, C., Kulasingam, V., Gunawardana, C. G., Smith, C. R., Batruch, I., and Diamandis, E. P. (2009) Mining the ovarian cancer ascites proteome for potential ovarian cancer biomarkers. *Mol Cell Proteomics.* **8**, 661–669
 16. Martin, K., Ricciardelli, C., Hoffmann, P., and Oehler, M. K. (2011) Exploring the immunoproteome for ovarian cancer biomarker discovery. *Int J Mol Sci.* **12**, 410–428
 17. Huang, H., Li, Y., Liu, J., Zheng, M., Feng, Y., Hu, K., Huang, Y., and Huang, Q. (2012) Screening and identification of biomarkers in ascites related to intrinsic chemoresistance of serous epithelial ovarian cancers. *PLoS One.* **7**, e51256
 18. Bery, A., Leung, F., Smith, C. R., Diamandis, E. P., and Kulasingam, V. (2014) Deciphering the ovarian cancer ascites fluid peptidome. *Clin Proteomics.* **11**, 13
 19. Zhang, Y., Xu, B., Liu, Y., Yao, H., Lu, N., Li, B., Gao, J., Guo, S., Han, N., Qi, J., Zhang, K., Cheng, S., Wang, H., Zhang, X., Xiao, T., Wu, L., and Gao, Y. (2012) The ovarian cancer-derived secretory/releasing proteome: A repertoire of tumor markers. *Proteomics.* **12**, 1883–1891
 20. Di Niro, R., Sulic, A. M., Mignone, F., D'Angelo, S., Bordoni, R., Iacono, M., Marzari, R., Gaiotto, T., Lavric, M., Bradbury, A. R., Biancone, L., Zevin-Sonkin, D., De Bellis, G., Santoro, C., and Sblattero, D. (2010) Rapid interactome profiling by massive sequencing. *Nucleic Acids Res.* **38**, e110
 21. Di Niro, R., D'Angelo, S., Secco, P., Marzari, R., Santoro, C., and Sblattero, D. (2009) Profiling the autoantibody repertoire by screening phage-displayed human cDNA libraries. *Methods Mol Biol.* **570**, 353–369
 22. Studier, F. W. (2005) Protein production by auto-induction in high density shaking cultures. *Protein Expr Purif.* **41**, 207–234
 23. Deantonio, C., Sedini, V., Cesaro, P., Quasso, F., Cotella, D., Persichetti, F., Santoro, C., and Sblattero, D. (2014) An Air-well sparging minifermenter system for high-throughput protein production. *Microb Cell Fact.* **13**, 132
 24. D'Angelo, S., Mignone, F., Deantonio, C., Di Niro, R., Bordoni, R., Marzari, R., De Bellis, G., Not, T., Ferrara, F., Bradbury, A., Santoro, C., and Sblattero, D. (2013) Profiling celiac disease antibody repertoire. *Clin Immunol.* **148**, 99–109
 25. Ganzfried, B. F., Riestler, M., Haibe-Kains, B., Risch, T., Tyekucheva, S., Jazic, I., Wang, X. V., Ahmadifar, M., Birrer, M. J., Parmigiani, G., Huttenhower, C., and Waldron, L. (2013) curatedOvarianData: Clinically annotated data for the ovarian cancer transcriptome. *Database.* 10.1093/database/bat013
 26. Ahmed, N., and Stenvers, K. L. (2013) Getting to know ovarian cancer ascites: opportunities for targeted therapy-based translational research. *Front Oncol.* **3**, 256
 27. Kristjansdottir, B., Levan, K., Partheen, K., Carlsohn, E., and Sundfeldt, K. (2013) Potential tumor biomarkers identified in ovarian cyst fluid by quantitative proteomic analysis, iTRAQ. *Clin Proteomics.* **10**, 4
 28. Staals, R. H., and Pruijn, G. J. The human exosome and disease. *Adv Exp Med Biol.* **702**, 132–142
 29. Shiba, N., Yoshida, K., Shiraishi, Y., Okuno, Y., Yamato, G., Hara, Y., Nagata, Y., Chiba, K., Tanaka, H., Terui, K., Kato, M., Park, M. J., Ohki, K., Shimada, A., Takita, J., Tomizawa, D., Kudo, K., Arakawa, H., Adachi, S., Taga, T., Tawa, A., Ito, E., Horibe, K., Sanada, M., Miyano, S., Ogawa, S., and Hayashi, Y. (2016) Whole-exome sequencing reveals the spectrum of gene mutations and the clonal evolution patterns in paediatric acute myeloid leukaemia. *Br. J. Haematol.* **175**, 476–489
 30. Sturm, D., Orr, B. A., Toprak, U. H., Hovestadt, V., Jones, D. T. W., Capper, D., Sill, M., Buchhalter, I., Northcott, P. A., Leis, I., Ryzhova, M., Koelsche, C., Pfaff, E., Allen, S. J., Balasubramanian, G., Worst, B. C., Pajtler, K. W., Brabetz, S., Johann, P. D., Sahm, F., Reimand, J., Mackay, A., Carvalho, D. M., Remke, M., Phillips, J. J., Perry, A., Cowdrey, C., Drissi, R., Fouladi, M., Giangaspero, F., Łastowska, M., Grajkowska, W., Scheurlen, W., Pietsch, T., Hagel, C., Gojo, J., Lötsch, D., Berger, W., Slavc, I., Haberler, C., Jouvett, A., Holm, S., Hofer, S., Prinz, M., Keohane, C., Fried, I., Mawrin, C., Scheie, D., Mobley, B. C., Schniederjan, M. J., Santi, M., Buccoliero, A. M., Dahiya, S., Kramm, C. M., Von Bueren, A. O., Von Hoff, K., Rutkowski, S., Herold-Mende, C., Frühwald, M. C., Milde, T., Hasselblatt, M., Wesseling, P., Rößler, J.,

- Schüller, U., Ebinger, M., Schittenhelm, J., Frank, S., Grobholz, R., Vajtai, I., Hans, V., Schneppenheim, R., Zitterbart, K., Collins, V. P., Aronica, E., Varlet, P., Puget, S., Dufour, C., Grill, J., Figarella-Branger, D., Wolter, M., Schuhmann, M. U., Shalaby, T., Grotzer, M., Van Meter, T., Monoranu, C. M., Felsberg, J., Reifenberger, G., Snuderl, M., Forrester, L. A., Koster, J., Versteeg, R., Volckmann, R., Van Sluis, P., Wolf, S., Mikkelsen, T., Gajjar, A., Aldape, K., Moore, A. S., Taylor, M. D., Jones, C., Jabado, N., Karajannis, M. A., Eils, R., Schlesner, M., Lichter, P., Von Deimling, A., Pfister, S. M., Ellison, D. W., Korshunov, A., and Kool, M. (2016) New Brain Tumor Entities Emerge from Molecular Classification of CNS-PNETs. *Cell*. **164**, 1060–1072
31. Porkka, K., Laakkonen, P., Hoffman, J. A., Bernasconi, M., and Ruoslahti, E. (2002) A fragment of the HMG2 protein homes to the nuclei of tumor cells and tumor endothelial cells in vivo. *Proc Natl Acad Sci U S A*. **99**, 7444–7449
 32. Hsu, C. Y., Lin, C. H., Jan, Y. H., Su, C. Y., Yao, Y. C., Cheng, H. C., Hsu, T. I., Wang, P. S., Su, W. P., Yang, C. J., Huang, M. S., Calkins, M. J., Hsiao, M., and Lu, P. J. (2016) Huntingtin-interacting protein-1 is an early-stage prognostic biomarker of lung adenocarcinoma and suppresses metastasis via AKT-mediated epithelial-mesenchymal transition. *Am. J. Respir. Crit. Care Med*. **193**, 869–880
 33. Garziera, M., Montico, M., Bidoli, E., Scalone, S., Sorio, R., Giorda, G., Lucia, E., and Toffoli, G. (2015) Prognostic role of serum antibody immunity to p53 oncogenic protein in ovarian cancer: A systematic review and a meta-analysis. *PLoS One*. 10.1371/journal.pone.0140351
 34. Kaaks, R., Fortner, R. T., Hüsing, A., Barrdahl, M., Hopper, M., Johnson, T., Tjønneland, A., Hansen, L., Overvad, K., Fournier, A., Boutron-Ruault, M., Kvaskoff, M., Dossus, L., Johansson, M., Boeing, H., Trichopoulou, A., Benetou, V., Vecchia, C. La, Sieri, S., Mattiello, A., Palli, D., Tumino, R., Matullo, G., Onland-Moret, N. C., Gram, I. T., Weiderpass, E., Sánchez, M., Sanchez, C. N., Duell, E. J., Ardanaz, E., Larranaga, N., Lundin, E., Idahl, A., Jirstrom, K., Nodin, B., Travis, R. C., Riboli, E., Merritt, M., Aune, D., Terry, K., Cramer, D. W., and Anderson, K. S. (2018) Tumor-associated autoantibodies as early detection markers for ovarian cancer? A prospective evaluation. *Int. J. Cancer*. 10.1002/ijc.31335
 35. Chatterjee, M., and Tainsky, M. A. (2010) Autoantibodies as biomarkers for ovarian cancer. *Cancer Biomarkers*. **8**, 187–201
 36. Kim, A., Ueda, Y., Naka, T., and Enomoto, T. Therapeutic strategies in epithelial ovarian cancer. *J Exp Clin Cancer Res*. **31**, 14
 37. Visintin, I., Feng, Z., Longton, G., Ward, D. C., Alvero, A. B., Lai, Y., Tenthorey, J., Leiser, A., Flores-Saib, R., Yu, H., Azori, M., Rutherford, T., Schwartz, P. E., and Mor, G. (2008) Diagnostic markers for early detection of ovarian cancer. *Clin Cancer Res*. **14**, 1065–1072
 38. Bjorge, L., Hakulinen, J., Vintermyr, O. K., Jarva, H., Jensen, T. S., Iversen, O. E., and Meri, S. (2005) Ascitic complement system in ovarian cancer. *Br J Cancer*. **92**, 895–905
 39. Chan, C.-P., Kok, K.-H., Jin, D.-Y., Panagopoulos, I., Moller, E., Dahlen, A., Isaksson, M., Mandahl, N., Vlamis-Gardikas, A., Mertens, F., Lu, R., Yang, P., O, P., Honma, Y., Kanazawa, K., Mori, T., Tanno, Y., Tojo, M., Kiyosawa, H., Takeda, J., Nikaido, T., Tsukamoto, T., Yokoya, S., Wanaka, A., Storlazzi, C., Mertens, F., Nascimento, A., Isaksson, M., Wejde, J., Brosjo, O., Mandahl, N., Panagopoulos, I., Omori, Y., Imai, J., Watanabe, M., Komatsu, T., Suzuki, Y., Kataoka, K., Watanabe, S., Tanigami, A., Sugano, S., Qi, H., Fillion, C., Labrie, Y., Grenier, J., Fournier, A., Berger, L., El-Alfy, M., Labrie, C., Smolik, S., Rose, R., Goodman, R., Abel, T., Bhatt, R., Maniatis, T., Vinson, C., Acharya, A., Taparowsky, E., Stirling, J., O, P., DenBoer, L., Hardy-Smith, P., Hogan, M., Cockram, G., Audas, T., Lu, R., Brown, M., Ye, J., Rawson, R., Goldstein, J., Bailey, D., O, P., Raggo, C., Rapin, N., Stirling, J., Gobeil, P., Smith-Windsor, E., O, P., Kondo, S., Murakami, T., Tatsumi, K., Ogata, M., Kanemoto, S., Otori, K., Iseki, K., Wanaka, A., Imaizumi, K., Kondo, S., Saito, A., Hino, S., Murakami, T., Ogata, M., Kanemoto, S., Nara, S., Yamashita, A., Yoshinaga, K., Hara, H., Imaizumi, K., Zhang, K., Shen, X., Wu, J., Sakaki, K., Saunders, T., Rutkowski, D., Back, S., Kaufman, R., Murakami, T., Saito, A., Hino, S., Kondo, S., Kanemoto, S., Chihara, K., Sekiya, H., Tsumagari, K., Ochiai, K., Yoshinaga, K., Chihara, K., Saito, A., Murakami, T., Hino, S., Aoki, Y., Sekiya, H., Aikawa, Y., Wanaka, A., Imaizumi, K., Vellanki, R., Zhang, L., Guney, M., Rocheleau, J., Gannon, M., Volchuk, A., Saito, A., Hino, S., Murakami, T., Kanemoto, S., Kondo, S., Saitoh, M., Nishimura, R., Yoneda, T., Furuichi, T., Ikegawa, S., Tanegashima, K., Zhao, H., Rebbert, M., Dawid, I., Fox, R., Hanlon, C., Andrew, D., Lee, M., Chanda, D., Yang, J., Oh, H., Kim, S., Yoon, Y., Hong, S., Park, K., Lee, I., Choi, C., Vecchi, C., Montosi, G., Zhang, K., Lamberti, I., Duncan, S., Kaufman, R., Pietrangelo, A., Adham, I., Eck, T., Mierau, K., Muller, N., Sallam, M., Paprotta, I., Schubert, S., Hoyer-Fender, S., Engel, W., Nagamori, I., Yomogida, K., Ikawa, M., Okabe, M., Yabuta, N., Nojima, H., Jin, D., Wang, H., Zhou, Y., Chun, A., Kibler, K., Hou, Y., Kung, H., Jeang, K., Ko, J., Jang, S., Kim, Y., Kim, I., Sung, H., Kim, H., Park, J., Lee, Y., Kim, J., Na, D., Eleveld-Trancikova, D., Sanecka, A., Hout-Kuijper, M. van, Looman, M., Hendriks, I., Jansen, B., Adema, G., Omori, Y., Imai, J., Suzuki, Y., Watanabe, S., Tanigami, A., Sugano, S., Chin, K.,

- Zhou, H., Wong, C., Lee, J., Chan, C., Qiang, B., Yuan, J., Ng, I., Jin, D., Aicha, S. Ben, Lessard, J., Pelletier, M., Fournier, A., Calvo, E., Labrie, C., Labrie, C., Lessard, J., Aicha, S. Ben, Savard, M., Pelletier, M., Fournier, A., Lavergne, E., Calvo, E., Chen, X., Shen, J., Prywes, R., Nadanaka, S., Okada, T., Yoshida, H., Mori, K., Chan, C., Mak, T., Chin, K., Ng, I.-L., Jin, D., Gao, H., Brandizzi, F., Benning, C., Larkin, R., Liu, J., Srivastava, R., Che, P., Howell, S., Hua, X., Nohturfft, A., Goldstein, J., Brown, M., Yang, T., Espenshade, P., Wright, M., Yabe, D., Gong, Y., Aebersold, R., Goldstein, J., Brown, M., Wu, M., Hill, C., Bailey, D., Barreca, C., O, P., Danno, H., Ishii, K., Nakagawa, Y., Mikami, M., Yamamoto, T., Yabe, S., Furusawa, M., Kumadaki, S., Watanabe, K., Shimizu, H., Gentile, C., Wang, D., Pfaffenbach, K., Cox, R., Wei, Y., Pagliassotti, M., Audas, T., Li, Y., Liang, G., Lu, R., Jang, S., Kim, Y., Kim, Y., Sung, H., Ko, J., Kim, H., Choi, K., Choi, H., Kang, H., Kim, M., Lee, Y., Lee, O., Lee, J., Kim, Y., Jun, W., Mertens, F., Fletcher, C., Antonescu, C., Coindre, J., Colecchia, M., Domanski, H., Downs-Kelly, E., Fisher, C., Goldblum, J., Guillou, L., Panagopoulos, I., Storlazzi, C., Fletcher, C., Fletcher, J., Nascimento, A., Domanski, H., Wejde, J., Brosjo, O., Rydholm, A., Isaksson, M., Franchi, A., Massi, D., Santucci, M., Lui, W., Zeng, L., Rehrmann, V., Deshpande, S., Tretiakova, M., Kaplan, E., Leibiger, I., Leibiger, B., Enberg, U., Hoog, A., Sheng, Z., Li, L., Zhu, L., Smith, T., Demers, A., Ross, A., Moser, R., and Green, M. (2011) CREB3 subfamily transcription factors are not created equal: Recent insights from global analyses and animal models. *Cell Biosci.* **1**, 6
40. Taniguchi, M., and Yoshida, H. (2017) TFE3, HSP47, and CREB3 Pathways of the Mammalian Golgi Stress Response. *Cell Struct. Funct.* **42**, 27–36
 41. Carim-Todd, L., Sumoy, L., Andreu, N., Estivill, X., and Escarceller, M. (2001) Cloning, mapping and expression analysis of C15orf4, a novel human gene with homology to the yeast mitochondrial ribosomal protein Ym130 gene. *DNA Seq.* **12**, 91–96
 42. Brown, A., Amunts, A., Bai, X. -c., Sugimoto, Y., Edwards, P. C., Murshudov, G., Scheres, S. H. W., and Ramakrishnan, V. (2014) Structure of the large ribosomal subunit from human mitochondria. *Science (80-)*. **346**, 718–722
 43. Staals, R. H. J., and Pruijn, G. J. M. (2010) The human exosome and disease. *Adv. Exp. Med. Biol.* **702**, 132–142
 44. Bluthner, M., and Bautz, F. A. (1992) Cloning and characterization of the cDNA coding for a polymyositis-scleroderma overlap syndrome-related nucleolar 100-kD protein. *J Exp Med.* **176**, 973–980
 45. Huynh, K. D., Fischle, W., Verdin, E., and Bardwell, V. J. (2000) BCoR, a novel corepressor involved in BCL-6 repression. *Genes Dev.* **14**, 1810–1823
 46. Martínez de Paz, A., and Ausió, J. (2016) HMGNs: The enhancer charmers. *BioEssays.* **38**, 226–231
 47. Porpaczy, E., Bilban, M., Heinze, G., Gruber, M., Vanura, K., Schwarzinger, I., Stilgenbauer, S., Streubel, B., Fonatsch, C., and Jaeger, U. (2009) Gene expression signature of chronic lymphocytic leukaemia with Trisomy 12. *Eur J Clin Invest.* **39**, 568–575
 48. Marimuthu, A., Chavan, S., Sathe, G., Sahasrabudhe, N. A., Srikanth, S. M., Renuse, S., Ahmad, S., Radhakrishnan, A., Barbhuiya, M. A., Kumar, R. V., Harsha, H. C., Sidransky, D., Califano, J., Pandey, A., and Chatterjee, A. Identification of head and neck squamous cell carcinoma biomarker candidates through proteomic analysis of cancer cell secretome. *Biochim Biophys Acta.* **1834**, 2308–2316
 49. Yang, Q., Bavi, P., Wang, J. Y., and Roehrl, M. H. (2017) Immuno-proteomic discovery of tumor tissue autoantigens identifies olfactomedin 4, CD11b, and integrin alpha-2 as markers of colorectal cancer with liver metastases. *J. Proteomics.* 10.1016/j.jprot.2017.06.021
-

8. Results Part II

8.1. Introduction to results

Here I would like firstly to remind briefly all step by step passages performed in the second part of the project, that have been already highlighted in the project summary.

1.Samples collection. Ascites from 153 patients (various disease conditions)

- 69 ascites patients with ovarian cancer
- 34 ascites patient with other cancers
- 50 non-cancerous control ascites

2.Identification of autoantibodies in ovarian cancer patient ascites. IF staining of OVCAR-3 cell membrane using ovarian cancer ascites → result showed that ascites contain high titer of autoantibodies recognizing some protein on the membrane → these antibodies able to activate CDC.

3.Anti-PDIA1 is the most abundant antibody in ovarian cancer ascites. SERPA analysis and MS identified that PDIA1 protein had the highest antibodies binding (Fig.8).

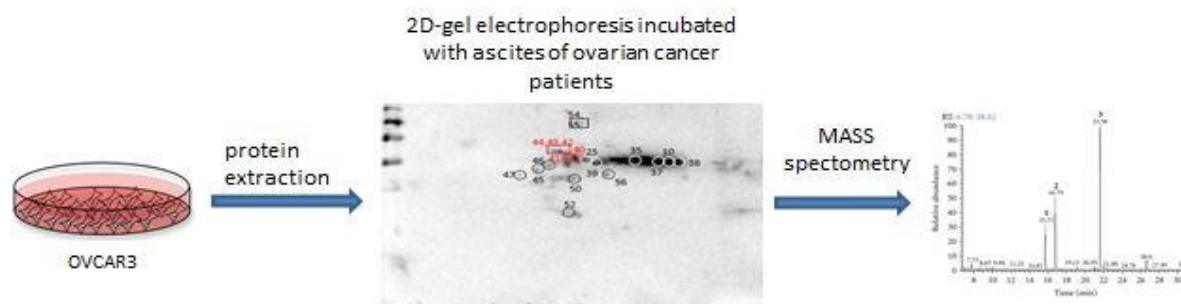


Fig.8. Scheme of anti-PDIA1 autoantibodies identification by SERPA. OVCAR-3 cell lysate was separated by 2D-gel electrophoresis, transferred to membrane and incubated with ascites of ovarian cancer patients. Spots, where antibodies showed binding were isolated and analyzed by mass spectrometry for protein identification.

4.ELISA assay confirmed high titer of anti-PDIA1 antibodies in ovarian cancer ascites. ELISA assay → testing antibodies from ovarian cancer/non-cancerous/other cancer ascites binding to PDIA1 protein → ovarian cancer ascites have significantly higher binding → higher titer of anti-PDIA1 antibodies positively correlate with higher survival rate of ovarian cancer patients.

5.Anti-PDIA1 antibodies activate CDC. Affinity purified from ovarian cancer ascites anti-PDIA1 antibodies showed its ability to activate CDC and lead to ovarian cancer cells killing.

6.Anti-PDIA1 scFv's were obtained by phage display library selection. Phage display selection → three scFv's had strong reactivity to PDIA1 → were used for further recombinant antibodies construction.

7.Recombinant anti-PDIA1 antibodies construction. scFv's were cloned into vector containing human Fc → vector was transfected into CHO cells → best antibody secreting CHO cells were obtained by monoclonal selection → antibodies secreting CHO cells were expanded and antibodies were collected from cells growing medium.

8. Antibodies showed it functionality in standard laboratory assays. Recombinant anti-PDI antibodies were tested in WB, ELISA, IF, IP, FACS → they showed it functionality and activity → specificity of antibodies to PDIA1 was confirmed by competition assay.

9. Antibodies epitopes were identified for complete antibody characteristic. Different length of PDI protein fragments were constructed → they were used in ELISA assay → all three antibodies recognize different epitope.

10. CDC assay. Recombinant antibodies were used in CDC assay → antibodies were “positive” in activation of complement that lead to 8% of ovarian cancer cell killing.

8.2. Tumor associated antigen identification

8.2.1. Ovarian cancer patient ascites antibodies identification

Ascites were collected from 153 patients representing various disease conditions that includes: 69 ascites from patients diagnosed with ovarian cancer, 34 ascites from patient that were having other cancers than ovarian and 50 non-cancerous ascites from female patients with no known history of cancer. Ovarian cancer ascitic fluid represents stage I-VI collected from both platinum sensitive and resistant patients with grade ranging from G1-G3. Cancer other than ovarian includes cancer of lung, liver, colon, fallopian tube, breast, gallbladder, pancreas, rectum, lymph nodes, lymphoma, various mesothelioma including peritoneal lining, adenocarcinoma of pulmonary, gastric and other organs. While, non-cancerous ascites were collected from patients having conditions such as cirrhosis, caused by various reasons, pulmonary fibrosis, cholestatic liver diseases, pneumonia, accumulation due to various transplantations, heteroplasia, inflammation etc.

These ascites were analyzed to identify antibodies present in ascitic fluids that are raised against ovarian cancer tumor associated antigens. To understand it, immunofluorescent staining was performed, where ovarian cancer cells OVCAR-3 were incubated by ascites from ovarian cancer patients. To exclude the possibility for cellular uptake of antibodies, incubations were performed at 4°C which, resulted only in binding to the cell membrane since cellular uptake does not occur at this temperature. Cell surface localization of tumor specific antibody was detected with anti-human immunoglobulin conjugated to Cy5. As result it was seen that antibodies from ascites of ovarian cancer patients bind the cell membrane proteins of ovarian cancer cells and give a very strong signal (in green, Fig. 9A). Nuclei were stained with propidium iodide (in red). On the contrary, non-cancerous ascites showed no staining (Fig. 9B). The mAb cMOV18 (humanized anti-Folate antibody) directed against the isoform α of the Folate receptors which are overexpressed by endothelial ovarian cancer cell on their cell surface was used as positive control for this assay (Fig. 9C).

Subsequently, a cell surface ELISA was performed on live OVCAR-3 cells to determine the presence and to quantify the amount of immun-reactive antibodies present in ascitic fluid directed against cell surface tumor antigen. 80% confluent live OVCAR-3 cells were incubated with 1:50 dilution of primary antibody (affinity-purified antibodies from ovarian, other cancer and non-cancerous control). Afterwards, secondary antibody was added to determine bound primary antibodies. Fig. 10A shows the cell surface result for set of 147 ascitic fluid. 34.78% (24/69) of ascitic fluid from patients with ovarian cancer shown to have significantly higher signal for the presence of specific antibodies against cell surface tumor antigen as compared to 4/28 ascitic fluid from other cancer patients. Except 1 out of 50, none of the non-cancerous controls (49/50) were able to produce any signal, leaving them below the cut off. Based on results of cell surface ELISA it was possible to quantify the signal of immune-reactive antibodies present in ascitic fluid directed against cell surface tumor antigen. In addition, this

assay provides a highly specific results that shows significant difference between ovarian cancer patients and non-cancerous patients as well as other cancer patients ascites with P-value<0.0001 for both cases.

Overall, our data confirms the presence of tumor specific antibodies in ovarian cancer ascites targeting surface antigen. After obtaining these results, it was further important to understand if these tumor specific antibodies when interact with cell surface antigen are capable to activate complement pathway and regulate tumor grown by complement dependent cytotoxicity. As it is represented in Fig.10B, 32 out of 68 ascitic fluid from ovarian cancer patients shown to have presence of tumor specific antibodies which are capable to activate C system leading to the killing. None of non-cancerous sample IgG's were able to cause killing, indicating the absence or presence of these specific antibody in very low concentration. Later, a comparative analysis was made between CDC assays and cell surface ELISA to understand their correlation. Scatter plot (Fig. 10C) shows 75% of cell surface ELISA positive ascites are capable to mediate complement dependent killing of the ovarian carcinoma cell line. Summarizing these results it was concluded that ascites of ovarian cancer patient contain a pool of antibodies specific to some proteins present on the cell membrane of ovarian cancer cells. Moreover, targeting these proteins antibodies are able to activate CDC that lead to cancer cells killing.

Characterization of ascitic fluid based on immune response

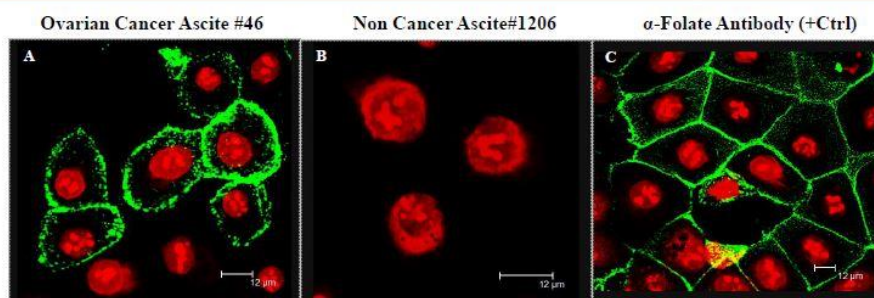


Fig.9. Characterization of ascitic fluid based on immune response. (A) Immunofluorescent staining of ovarian cancer cells surface previously incubated by ovarian cancer ascites of patient #46. (B) Immunofluorescent staining of cell surface of ovarian cancer cells previously incubated by non-cancerous ascite of patient #1206. (C) anti-Folate staining of ovarian cancer cell surface.

Ascites antibodies in Cell Surface ELISA and CDC assay

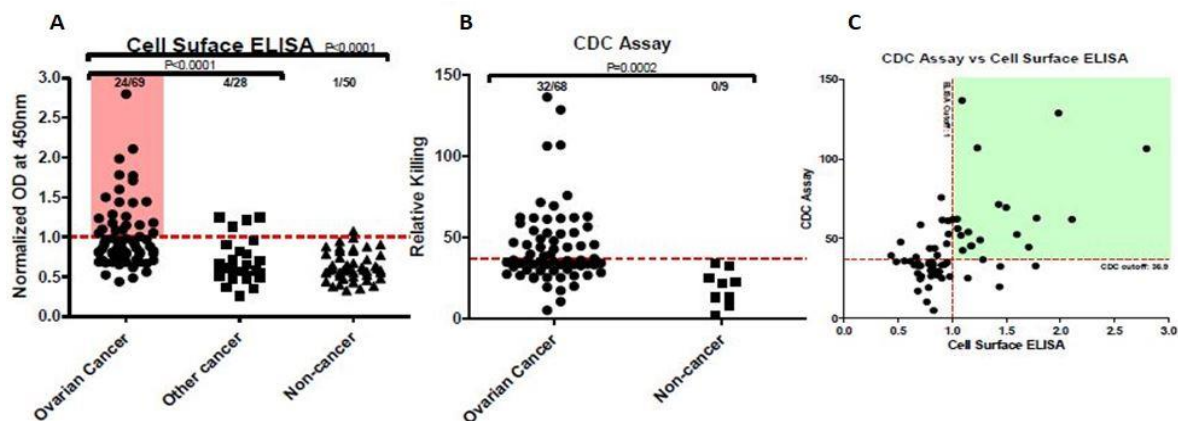


Fig.10. Ascites antibodies in Cell Surface ELISA and CDC assay. (A) Cell Surface Elisa. (B) Complement Dependent Cytotoxicity Assay. (C) Comparative analysis of CDC assay versus cell surface ELISA of all ovarian cancer ascites

8.2.2. SERPA tumor associated antigens identification

After autoantibodies present in ascites of ovarian cancer patients were discovered, it was essentially, as the next step, to understand which protein exactly on the cell membrane is triggering so strongly antibody production. To answer this question, was performed Serological Proteome Analysis (SERPA). SERPA is a tool for the identification of tumor antigens able to trigger immune responses and antibody production. This approach combines classical 2-DE SDS-PAGE with Western blotting and MS. Big advantage of SERPA is that it analyze proteins in its nature form and can recognize post-translationally modified proteins as a source of potential TAA. To perform SERPA, OVCAR-3 cell lysate was separated on gel by 2-DE SDS-PAGE. 2D electrophoresis is the classical technique for proteome analysis that separate proteins in a mix based on their isoelectric points and molecular weights. 2D electrophoresis is still the best technique for the high-resolution separation of a complex mixture of proteins that can differentiate post-translationally modified proteins and protein isoforms. Afterwards, protein were transferred to nitrocellulose membrane by electroblotting and subsequently incubated by ovarian cancer patient ascites and non-cancerous ascites. Antibodies present in ascites bound proteins on the membrane and were visualized with secondary anti-human antibodies. The cancer-associated antigenic spots were identified by MS and immuno-reactive profiles of ovarian cancer and non-cancerous ascites were compared. One of the identified proteins that showed the most abundant antibody binding result was PDIA1. Non-cancerous ascites that was used as a negative control didn't show proteins binding in SERPA (Fig.11). Based on these results, it was concluded that anti-PDIA1 antibody is the most abundant antibody in the antibodies pool in ovarian cancer patient ascites.

Serological Proteome Analysis (SERPA)

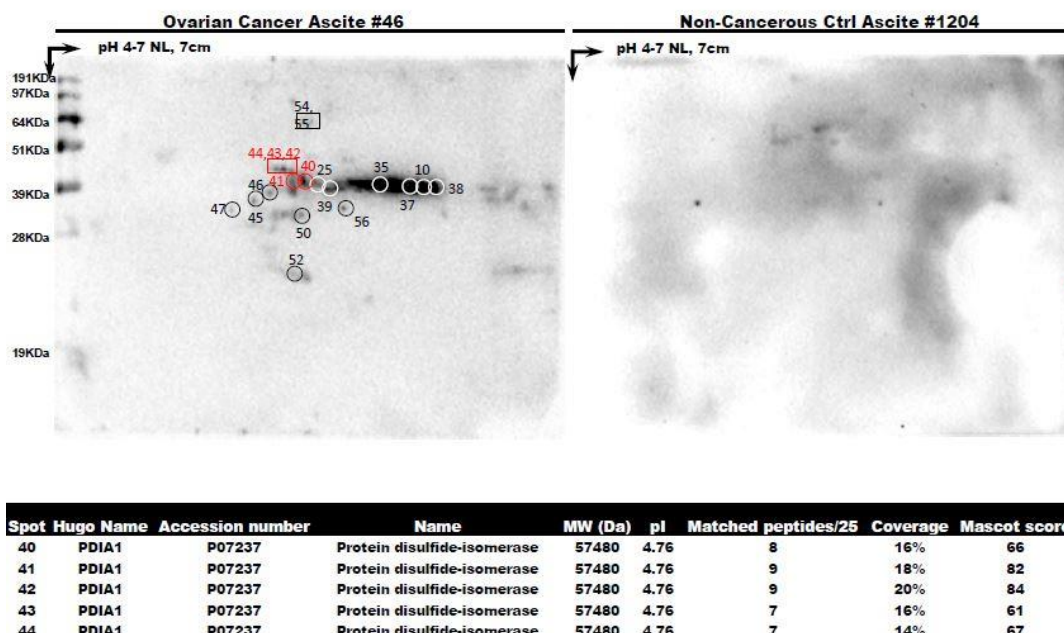


Fig.11. Serological Proteome Analysis. Recognition of OVCAR-3 cell lysate proteins separated by 2D-gelectoforesis and transferred to membrane by ovarian cancer (left panel) and non-cancerous (right panel) patient ascites and identification PDI as the most abundant antibody binding protein by MS (under panel).

8.2.3. ELISA assay PDI specificity of ovarian cancer patient ascites antibodies

As the next step, indirect ELISA assay was performed to determine whether the antibodies present in the ascitic fluid from the ovarian cancer patients specifically recognize PDIA1 protein identified by SERPA. This techniques offer a higher level of sensitivity to measured autoantibodies even at a very low concentration. Each well of ELISA plate was coated with 1 μ g of recombinant PDIA1 protein in 100 μ l PBS. Antibodies from ovarian cancer, non-cancerous and other cancer ascites were purified, normalized by it concertation and used in ELISA assay. 44 out of 68 ovarian cancer ascites showed a binding higher than cut-off value. Cut-off value was calculated separately for each antigen as mean + 2 times standard deviation of the OD from all non-cancerous control wells. The prevalence of autoantibodies in ovarian cancer patient is described by the P-value, calculated using two tailed unpaired t-test: antigens with P-value<0.05 was considered significant (Fig.12).

A significant association of autoantibody responses with better clinical outcome was found by comparing differences between curves with the log-rank method. Subsequently, clinical data of the corresponding patients were analyzed after the experimental phase of this study was completed. A log-rank method was used to evaluate their significance. Extraordinarily, the result showed a significant difference in survival time between patients whom were having higher response to PDIA1 in ELISA assay compared to the other patients with lower signal to PDIA1 (Fig.12). These results, made to conclude that anti-PDIA1 antibody are specifically present in ascites of ovarian cancer patients and it higher titer is positively influencing overall survival of the patients.

Validation of PDIA1 and Patient Survival

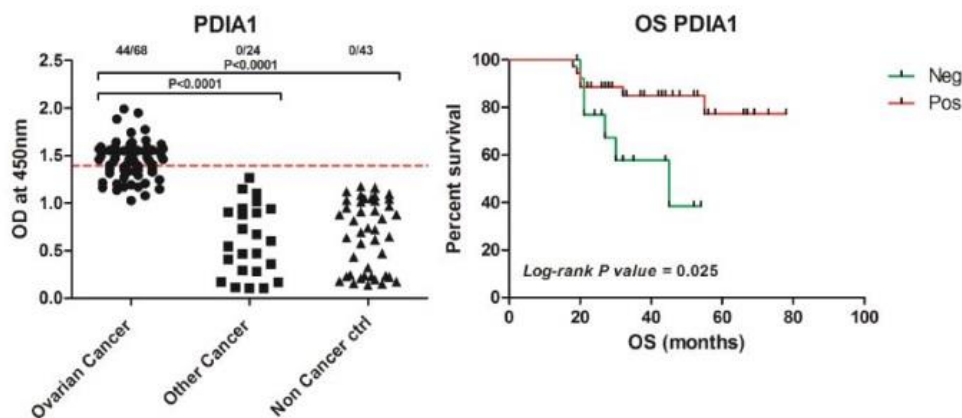


Fig. 12. ELISA assay and Overall patient Survival analysis. Affinity purified antibodies of ovarian cancer, other cancer and non- cancerous ascites reactivity to recombinant PDIA1in ELISA assay (left panel). Analysis of overall survival of ovarian cancer patients, which ascites showed Positive (above threshold) and Negative (bellow threshold) response to PDI in ELISA assay (right panel).

8.2.4. CDC assay

Going further, one of the most important questions to understand is if anti-PDIA1 antibodies present in ascites of patients have its immune functionality. To answer it, anti-PDIA1 antibodies from ovarian cancer patient ascites were affinity purified and used to perform CDC assay. To purify specific anti-PDIA1 antibodies CNBr-activated Sepharose 4B beads were coated with recombinant PDIA1 protein.

Incubated with ovarian cancer patient ascites beads made anti-PDIA1 antibodies present in ascites recognize PDIA1 protein and get purified together with beads. Antibodies afterwards were eluted by pH change. To perform CDC assay, confluent OVCAR cells were incubated with affinity purified anti-PDIA1 antibodies from ovarian cancer patient ascites. In parallel with affinity purified antibodies, commercial anti-PDI antibodies (SIGMA) were also tested in this experiment. To represent specificity of affinity purified and commercial antibodies for PDIA1 protein both types of antibodies were additionally blocked by added PDI protein. Pre-blocked antibodies were expected to have no activity in CDC assay. Antibody mixture of cMOV18 and cMOV19 anti-Folate receptor antibodies was used as a positive control. cMOV18/19 were selected for positive control, as its functionality in activation of CDC and ovarian cancer cells killing has been studied and widely described (55). Further, NHS containing complement factors were added to the cells to activate complement pathway which resulted in formation of membrane attack complex (MAC) on their cell membrane and lead to complement dependent cytotoxicity. The residual viable cells as well as number of killed cells were estimated by the MTT assay. The resulting purple solution is spectrophotometrically measured at 570nm and can be directly related to the number of viable (living) cells. Considering the cells with only NHS ('no antibody') as 100% living cells, the percentage of dead cells was calculated as: % of dead cells = 100 - [100 x (average of cells +Abs)/ (Average of cells +NHS)]. As expected, a 25-30% of OVCAR-3 cells killing was attained by the mixture of cMOV18 and cMOV19 via complement activation. Anti-PDIA1 antibodies were able to activate complement dependent cytotoxicity and result in almost 25% of ovarian cancer cells killing. Inhibited antibodies showed decreased killing ability, which confirms specificity of antibodies (Fig. 13). Overall, CDC assay showed fascinating results, that made it concluded that anti-PDIA1 antibodies from ovarian cancer patient ascites target PDIA1 on the cell surface and trigger immune response.

αPDIA1 Mediated Complement-Dependent Cytotoxicity

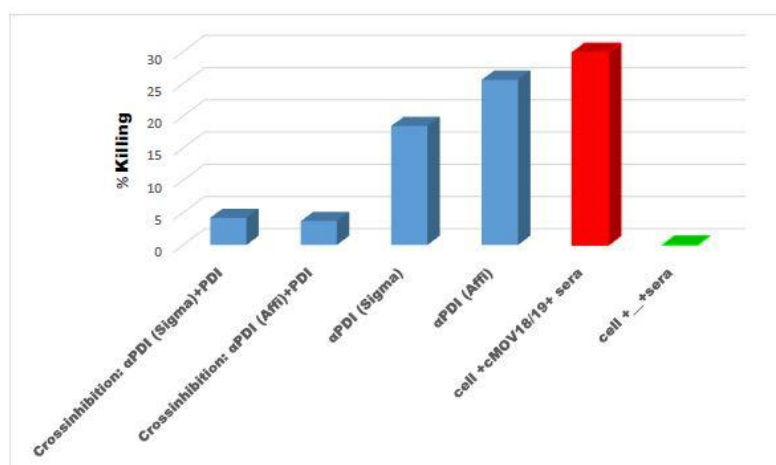


Fig.13. Anti-PDIA1 mediated complement dependent cytotoxicity. Affinity purified anti-PDI antibodies from ovarian cancer patient ascites, commercial anti-PDI and anti-Folate (used as positive control) antibodies activation of CDC. Affinity purified and commercial anti-PDI antibodies were cross-inhibited by incubation with PDI protein to represent its specificity.

8.2.5. OVCAR-3 surface PDI staining

It is, however, known that PDI is an intracellular protein, localized in endoplasmic reticulum (ER) and in normal cells is not expected to be represented on cell surface. Further literature studies confirmed that in cancer cells chaperon proteins can be translocated to the cell surface. To confirm PDI presence on the cell surface, PDIA1 protein was shown by Immunofluorescent staining using commercial anti-PDI antibodies on living, not permeabilized OVCAR-3 cells. In Fig.14 PDI staining is represented in green. Mixture of cMOV18 and cMOV19, that target anti-Folate receptor was used for membrane surface staining (in red). As result we were able to represent presence of PDIA1 protein on the cell surface of ovarian cancer cells. PDI, present on the cell surface, shows not homogeneous dot staining

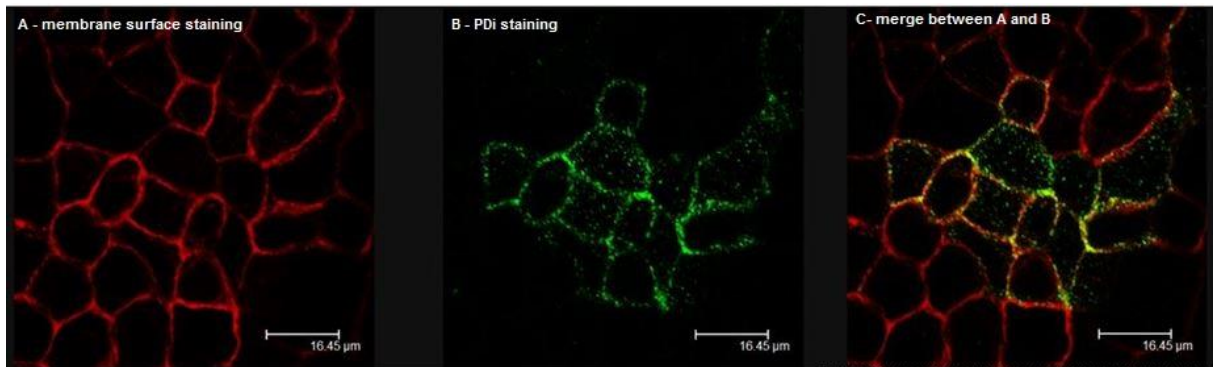


Fig.14. PDI surface staining on not permeabilised OVCAR-3 cells. (A) membrane surface staining (anti-Folate receptor staining). (B) surface PDIA1 staining. (C) merge between A and B.

Summarizing all results our findings indicate that PDIA1 protein is a potential tumor associate antigen, present in ovarian cancer ascites that is able to trigger immune system and correlate with higher survival of patients. Antibodies raised by organism against PDIA1 showed it ability to activate CDC and lead to ovarian cancer cells killing. As conclusion PDIA1 is proposed to be promising target for potential ovarian cancer immunotherapy.

8.3. Recombinant antibodies production

8.3.1. Phage display antibodies selection

Based on our hypothesis that PDIA1 is a promising tumor associated antigen, we decided to engineer recombinant anti-PDIA1 antibodies. For it, PDIA1 specific scFv's were selected from the naïve antibodies scFv's phage display library, present in Department of Life Science at the University of Trieste. The following steps briefly summarizes selection of PDIA1 specific scFv's from phage antibody library.

1. Library amplification and phage particle production.
2. Immuno-tube coated by protein of interest overnight.
3. Immuno-tube incubation with phage preparation.
4. Washing steps: Extensive washes were performed to remove unbound phages.
5. Elution and amplification of bound phages by infecting host bacteria: Bound phages were eluted with DH5 α F' bacterial culture and plated onto agar plates.
6. Individual colonies can be picked from agar plate and screened for it specificity in phage ELISA assay.

After two rounds of phage display selection 193 different colonies were manually picked and screened for it specificity to PDIA1 in phage ELISA assay. 36% of all colonies were having a strong reactivity

signal in ELISA assay. 27% were having less strong signal and 35% were having low or no signal to PDIA1 as shown in Fig.15.

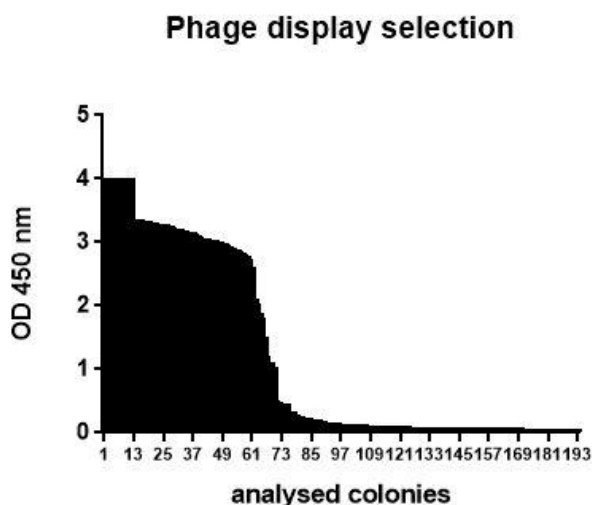


Fig.15. Specific for PDI clones, identified during phage selection. 193 different colonies manually picked during phage display selection arranged in them reactivity to PDI protein. 36% of all colonies showed a strong reactivity signal in ELISA assay

On most reactive clones was performed finger printing analysis. Here PCR reaction was performed for individual colonies using scFv specific primers. Afterwards PCR product was digested using HaeIII and BstnI restriction enzymes and determined by running of a 1% agarose gel. Different sequence of scFv's gives different cut patron of PCR product and can give initial idea about which antibodies were selected (figure not shown).

After finger printing 6 clones were selected that showed different cut pattern. The heavy (VH) and light chains (VL) of scFv's genes were sequenced, and the gene segments were assessed using the ImMunoGeneTics/V-QUEST tool in the ImMunoGeneTics information system (<http://www.imgt.org/>) (56). This way it was confirmed that VH and VL fragments sequence of 6 selected clones were different from each other (Tab.2).

ID	VL gene	VL CDR3	VH gene	VH CDR3
A8	IGKV1-39*01	CQQSYNMPPTF	IGHV3-23*04	CAKTGAYTPL
H7	IGKV3-15*01	CQQYYSAPYTF	IGHV3-23*04	CARGATRTYYYDSSGYYYAYW
H12	IGKV3-20*01	CQQYGSSPRTF	IGHV1-2*02	CAYGPPRGYSYARTVYFDYW
B10	IGKV1-5*03	CQQYNNWPRTF	IGHV1-69*14	CARAYSGSYSGAFDIW
D9	IGLV7-46*01	YLVSYSGDRV	IGHV4-38-2*01	CARAPRGYSYGYVFGGRRYFDLW
D2	IGLV2-8*01	CNSYAGNTVLF	IGHV4-59*01	CASSPLLWFGEKNGGSLDYW

Tab.2. Specific for PDI clones selected as result of sequencing of plasmid.

Further, selected clones were tested for it specificity to PDIA1 by performing phage ELISA assay. Selected scFv's were produced fused to pIII protein on the phage particle and screened against coated proteins. Specificity of the clones in phage ELISA experiment was tested to folded GST-PDI, folded HIS-PDI and denatured in 8M urea HIS-PDI, GST, HIS-TG2 . Binding to HIS-TG2 and GST proteins was performed as a control (Fig.16) to see if antibodies were not selected against GST and HIS tag. Result showed that H12, B10 and H7 were having the strongest signal in phage ELISA. H12 antibody

had also strong signal recognizing PDI in denatured conditions, while B10 and H7 recognize PDI only its native conformation.

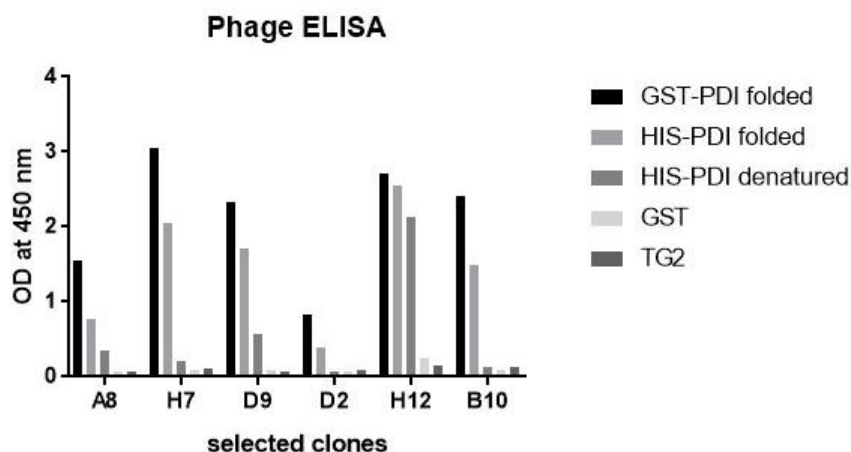


Fig.16. Phage ELISA for selected clones A8, H7, D9, D2, H12 and B10. Phage clones were tested for its reactivity to GST-PDI folded, HIS-PDI folded, HIS-PDI denatured, GST and HIS-TG2 proteins (used as a control proteins to show that scFv's were selected against PDI protein and not to its tag, which were GST and 6xHIS).

Clones H12, H7, B10 were selected for further cloning and recombinant antibodies engineering (Tab.3).

ID	VL gene	VL CDR3	VH gene	VH CDR3
H12	IGKV3-20*01	CQQYGSSPRTF	IGHV1-2*02	CAYGPPRGYSYARTVYFDYW
B10	IGKV1-5*03	CQQYNNWPRTF	IGHV1-69*14	CARAYSGSYSGAFDIW
H7	IGKV3-15*01	CQQYYSAPYTF	IGHV3-23*04	CARGATRTYYDSSGYYYAYW

Tab.3. Clones selected for TAG mutagenesis and further antibody production.

Finger printing analyze using HaeIII and BstNI restriction enzymes performed on H12, H7 and B10 clones showed three different cut pattern as represented in Fig. 17.

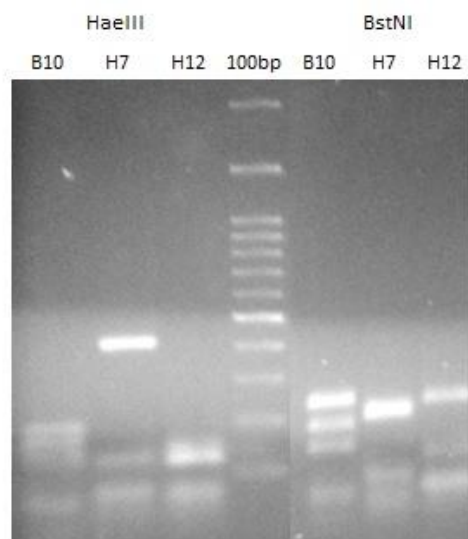


Fig.17. Finger printing analyze. B10, H12, H7 clones restricted by HaeIII and BstNI restriction enzymes that represent different cut patterns for each antibody confirming that antibodies are different from each other.

8.3.2. Antibody production

As the next step selected scFv's had to be produced as antibodies in eukaryotic cells. For it scFv's sequences were cloned in eukaryotic expression vector. Fig. 18 represents all passages performed for complete antibody production.

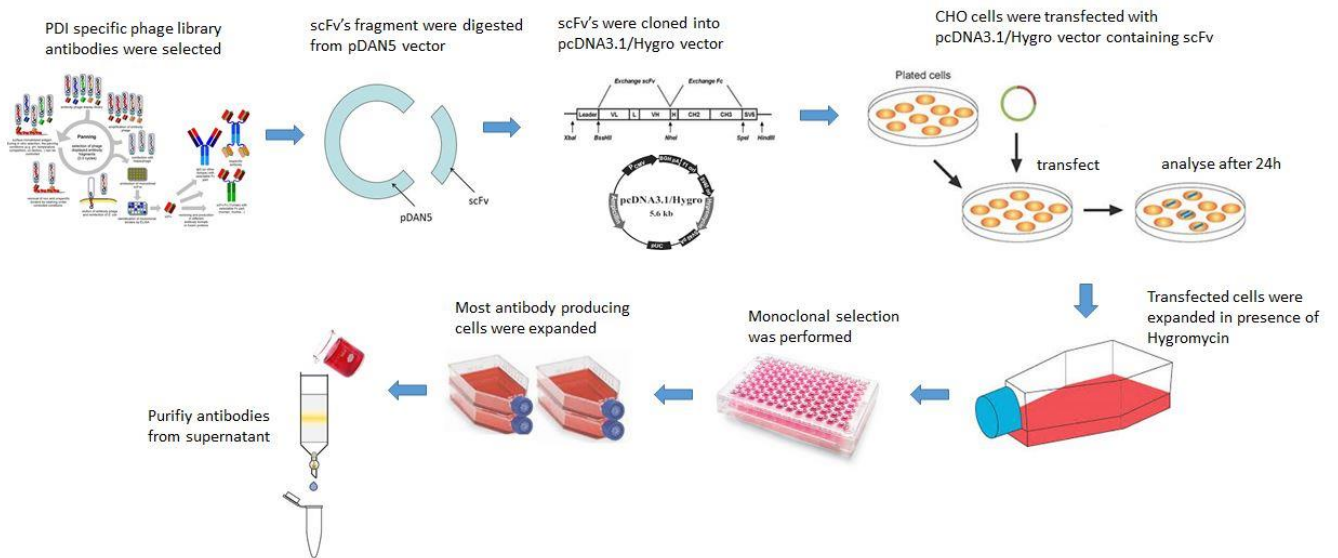


Fig.18. Schematic representation of H12, H7 and B10 antibodies (minibodies) production. Plasmid pDAN5 present in selected phage clones was extracted. scFv's were digested from pDAN plasmid and cloned into pcDNA3.1/Hygro(+) vector. This vector was analyzed for its correct sequence and transfected into CHO cells. Transfected CHO cells were grown under Hygromycin selection for two days. Cells that developed resistance to Hygromycin were grown in 96 well plates in concentration 1 cell/well for monoclonal selection. Best antibody producing cells were selected based on WB and ELISA results and were expanded. Supernatant of it was collected and used to purify antibodies.

For it, scFv's of H12, H7 and B10 clones were digested from pDAN5 vector using restriction enzymes BssHIII and NheI and cloned into pcDNA3.1/Hygro(+) vector. Fig. 19A represents a schematically cloned minibody, where variable regions of heavy (VH) and light (VL) chains conjugated by linker (L) were cloned into vector that already contained Human Fc domains sequence (CH2-CH3) and small SV5 tag sequence. Using this approach it is possible to produce minibodies with Fc of different species, depends on the model organism used in the experiments. pcDNA3.1/Hygro(+) plasmids with H12, H7 and B10 were transfected into CHO cells. pcDNA3.1/Hygro(+) vector contains a gene for hygromycin resistance, that allow to select those cells that received plasmid and incorporated in its genome correctly by growing cells in presence of hygromycin. Afterwards the most stable and best antibody producing cell was obtained by performing monoclonal selection. Supernatant of those wells where cells were growing was tested for produced and secreted antibodies in ELISA assay or WB. Cells that showed best antibody production were expanded and were grown in T75 flasks till it confluency. Supernatant was collected and antibodies were purified by incubating it with Protein A agarose. The yield of purified antibodies was around 0,2-0,5mg/L. Fig.19B represents recombinant antibody validated and quantified by SDS-PAGE. The predicted molecular weight of the miniantibodies is about 55 kDa but in acrylamide gel is running between 55 and 70 kDa due to its glycosylation. Moreover, recombinant antibodies H12, B10 and H7 were visualized in WB using anti-human conjugated HRP antibody and anti-SV5 antibody (Fig.19B).

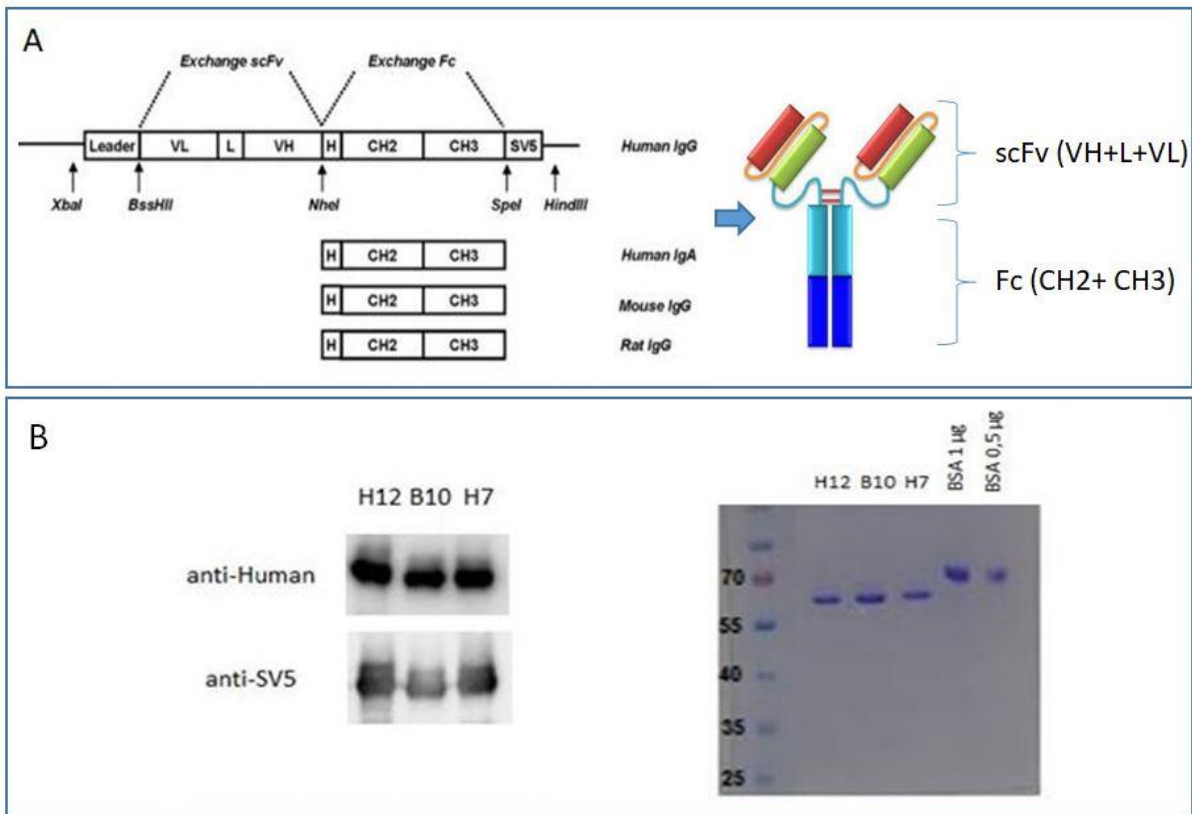


Fig.19. Minibody production. (A) Scheme of selected scFv's cloning into pcDNA3.1/Hygro(+) vector already containing Fc fragment that can be of different species (1). (B) Produced antibodies were visualized in Western Blotting by anti-human and anti-SV5 antibodies. Produced antibodies were visualized and quantified in SDS-PAGE gel.

8.3.3. ELISA assay

Recombinant antibodies were validated in different assay to represent its functionality. It was shown that recombinant antibodies can be used in ELISA assay and are able to recognize recombinant HIS-PDI protein at different concentrations (Fig.20.).

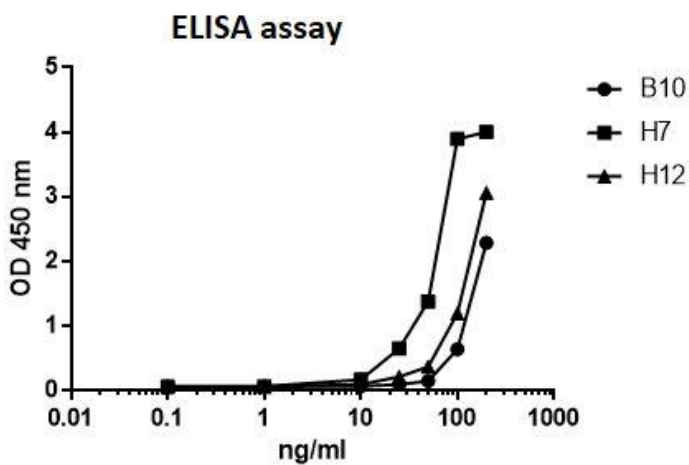


Fig.20. ELISA assay. ELISA wells were coated with 1µg/well recombinant HIS-PDI. Recombinant antibodies were used in different concentration to represent its reactivity to PDI.

Based on the ELISA assay values we calculated affinity of antibodies to PDI. In this method, the binding of an antibody to antigen is measured by ELISA using serial dilutions of antibody. OD measured after the antigen antibody interaction was plotted against the concentration of Ab, that gives a hyperbolic curve. Here, antibody concentration in ELISA assay was plotted against normalized activity of antibodies. Saturating value of each antibody in ELISA assay was considered as maximum binding of antibody to available epitopes and was normalized till 1.0. As it can be seen in Fig. 21 all three antibodies are having quit similar affinity to the PDI protein.

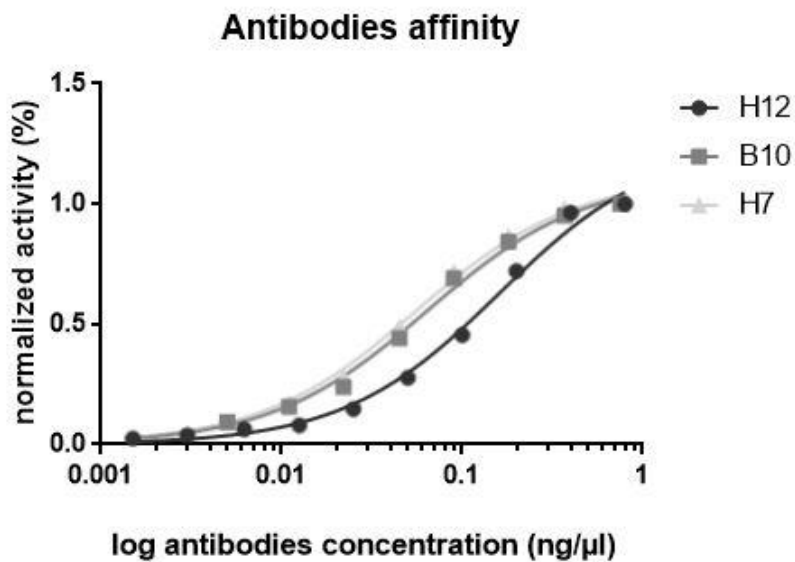


Fig.21. Antibodies affinity. Saturating value of each antibody in ELISA assay was considered as maximum binding of antibody and was normalized till 1.0.

8.3.4. Epitope mapping

Epitope is the part of an antigen that is recognized by antibody. To understand which domain of PDIA1 protein is recognized by recombinant antibodies, different length fragments of PDIA1 protein were produced. For it were created specific primers for amplification of different fragments of PDI protein. These fragments were cloned and expressed as proteins to perform epitope mapping for H12, H7 and B10 antibodies. Recombinant PDI protein as all PDI fragments were cloned into pTrcHis B vector (Fig.22) using BamHI and EcoRI restriction sites.

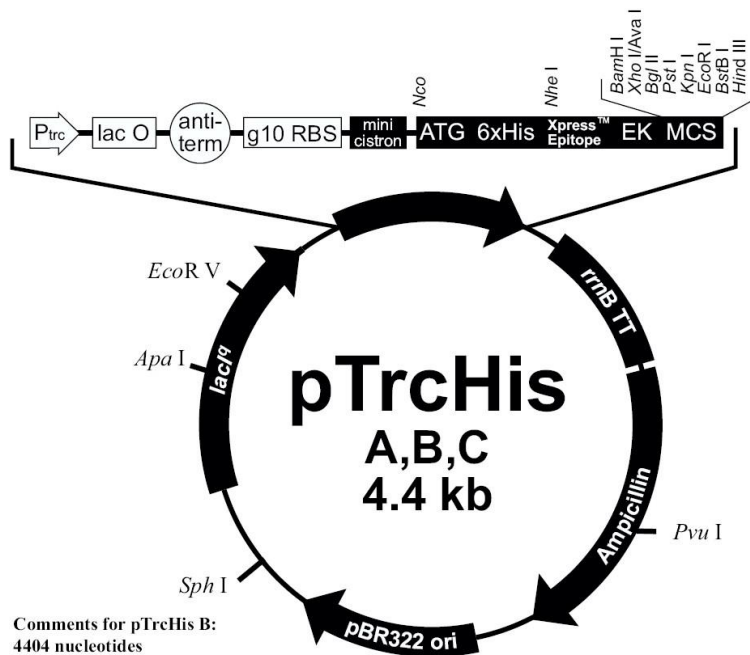


Fig.22. pTrcHis B vector map

Different size PDI fragments were cloned as represented in Fig.23. Full PDIA1 protein contains domains A, B, B', linker (represented in black), A' and C. Construct 1 contains A, B, B', linker and A' domains. Construct 2 contains A, B, and B' domains. Construct 3 contains A and B domains. Construct 4 contains B', linker and A' domains. Construct 5 contains A' and C domains. Construct 6 contains B' domain, Construct 7 contains linker and A' domains. Construct 8 contains half of B', linker and A' and C domains. Each domain is about 300-400 bp, linker is a fragment of 50 bp and C is a terminus sequence about 100bp. Each construct was produced as recombinant protein, purified, validated and quantified by SDS-PAGE (figure not shown).

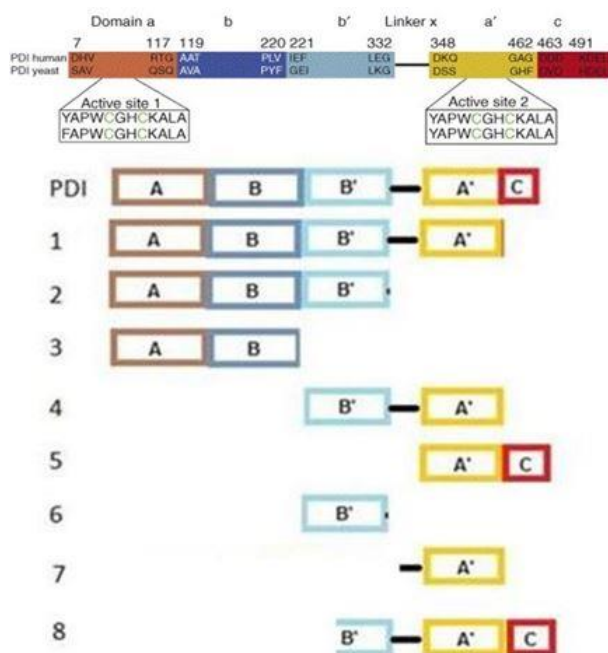


Fig.23. Different length PDI constructs. Schematic representation of different constructs of PDI produced as separate proteins for epitope mapping. Domain A, B, B', linker, A', C correspond to domains as describes by Gruber *et.al.* (57).

Reactivity of recombinant antibodies to each construct was tested in ELISA assay. As result H12 antibody showed it ability to recognize strongly full PDI protein, constructs 1 and 4. H12 gives also a bit lower signal to construct 2 and 8. It made us to conclude that epitope of H12 antibody might be located on the end sequence of B' domain and begin sequence of linker of PDIA1 protein (Fig.24). It is remarkable that presence of a fragment of B' domain, as in construct 8, is already contributing to the antibody signal compare to the construct 7 where signal is absent. This result was confirmed by performing epitope mapping using Western Blotting technique. Fig.25 represents WB results where H12 was used as a primary antibody. As it can be seen, result of epitope mapping ELISA can be confirmed by WB.

ELISA epitope mapping also showed that H7 antibody epitope can be restricted to the fragment of PDI that involves fragment 4. B10 antibody epitope was quite difficult to identify, as this antibody was giving signal only to PDI protein and construct 1 in ELSIA, where conformation of protein is most conserved. B10 might recognize complex conformational epitope (Fig.24). B10 and H7 are conformational antibodies and were not able to be used in WB. It is difficult to take exact conclusion about epitope for H7 and B10, however epitope ELISA assay showed that all three antibodies recognize three different epitopes. Fig. 26 represents fragments of PDI that we concluded are possible epitope sides for antibodies.

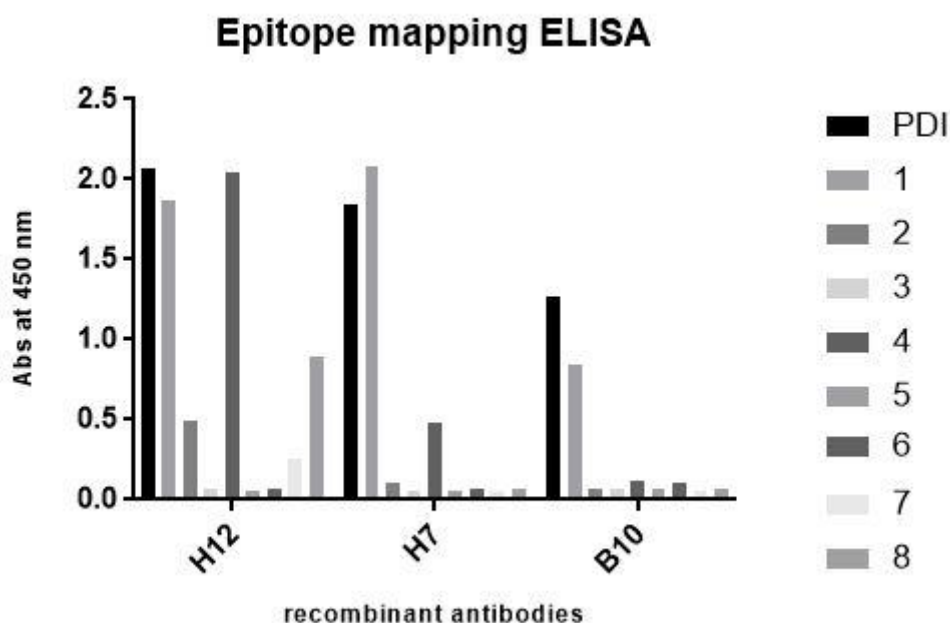


Fig.24. Epitope mapping using ELISA assay. ELISA wells were coated with 1µg/well of each PDI fragment (1-8 numbers correspond to the fragments in Fig.23). Recombinant antibodies show different pattern of epitope recognition.

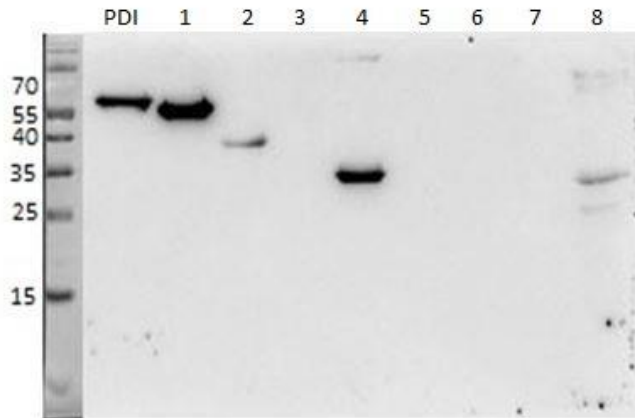


Fig.25. WB epitope mapping of H12 antibody. H12 antibody recognize PDI, constructs 1, 4 and less strongly constructs 2 and 8, that correspond to result in epitope mapping ELISA. Constructs correspond to it predicted weight.

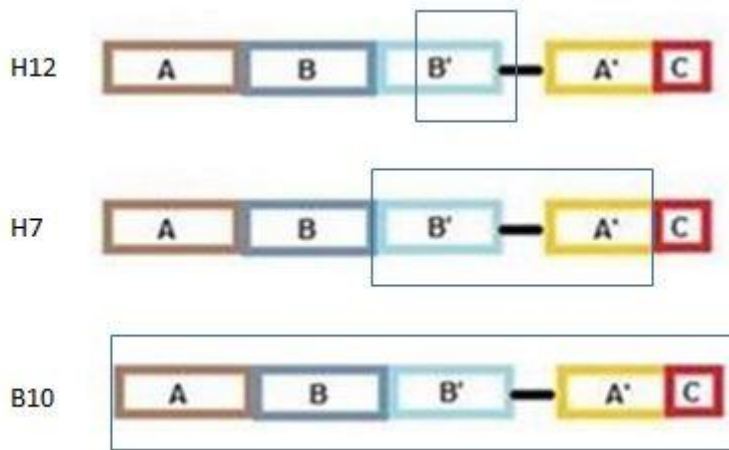


Fig.26. Epitope sites for H12, H7 and B10 antibodies. Representation of PDI protein site supposed to be epitopes of recombinant antibodies. H12 antibody might recognize epitope located in between half of B' domain and part of the linker. H7 antibody recognize epitope in a fragment restricted to B', linker, A' domain. B10 antibody has a complex conformational epitope and can recognize only full correctly folded PDI protein.

8.3.5. Immunofluorescent staining

Recombinant antibodies were tested for it functionality in Immunofluorescent staining. For it OVCAR-3 cells were grown on the microscope glass. Afterwards cells were fixed, permeabilized and stained with recombinant H12, H7 or B10 antibodies. It was shown that H12, H7 and B10 (Fig.27) are able to recognize endogenous PDIA1 protein (in bleu) and give intracellular staining.

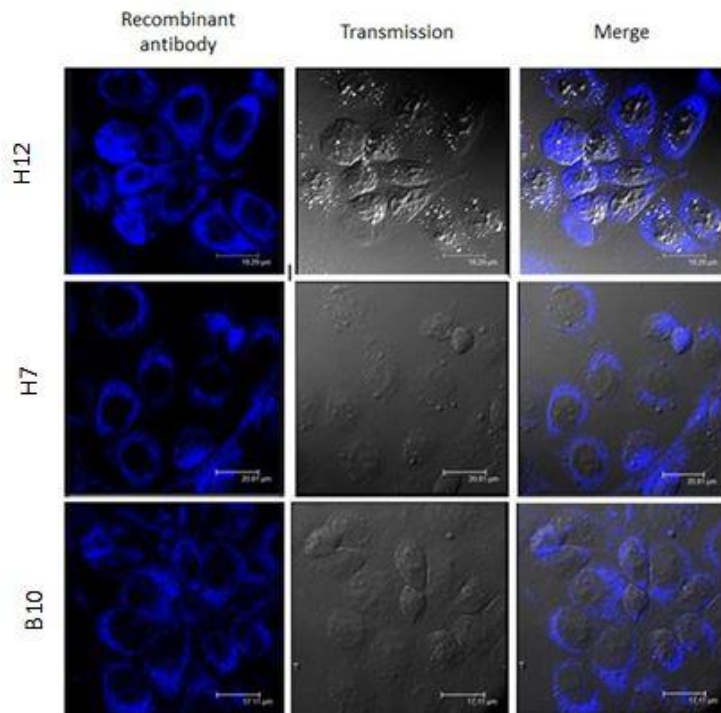


Fig. 27. Immunofluorescent staining of intracellular PDI. OVCAR-3 cell line were permeabilized and stained with recombinant antibodies H12, H7 and B10. Transmission field represents position of the cells on slide. Merge between recombinant antibodies staining and transmission field shows that PDI staining is present in cytoplasm.

To confirm that recombinant antibodies are specific for PDI protein recombinant antibodies were used for intracellular PDI staining in parallel with commercial monoclonal anti-PDI antibodies. Here OVCAR cells were fixed and permeabilised. Afterwards recombinant antibodies were used in the same staining as commercial mouse anti-PDI antibodies. As secondary were used anti-human CY5 antibodies, that recognize recombinant antibodies Fc and anti-mouse CY3 antibody that recognize commercial antibody. It was seen that H12, H7 and B10 antibodies (in bleu) are giving a perfect co-staining with commercial anti-PDI antibodies (in red) (Fig. 28).

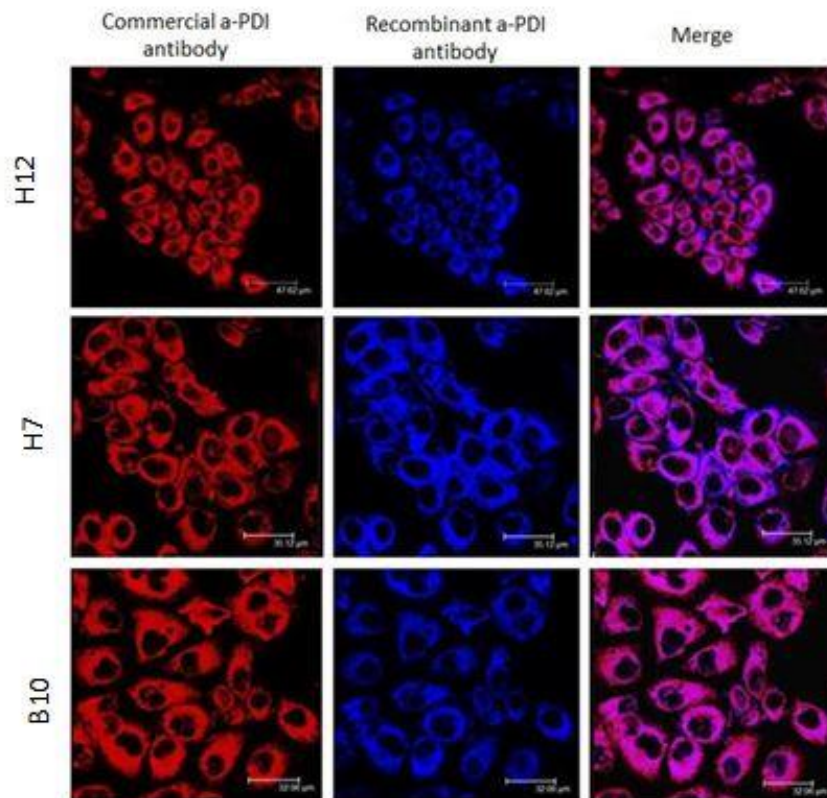


Fig. 28. Immunofluorescent co-staining of intracellular PDI. OVCAR-3 cell line were permeabilized and stained with recombinant antibodies H12, H7 and B10 (bleu) in parallel with commercial anti-PDI antibodies (red). Merge between commercial anti-PDI and recombinant antibodies staining shows that staining correspond each other, what confirm specificity of recombinant antibodies to PDI protein.

Recombinant antibodies were used to represent PDI protein present on the surface of OVCAR-3 not permeabilised cells. OVCAR cells were kept alive, were not permeabilised and staining was performed on 4°C. H12 , H7 and B10 (Fig. 29) were able to stain surface PDI (in bleu). Membrane staining was performed using *Triticum vulgare* FITC conjugate (in green).

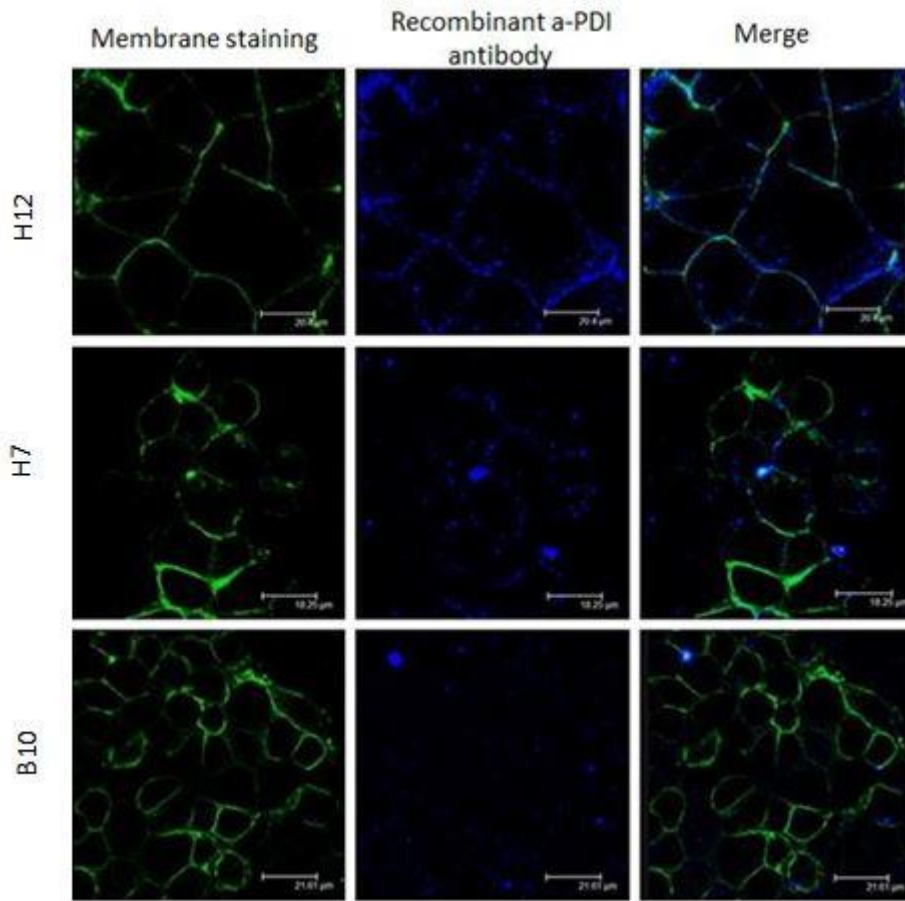


Fig. 29. Immunofluorescent staining of surface PDI in OVCAR-3 cells. Membrane staining performed by *Triticum vulgare* FITC conjugate (that recognizes glycoproteins and on not permeabilised cells gives membrane staining) is represented in green. Recombinant antibodies PDI staining is represented in blue. Merge between membrane and PDI staining represent that PDI is located on cell surface.

8.3.6. PDI surface staining analyzed by FACS

Present on cell surface PDI protein was confirmed by performing staining of it with recombinant antibodies H12, H7 and B10 and its visualization by FACS analysis. Here, OVCAR-3 cells were stained with primary antibodies in concentration 1 µg/immune-tube and secondary anti-human CY5 antibodies. All three antibodies were able to represent cell surface PDI protein (Fig 30).

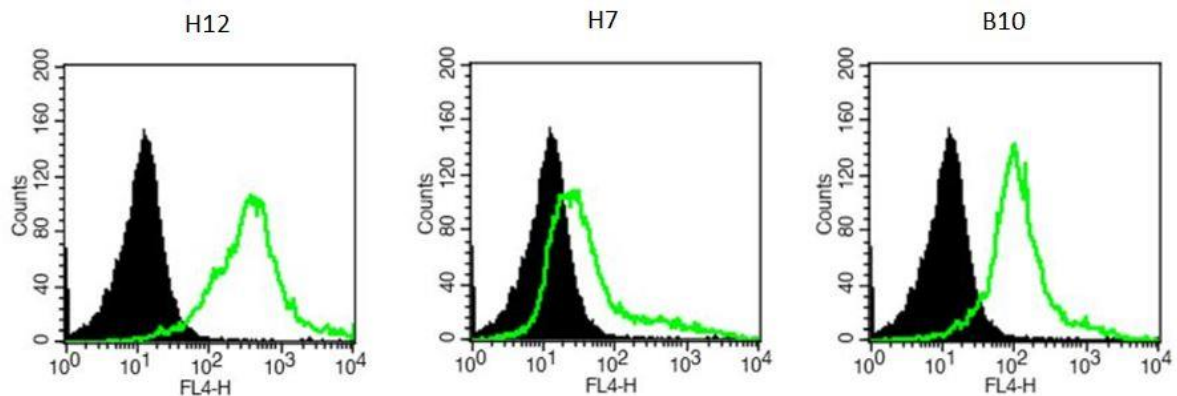


Fig.30. Surface PDI staining in OVCAR-3 cells. FACS analysis of present on the cell surface PDI protein in not permeabilised OVCAR-3 cells using H12, H7 and B10 antibodies (green graphic). Negative control (black filled graphic) is anti-human CY5 antibody staining.

8.3.7. Immunoprecipitation

Recombinant antibodies were used to test its ability to immune-precipitate endogenous protein in OVCAR-3 cells. For it, OVCAR-3 cells lysate as the first was pre-cleaned by incubating it with Protein A beads to remove all not specific proteins that might bind to protein beads. Further cell lysate was incubated with recombinant antibodies H12, B10 and H7 for 1h on rotation. These antibodies were tested in parallel with commercial monoclonal anti-PDI antibody to compare its functionality. Afterwards cell lysate was incubated with Protein A beads that captured antibody-PDI complex. Negative control was incubated only with Protein A. Small fraction of cell lysate, which correspond to approximately 6% of total cell lysate, was loaded on the gel in order to understand a total amount of PDI present in lysate and be compared to pull down PDI protein. Fig.31 represents that all three antibodies are able to pull down endogenous PDI in low quantity. H12 showed the strongest ability to pull down endogenous PDI.

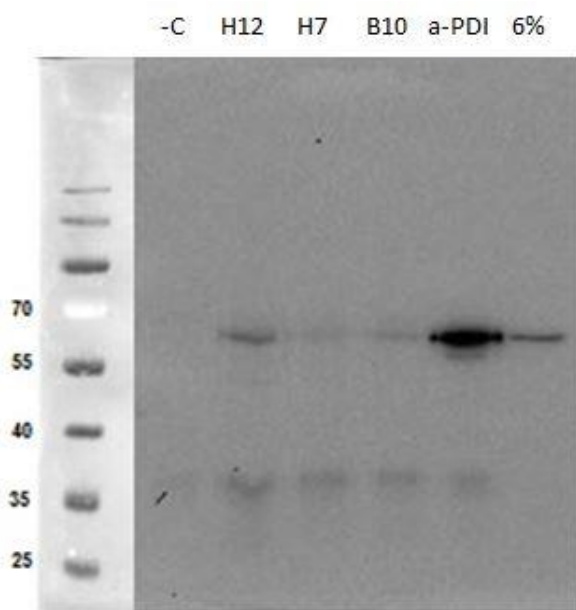


Fig.31. Immunoprecipitation assay. IP of endogenous PDI in cell lysate of OVCAR-3 cell. Preliminary cell lysate was incubated with protein A beads to remove proteins that might bind protein A not specifically. Afterwards, equal amount of cell lysate was incubated with H12, H7, B10 and commercial anti-PDI antibodies. Antibody-protein complex was precipitated with protein A beads. Negative control (-C) was incubated only with protein A beads. A small fraction of cell lysate (correspond to approximately 6%) was loaded on the gel to represent total amount of endogenous PDI in cell lysate.

8.3.8. Competition assay

To confirm that recombinant antibodies are specific for PDI protein competition assay was performed. Fig. 32 gives schematic representation of experiment. For it, recombinant antibodies used for cell surface PDI immunofluorescent staining were preincubated with HIS-PDI or HIS-TG2 recombinant protein. HIS-TG2 protein was chosen as it was also labeled with 6xHIS, to show that recombinant antibodies have been selected exactly to PDI protein and not to its tag. HIS-PDI and HIS-TG2 protein was used in concentration 40 times higher than concentration of antibodies. Antibodies were incubated on rotation for 2 hours at room temperature. Fig. 33A represent that H12, H7 and B10 are giving a good PDI surface staining (in blue) on OVCAR-3 not permeabilised living cells when are incubated with HIS-TG2 protein. On the other side PDI staining is completely absent (blue staining is not visible) when antibodies were inhibited with HIS-PDI protein (Fig.33B). Membrane staining was performed using *Triticum vulgaris* FITC conjugate (in green).

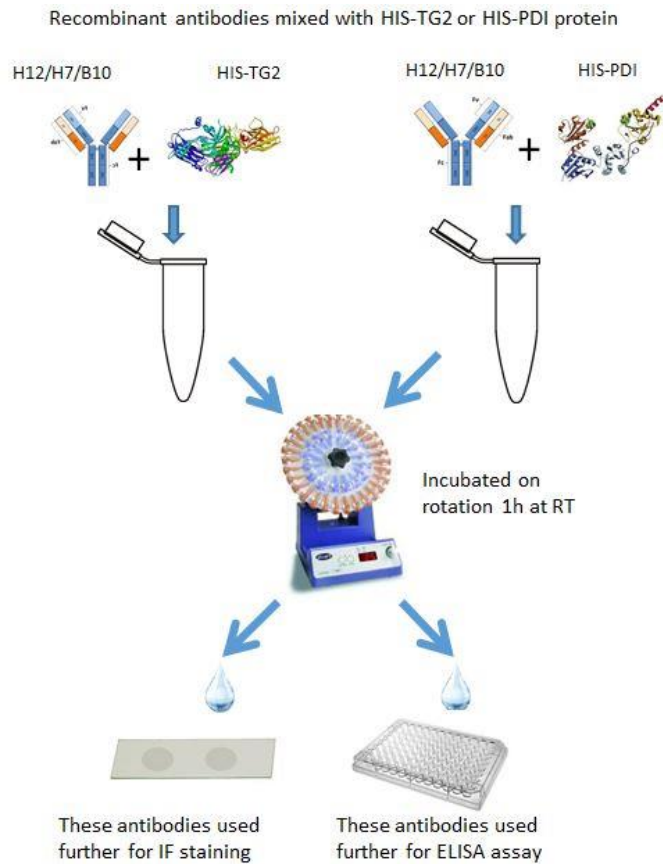


Fig.32. Schematic representation of competition experiments. Recombinant antibodies H12, H7 and B10 were mixed with HIS-PDI. In parallel the same antibodies were also mixed with HIS-TG2 protein. Incubation took 1 hour on rotation at RT. Afterwards these antibodies were used for surface IF staining of PDI protein on not permeabilised OVCAR-3 cells and in ELISA assay on the wells pre-coated with PDI protein.

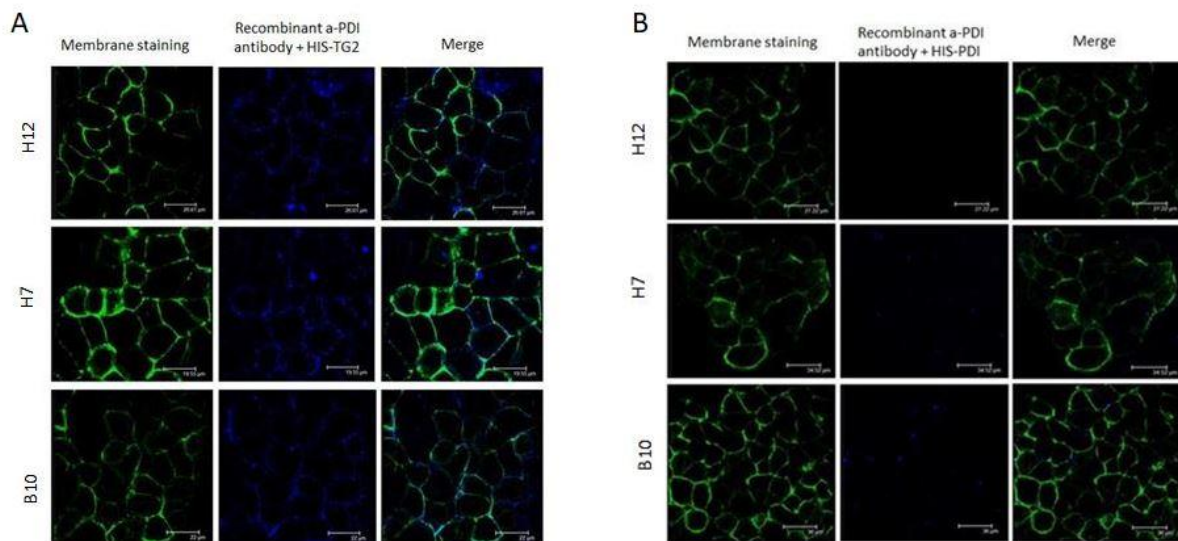


Fig.33. Immunofluorescent staining of surface PDI in OVCAR-3 cells. (A) H12, H7, B10 staining of cell membrane PDI after being preincubated with HIS-TG2 (in blue). (B) H12, H7, B10 staining of cell membrane PDI after being preincubated with HIS-PDI (in blue). Membrane staining performed by *Triticum vulgaris* FITC conjugate (that recognize glycoproteins and on not permeabilised cells gives membrane staining) is represented in green.

Moreover competition of recombinant antibodies was presented by performing ELISA assay. Here ELISA wells were coated with recombinant PDI protein in concentration of 1µg/well overnight at 4°C. Recombinant antibodies were preinhibited with HIS-PDI and HIS-TG2 in concentration 0µg, 0,5µg, 1µg on rotation at room temperature for 1 hour. Later these antibodies were used to recognize PDI protein. Afterwards secondary anti-human labeled HRP antibody were used to visualize the binding. As it is shown in the Fig. 34, H12, H7 and B10 antibodies were inhibited by pre-incubation with HIS-PDI and were having a strong signal when they were incubated with HIS-TG2.

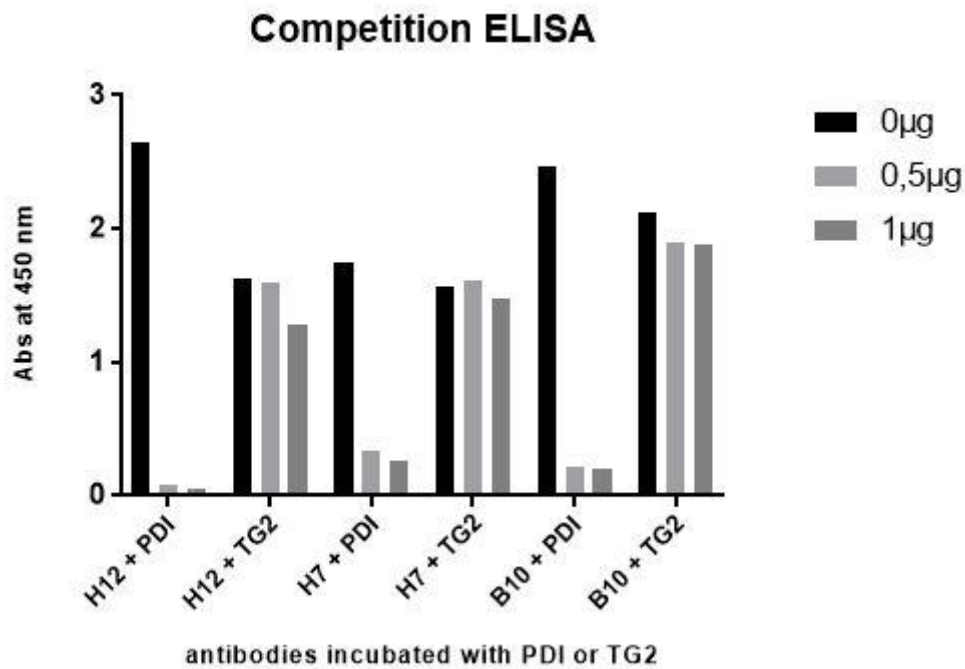


Fig.34. Competition ELISA. ELISA wells were pre-coated with 1µg/well PDI protein overnight at 4°C. H12, H7 and B10 antibodies used in ELISA assay were preinhibited with 0µg, 0,5µg, and 1µg of HIS-PDI or HIS-TG2.

8.3.9.CDC assay

An important characteristic of therapeutic antibodies is its capability to kill the target cells. Antibodies mediate killing in different ways such as apoptosis, complement dependent cytotoxicity, antibody-dependent cellular cytotoxicity. Accordingly, recombinant antibodies were tested in complement dependent cytotoxicity assay to understand if these antibodies are able to activate CDC and lead to ovarian cancer cell killing. For it, firstly, was performed Cell Surface ELISA. It was important to understand how much antibodies are binding on the surface of ovarian cancer cells. Here IGROV ovarian cancer cells were used. Recombinant antibodies were used separately in concentration 2µg/ml or as a mix of three antibodies in concentration 2µg/ml or 6µg/ml. Anti-Folate receptor antibody was used as a positive control (cMOV18). Result is represented in Fig. 35. Here we can see that recombinant antibodies recognize it target on the cell surface of the cells. Three antibodies together give about 40% signal compare to the positive control, which is considered 100% of binding.

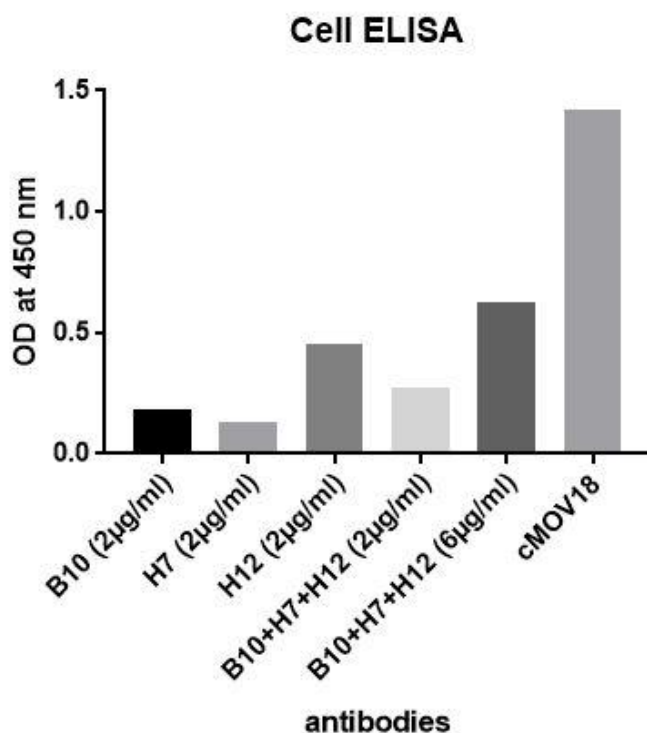


Fig.35. Cell surface ELISA assay. Not permeabilised IGROV ovarian cancer cells were incubated with recombinant antibodies H12, B10 and H7 each of it separately or in combination of three antibodies together B10+H7+H12. cMOV18 anti-Folate antibody was used a positive control.

Further recombinant antibodies were also used in CDC assay. Fig. 36 represents observed results. Here recombinant antibody H12, B10 and H7 were used in concentration 2µg/ml. Anti-Folate receptor antibodies cMOV18 and cMOV19 were used as a positive control in concentration 2µg/ml each. Antibodies were added to the cells and normal human serum (NHS) containing complement factors were added to the cells to activate complement pathway which resulted in formation of membrane attack complex (MAC) on their cell membrane and lead to complement dependent cytotoxicity. The residual viable cells as well as number of cells killed was estimated by the MTT assay (3-(4,5-dimethylthiazol-2-yl)2,5-diphenyltetrazolium bromide assay). The resulting purple solution is spectrophotometrically measured at 570nm and can be directly related to the number of viable (living) cells. Considering the cells with only NHS ('no antibody') as 100% living cells, the percentage of dead cells was calculated as: % of dead cells = 100 - [100 x (average of cells +Abs)/ (Average of cells +NHS)]. In the Fig. 36 NHS represents a negative control, cells that were incubated only with NHS, so the value of it was subtracted from the values of other antibodies to avoid false-positive results. As result we can see recombinant antibodies H12 and H7 are able to activate up to 5% of cells killing. This value is becoming about 8% when three antibodies are mixed together. Anti-Folate receptor antibodies represent 25-30% of killing as it was expected.

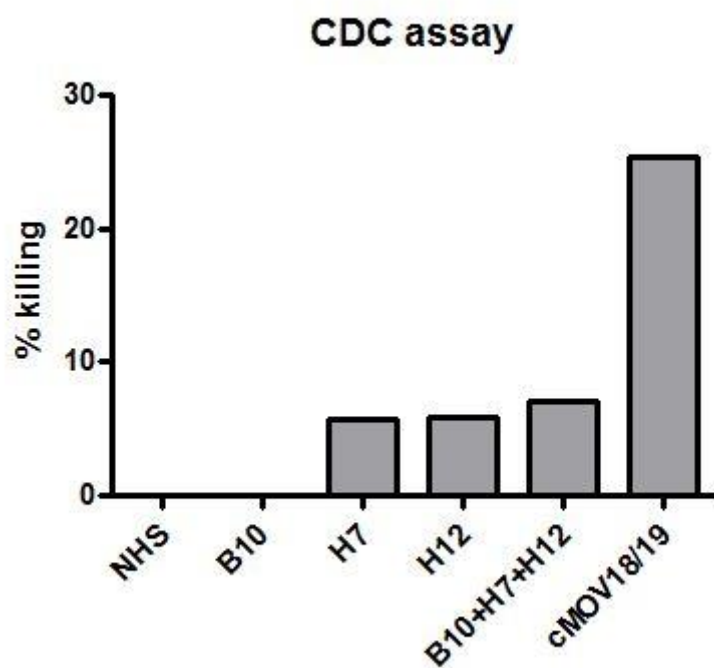


Fig.36. CDC assay. H12, B10 and H7 used in concentration 2 μ g/ml. Positive control anti-Folate receptor antibodies (cMOV18/19) used in concentration 2 μ g/ml each. Normal human serum (NHS) represents a negative control, cells that were incubated only with NHS.

Chapter 4

9. Discussion

9.1. Tumor associated antigen identification

Ovarian cancer is one of the most common and hard to be diagnosed gynecological cancers between women. Among the gynecologic cancers (uterine, ovarian, cervical), ovarian cancer has the highest rate of deaths. Treatment of patients with ovarian cancer is limited and is not much promising. Old methods are damaging and giving a row of complications. Surgery is remaining the main treatment method for ovarian cancer already in the last stages and consists of an effort to remove all visible disease in the abdomen, commonly called surgical debulking. It results in removal of a lot of nearby good tissue, both tubes and ovaries, the uterus (hysterectomy), removal of the omentum, lymph node biopsies and any other organ involved in the disease, that can be very damaging for the organism. Chemotherapy is a standard treatment for ovarian cancer but gives a lot of side effects, damage normal dividing cells and immune system of the patients.

Immunotherapy is a modern alternative way for cancer treatment that shows some promising results. Immunotherapy includes monoclonal antibodies, checkpoint inhibitors, cancer vaccines or other non-specific immunotherapy. Many different monoclonal antibodies are already approved for cancer treatment; some others are still in clinical trials. Some monoclonal antibodies therapies results in cancer shrinking and increase of overall survival but on the other side monoclonal antibodies therapy can give some side effects. These can vary depending on the type of antibody is used and which protein it target. It is crucial nowadays to discover more new tumor associated antigen that can be specific only for cancer tissue and develop monoclonal antibodies that can target this antigens.

Ovarian cancer patient ascites antibodies

Ascites have been already described as a perfect fluid to study ovarian cancer antigens. Ascites fluid contains many tumor cells and other soluble growth factors that have been associated with invasion and metastasis. Moreover it contains the secretome of ovarian cancer cells while reflecting other micro-environmental factors of the malignancy. Complex biological fluids such as serum and ascites fluid contain thousands of proteins with a concentration range spanning at least 9 orders of magnitude (24).

For this study 153 ovarian cancer patient ascites were collected. Ovarian cancer ascitic fluids represent stage I-VI collected from both platinum sensitive and resistant patients with grade ranging from G1-G3. Non-cancerous ascites and other cancer ascites were collected to use as negative control.

For the begin, OVCAR 3 cells were incubated by ascites of ovarian cancer patient and non-cancerous ascites in immunofluorescent assay. Result showed that antibodies present in ovarian cancer ascites bind to some membrane proteins in OVCAR-3 cells while non-cancerous ascites showed no staining. Anti-Folate antibodies staining was used as a positive control staining of OVCAR cells membrane, due to the fact that folate receptor is highly expressed on the ovarian cancer cell surface. Performing cell surface ELISA assay confirmed this result. Ovarian cancer ascites showed significantly higher binding to cell surface proteins comparing to non-cancerous ascites. The cut-off value was calculated as cumulative mean + 2 times SD (standard deviation) of the absorbance from non-cancerous control

samples. Furthermore it was shown that antibodies purified from ascites of ovarian cancer patients are able to kill OVCAR-3 cell in CDC assay. Antibodies from non-cancerous ascites did not show killing.

SERPA identification of anti-PDI antibodies

To understand better which proteins exactly triggering antibody production in ovarian cancer patient ascites, SERPA analysis was performed. SERPA is widely used technique for identification of autoantibodies in human serum or other fluids. SERPA was firstly described by Klade *et al.* which identified two TAAs (SM22-alpha and CAI) in kidney cancer patients (58). After that, different other studies used SERPA to identify new cancer antigens. Kellner *et al.* identified cytokeratin 8, stathmin and vimentin are potential TAAs in renal cell carcinoma subtypes from the normal renal epithelium tissues (59). Using SERPA has been identified calreticulin and DEAD-box protein 48 (DDX48) in pancreatic cancer (60). SERPA has been applied in the study of many cancers, such as neuroblastoma, lung carcinoma, breast carcinoma, renal cell carcinoma, hepatocellular carcinoma and ovarian cancer (61).

OVCAR-3 cell lysate proteins were separated by 2D-gel electrophoresis and transferred to the membrane. Membrane incubated with ovarian cancer patient ascites showed a strong binding to proteins compare to non-cancerous ascites. MS identified spots with highest antibody binding. It was shown that anti-PDIA1 was the most abundant antibody in ascites of ovarian cancer patients, while it showed no anti-PDIA1 antibodies in non-cancerous ascites.

CDC assay using anti-PDI antibodies

CDC assay was one of the most important experiments to understand if anti-PDI antibodies discovered in ascites of ovarian cancer patients have its immune activity. Affinity purified anti-PDIA1 antibodies were tested in parallel with commercial antibodies. Both affinity-purified and commercial antibodies showed its immune functionality to activate CDC. Affinity purified antibodies showed about 25% of killing. In parallel these antibodies were also blocked by recombinant protein as control, which represented that killing happens exactly due to the presence of anti-PDIA1 antibodies.

Here anti-Folate receptor antibodies were used as positive control. Immunohistochemical studies revealed that Folate receptor is a tissue specific fetal antigen expressed at high levels on malignant ovarian tumor cells. Specially, it is highly expressed on epithelial ovarian cancer cells. Anti-Folate receptor antibodies cMOV18 and cMOV19 were selected to use as positive control for CDC activation. cMOV18 and cMOV19 activation of CDC and killing of ovarian cancer cells has been already described (55). In its research was possible to show that mixture of cMOV18 and cMOV19 antibodies caused deposition of MAC on OVCAR-3 and induce C-dependent killing of several EOC cell lines. It has been also showed that each antibody separately is not giving strong CDC activation (about 5%). However surprisingly, combination of two antibodies together increases ovarian cancer cells killing significantly, and shows about 25-30% of killing (55).

OVCAR-3 membrane PDIA1 staining

To be able to activate complement cytotoxicity anti-PDIA1 antibodies has to bind PDIA1 protein on the cell membrane of ovarian cancer cells. As it has been known that PDI is intracellular protein and is localized in endoplasmic reticulum, it is not immediately evident that PDI is localized on the cell surface. Accordingly, has raised a question, how PDI is able to go to extracellular matrix and activate immune system response? There must be a mechanism that brings PDI to the cell surface for a certain purpose. Further analysis of literature confirmed that endoplasmic reticulum stress trigger PDI relocalisation to cell surface. The endoplasmic reticulum is cell organelle that plays an important role

in synthesis, folding, and accurate processing of proteins. ER contains proteins that play an important role in correct quality controlled folding and assembly of newly synthesized proteins. These proteins are ER chaperones HSP47, binding immunoglobulin protein (BiP), ERP57, protein disulfide isomerase (PDI), gp96 (GRP94; HSP90), and calreticulin. Chaperones are also involved in protein repair after cell stress, such as thermal shock and formation of MHC class I and II molecules and antigen peptide loading.

Correct protein folding requires a balance between the ER protein load and the folding process. Disturbing physiological cell conditions by some pathological signals, viruses, environmental toxins, inflammation processes, mutation in proteins can lead to interruption of ER homeostasis and accumulation of misfolded and unfolded proteins. This cell condition is known as ER stress. It leads to stimulation of signaling pathway in order to decrease ER stress and restore homeostasis, known as Unfolded Protein Response (UPR). Cell that is not able to restore homeostasis loses its correct functionality or dies. The UPR adaptation of cell involves overexpression of molecular chaperones and protein processing enzymes that handle folding of overexpressed proteins (62). As a result, chaperones can be relocated to cell surface via a number of pathways and also secreted into the extracellular space. Some overexpressed chaperones on the cell surface becoming a target signal for immune system to recognize abnormally growing cell, but its mechanism is not fully understood, however is often associated with the receptor CD91(63). Some studies showed that ER chaperones like calreticulin, BiP, and gp96 can activate the immune system once secreted in the extracellular space. Chaperones BiP (64) and gp96 (65) present in extracellular space are able to initiate antigen-specific anti-tumor responses by activating CD⁸⁺ T-cells.

Moreover, it is known that ER chaperones such as BiP, gp96 and PDI have a carboxyl terminus sequence of Lys-Asp-Glu-Leu (KDEL) that allows protein trafficking between the ER and Golgi complex and chaperones returning to the ER. Some researchers suggest translocation of chaperones to the cell surface as result of mutation in KDEL sequence (66), (67). When KDEL receptors become saturated with chaperones, non-bound chaperones may escape the retrograde retrieval system and fail to return to the ER (68). Some further literature studies suggest that PDI can be found extracellular in the cancer derived exosomes. When PDI is secreted in the extracellular space it remains on the cell surface due to electrostatic interactions (69), (70), (71). Secretion of chaperones and its presence on the cell surface is associated with cancer and autoimmune diseases (68). Some studies also propose that chaperones are engaged directly in the spread of tumors by promoting cell proliferation, migration, and metastasis (72).

To confirm the presence of PDI on cell membrane immunofluorescent staining of PDI on cell surface in not-permeabilised OVCAR-3 cells was performed using commercial anti-PDIA1 antibody. We were able to confirm that PDI protein is present on the cell surface and due to it able to trigger immune production of anti-PDIA1 antibodies.

9.2. Protein Disulfide Isomerase (PDI)

Structure and function

Protein Disulfide Isomerase (PDI) is a 57-kDa chaperone protein. PDI belongs to the family of 20 related mammalian proteins and is located in the endoplasmic reticulum. The members of PDI family have different length and domain composition, but share the common structural characteristics of having at least one domain with a thioredoxin-like structural fold, $\beta\alpha\beta\alpha\beta\alpha$.

PDI can function as reductase, oxidase, isomerase and maintaining cellular homeostasis by mediating oxidative protein folding, catalyzes disulfide bond breakage, formation, and rearrangement. It has been showed that PDI has also chaperone activity independent of the redox status of active site thiols, as a chaperone PDI makes wrongly folded proteins reach a correctly folded state without enzymatic disulfide shuffling. Most PDI family members contain both catalytic and non-catalytic thioredoxin like domains that are named “a” or “b”. PDI is composed from four domains, a, b, b’ and a’ (Fig.37).

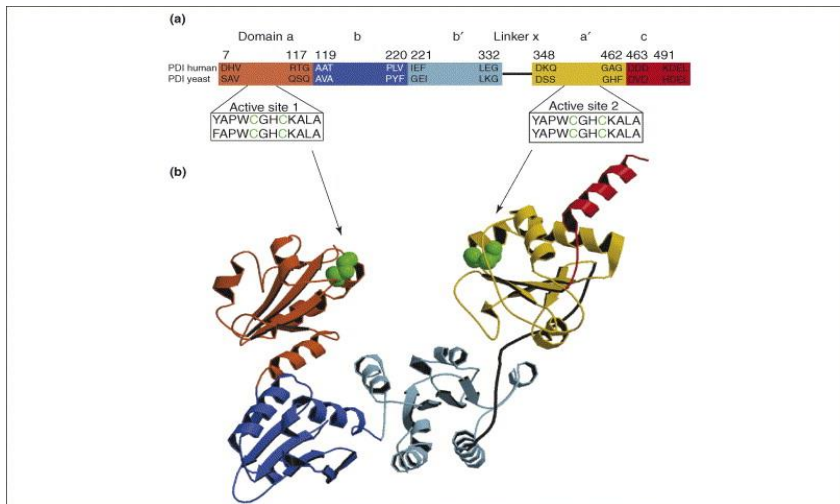


Fig.37. Domains organization of PDI. (A) Models of human PDI and yeast PDI. (B) Ribbon diagram based on the crystal structure of yeast PDI showing the active-site cysteines in green space-filling representation. Colors of the domains are the same as in (A) (57).

The a and a’ domains functionally are similar to thioredoxin, and contains catalytic Cys-x-x-Cys motifs. It reacts with thiols of newly produced proteins to confer disulfide oxidoreductase activity. Due to this sequence PDI is able to change between oxidized (disulfide) and reduced (dithiol) states. The b and b’ domains, although structurally similar to thioredoxin, do not contain catalytically active cysteines. Instead, the b and b’ domains play a role of spacers and are often responsible for proteins recruitment. Domain b’ has been identified as a chaperone domain. It has been seen that amino acid residues of the b’ domain was able to interact with unfolded RNase A, an often used enzyme to assay the chaperone activity of PDI. The b’ domain contains a large multivalent hydrophobic surface allowing for a structurally promiscuous binding site (73). Extensive research has assessed the roles of b’ domain to be the primary peptide- or protein-binding domain (74). Between b’ and a’ domains is located a small interdomain region known as the x-linker. Structural studies on PDI showed that its four domains folded in ‘U’ shape, suggesting how substrates may be positioned relative to the two catalytic domains. C-terminal tail folds back and makes contacts with the a and b’ domains (75) .

PDI role in disease development

PDI is a complex protein that plays a role in both physiology and pathophysiology. Different research groups showed that PDI is involved in the development of other diseases. It has been shown that internalization of some pathogens is modulated by PDI. PDI is hypothesized to play a role in the reduction of the disulfide bonds present on the parasite, which may help with it internalization. Recent research has described the role of PDI in HIV infections. Both PDI and thioredoxin1 (Trx1) have been shown to reduce disulfides on the virally co-protein gp120 causing the internalization of HIV-1. PDI on the surface of platelets plays a crucial role in the formation of thrombus in collagen-coated platelets. In monocytic cells, cell surface PDI is required for anti-thymocyte globulin decryption of tissue factor. Recent studies have shown that free thiols and isomerization are associated with the

process of coagulation. Protein aggregation has been shown to occur in a variety of neurodegenerative diseases, such as cerebral ischemia and amyotrophic lateral sclerosis, Alzheimer disease and Parkinson's disease (73). In neurodegenerative diseases nitric oxide (NO)-induced S-nitrosylation of PDI and inhibits its enzymatic activity, leading to the accumulation of polyubiquitinated proteins, and activates the unfolded protein response, which lead to ER stress and apoptosis in neuronal cells (76).

Latest research associated increased PDI expression in a variety of human cancers, including ovarian, prostate and lung cancers as well as lymphoma, glioma, acute myeloid leukemia and melanoma (3). Compared to normal tissues, protein disulfide isomerase (PDI) is overexpressed in ovarian tumors (77). It has been shown that inhibition of PDI activity leads to apoptosis in cancer cells. Due to it PDI is considered to be a promising druggable target (3).

PDI inhibition studies

Different researchers are trying to find a good inhibitor for PDI. Shili Xu and his group have studied effect of PDI inhibition on ovarian cancer progression. They created safe small-molecule propynoic acid carbamoyl methyl amides (PACMAs) which inhibits PDI protein in human ovarian cancer cell lines. It forms covalent bond with the active site cysteines of PDI. Liquid chromatography MS/MS identified that PACMA modify Cys397 or Cys400 in the active sites of purified recombinant PDI protein and inhibit its enzymatic activity. In vivo and in vitro, PACMAs showed tumor targeting ability and significantly suppressed ovarian tumor growth without causing toxicity to normal tissues. Shili Xu and his group showed that inhibition of PDI by either small-molecule compounds or PDI siRNA resulted in substantial cytotoxicity in human ovarian cancer cells (78). In other study Lappi *et.al.* discovered an active biotinylated analog of CCF642, that showed its ability to bind PDI isoenzymes and inhibit it function in multiple myeloma. CCF642 act through causing acute ER stress in cancer cells accompanied by apoptosis inducing calcium release. They showed that CCF642 is 100 times more active than PACMA inhibitor in mouse model and prolong mouse lifespan (79), (80). Moreover, Jingyan *et.al.* described phenyl vinyl sulfonate-containing small molecule (P1) as cell permeable, a relatively potent and specific inhibitor of endogenous human PDI in several mammalian cancer cells (81). In one more article, Gregoire *et.al.* described XCE853, a synthetic small molecule that inhibits in vitro recombinant PDI activity. XCE853 inhibited human tumor cells proliferation through an irreversible cytolysis, leading to a tumor cell death by autophagy and particles release (vesicles or protein aggregates). XCE853 showed to be active on a large panel of drug resistant human cancer cells (82). Furthermore, Di Santo *et.al.* proposed Nitazoxanide [NTZ: 2-acetyloxy-N-(5-nitro-2-thiazolyl)benzamide] that acts as PDI inhibitor for cancer treatment. NTZ is used for the treatment of anaerobic intestinal parasites. Di Santo and his group assume, that the antiparasitic drug NTZ may show anti-PDI activity similar to that of the PACMAs (10). Goplen *et.al.* studied function of PDI inhibitor bacitracin on cell migration and tumor. Result showed effectively inhibition of glioma cell invasion. Effect of bacitracin was reversible after withdrawal of the inhibitor, indicating a specific, non-toxic effect (83). Some other studies analyzed effect of PDI-knockdown in three cell lines, namely MCF-7, SH-SY5Y and HeLa. It has been shown that PDI-knockdown activates caspase-dependent apoptosis pathway, however level of cytotoxicity triggered by PDI knockdown was different between cell lines. In MCF-7 and human neuroblastoma SH-SY5Y cells it resulted in apoptosis (84). Different studies suppose that apoptosis in response to ER stress in cancer cells can be increased using a PDI inhibitor to disable homeostatic mechanisms. It has been shown that fenretinide and velcade induce ER stress in melanoma cells and PDI inhibitor bacitracin raises cell death as a result of ER stress. The approach to induce ER-stress apoptosis using PDI inhibitors showed significant dying of melanoma cells. It has been supposed that small-molecule PDI inhibitors that are able to bind PDI active site may have significant potential as powerful tools for enhancing the efficacy of chemotherapy in a wide

range of cancers (85). As describes before, PDI seems to play important role in ovarian cancer grow and PDI is hypothesized to be a potential target for cancer treatment (78-85).

9.3. Recombinant antibodies production

Phage display selection

Altogether, identification of a high titer of anti-PDIA1 antibodies in ascites and its association with better overall survival of ovarian cancer patients; moreover confirming anti-PDIA1 antibodies ability to activate CDC and kill ovarian cancer cells, made us suggest that PDIA1 is a promising tumor associated antigen. Moreover literature research suggests that PDI is involved in some cancers progression and search for PDI inhibitors is already going on. Based on these results further aim of my project was to design and produce recombinant antibodies that target PDIA1 for a possible monoclonal antibodies therapy of ovarian cancer. To achieve this goal, as a first, specific for PDIA1 scFv's were selected from phage display naïve library, that contain huge pool of scFv's. 193 bacterial colonies that contain phage with coding scFv were manually picked and screened in phage ELISA for its specificity to PDIA1. Third of the randomly selected colonies were giving a strong signal in phage ELISA. To understand if these colonies contain the same phage, scFv's were amplified by PCR and a product was digested by restriction enzymes in a finger printing assay. The colonies that showed the same cutting pattern by digesting enzymes were having the same sequence. 6 clones showed different cutting pattern and were selected for further analyzing. Specificity of selected clones was tested in phage ELISA assay to PDIA1 protein in its native conformation and denatured form and unrelated proteins that were having the same tag as recombinant PDIA1 protein. H12, B10 and H7 clones were having strong signal to PDIA1 and were selected to proceed further with antibodies design.

Antibodies production

scFv were subcloned into pcDNA3.1/Hygro(+) vector containing Fc fragment of human origin. pcDNA3.1/Hygro(+) vector with cloned H12, B10 and H7 were transfected into CHO cells, which are standardly used stable expressing cell line for transfection and antibodies production.

Recombinant antibodies expression can be performed in CHO, NS0, Sp2/0, HEK293, and PER.C6 cell line. However, most literature is available for CHO cells, which is exploited for 70 % of today's industrially produced protein therapeutics. CHO cells have a good capacity for high-rate recombinant antibodies production with mammalian posttranslational modifications. CHO transfected using polyethylenimine and lipid-based reagents and grown in optimized conditions result in antibody production yield from 10 to 250 mg/L for typical IgG (86). However, yield of antibodies obtained from purification in my experiments was lower than expected and resulted 0,2-0,5mg/L. Different aspects can influence rate of antibody production, namely cell culture conditions such as temperature, pH, osmolarity, and media additives. It is not completely clear why CHO cells were producing so low amount of antibodies. It has been suggested that there must be some biological mechanism behind.

9.4. Antibodies characterization in standard laboratory assays

ELISA assay

Recombinant antibodies were validated in different assay to represent its functionality. Antibodies were validated by SDS-PAGE and WB. To understand more about reactivity of recombinant antibodies to PDIA1 protein different concentrations of recombinant antibodies were used to perform ELISA assay.

It was shown that recombinant antibodies can be used in ELISA assay and are able to recognize recombinant HIS-PDI protein.

Epitope mapping

Epitope mapping was performed to understand which part of PDIA1 protein antibodies bind. For it, different length constructs of PDIA1 protein were cloned and produced as proteins. ELISA and WB assay were performed to identify to which constructs recombinant antibodies were reactive. Result showed that all three antibodies recognize different epitopes of PDIA1 protein. H12 antibody recognize end sequence of B' domain and begin sequence of interdomain linker. This result was confirmed by performing epitope mapping using Western Blotting technique. Linker is a stretch of approximately 20 residues and is described as flexible part of PDI protein. Its flexibility gives to PDI protein U shape and brings active sites on domain A and A' in proximity with each other (75). U shape form of PDI makes linker to be well exposed for antibodies. H7 and B10 antibodies recognize conformational epitope. Epitope mapping ELISA assay showed that H7 antibody epitope is localized on the construct B', linker, A' domain. Exact epitope of B10 antibody was not possible to identify, as this antibody recognizes complex conformational epitope.

Immunofluorescent staining

Recombinant antibodies were tested for their functionality in immunofluorescent staining. It was seen that antibodies are able to bind intracellular PDIA1 protein and its binding corresponds to commercial anti-PDIA1 staining. Moreover, recombinant antibodies were able to bind PDIA1 on the surface of non-permeabilized cells. Binding of antibodies to the cell membrane PDIA1 was also visualized by FACS.

Immunoprecipitation

Recombinant antibodies were tested for their ability to recognize endogenous PDI in OVCAR-3 cells by performing immunoprecipitation. All three recombinant antibodies were able to pull down PDI, but in very low quantity. H12 showed the stronger ability in PDIA1 binding. It can be due to the fact that H12, compared to B10 and H7, recognizes not conformational epitope.

Competition assay

Specificity of recombinant antibodies for PDIA1 protein was confirmed by performing competition of recombinant antibodies by incubating them with HIS-PDIA1 protein or HIS-TG2 (not related HIS tagged protein). As a result we saw that incubated with PDIA1 antibodies were not able to give surface PDIA1 staining in OVCAR-3 cells, while, if antibodies were incubated with TG2, were still able to bind PDIA1 protein on cell surface. Competition of recombinant antibodies was also confirmed by performing ELISA competition assay. Here, recombinant antibodies that were preincubated with HIS-PDIA1 protein were not giving a signal in ELISA assay. Recombinant antibodies that were preincubated with HIS-TG2 protein were still able to show strong binding to coated PDIA1 protein.

CDC assay

As the first, recombinant antibodies were tested in Cell Surface ELISA. It gave us a general idea about how much antibody is binding to the cell surface PDI protein. It was seen that three antibodies mixed together can give about 40% of binding to a target compared to positive control. CDC assay using recombinant antibodies gave a "positive" result. It is visible that killing is slightly increased when antibodies are used together as a mix. However, recombinant antibodies were not giving signal as strong as positive control, anti-Folate receptor. It can be explained by the fact that Folate receptor is a

membrane protein, normally present on the cell surface in a very abundant amount. PDI is not a membrane protein and is secreted by cancer cells as result of endoplasmic reticulum stress as it was described. PDI remain on the surface due to some interactions with other protein. It is not exactly known with which proteins PDI interact on the cell surface, but its bonds are not strong and PDI can be easily lost. Different studies suggest that PDI interact with integrin's on the cell surface and this way can play role in metastasis and cancer cell adhesion and proliferation (87-89)

10. Conclusions

Overall, our findings indicate that organism of cancer patient is able to raise antibodies against tumor associated antigens. Analyzing ovarian cancer patient ascites we were able to show that it contain a big pool of antibodies that recognize membrane proteins on ovarian cancer cells surface. Further, trying to understand which proteins exactly are triggering most antibody production, we were able to identify that these ascites contain high titer of antibodies against PDIA1 protein. Furthermore, we showed that higher titer of anti-PDIA1 antibodies in ascites benefit a higher survival of patients. Other cancer ascites and non-cancerous ascites showed significantly lower concentration of anti-PDIA1 antibody. Further, experiments using affinity purified anti-PDIA1 antibodies confirmed that these antibodies activate CDC can induce ovarian cancer cell killing. Moreover, we were able to show PDI present on the cell membrane using immunofluorescent staining. These data brought us to conclusion that PDIA1 is a novel tumor associated antigen, able to trigger immune system of patients to produce antibodies against it and activate CDC. Based on these results, it was hypothesized that recombinant antibodies targeting PDIA1 protein can be a potential monoclonal therapy for ovarian cancer. PDIA1 specific scFv's were selected from naïve phage display antibodies library and cloned for dimerized minibody production. Produced recombinant antibodies confirmed it specificity and functionality in main laboratory assays. These antibodies were tested in CDC assay and showed "positive" killing of ovarian cancer cells. In the future it will be important to test these recombinant antibodies in mouse model for its ability to activate cancer killing in organism. Afterwards monoclonal antibodies can undergo further steps required for development of monoclonal antibodies therapy. mAb can be tested in combination with other monoclonal therapies or standard chemotherapies. mAb can be also used as after-surgery treatment to remove metastatic cells possible present in the bloodstream. On the other hand it is also possible to conjugate these antibodies to a chemical or radioactive drug and use it as a drug delivery tool for ovarian cancer treatment. Obviously that these recombinant antibody can continue different pathway to find it best functionality for potential cancer immunotherapy.

Chapter 5

11. Materials and methods

11.1. Section 1: Abbreviations

Ab, antibody

AP, Alkaline Phosphatase

BCIP, 5-bromo-4-chloro-3-indolyl-beta-D-galactopyranoside

B-PER, bacterial protein extraction reagent

BSA, Bovine Serum Albumine

DMSO, Dimethylsulfoxide

dNTPs, deoxynucleotides

DTT, dithiothreitol

GSH, glutathione

HRP, HorseRadish Peroxidase

IPTG, Isopropyl β -D-1-thiogalactopyranoside

NBT, NitroBlue Tetrazolium

NC, nitrocellulose

O/N, over night

PBS, phosphate buffered saline

PEG, polietilenglicole

RT, Room Temperature

TMB, Tetrametilbenzidine

11.2. Section 2: Solutions and buffers

- **PBS:** 8 g NaCl, 0.2 g KCl, 1.44 g Na₂HPO₄, 0.24 g KH₂PO₄ in 1000 mL H₂O, final pH 7.4.
- **TAE buffer for DNA electrophoresis on agarose gels:** 0.04 M Tris-acetate, 0.001 M EDTA.
- **2xTY liquid broth for bacteria:** 16 g Bacto-tryptone, 10 g Bacto-yeast, 5 g NaCl, final pH 7.0. If required, ampicillin 100 μ g/mL, chloramphenicol 34 μ g /mL, streptomycin 75 μ g /mL
- **2xTY Agar plates:** 16 g Bacto-tryptone, 10 g Bacto-yeast, 5 g NaCl, 15 g Bacto-agar, final pH 7.0. If required, ampicillin 100 μ g/mL, chloramphenicol 34 μ g /mL, streptomycin 75 μ g /mL.

- **CCMB80 for preparation of competent *E.coli* cells:** 11,8 g CaCl₂ (dihydrate), 4,0 g MnCl₂ (tetrahydrate), 2,0 g MgCl₂ (hexahydrate), 10mM K-acetate (pH7), 10% Glycerol, H₂O to 1L. Adjust pH to 6.4 . Filtration with 0.2 µm filter.
- **Glycerol Buffer for preparation of electrocompetent *E.coli* cells:** 10% glycerol in milliQ water. Autoclave before use.
- **PBST:** PBS added with 0.1% Tween 20
- **MPBS:** PBS added with 2% non-fat milk powder.

Bacterial strains:

The bacterial strains used in this study were:

- *Escherichia coli* DH5αF' (Gibco BRL), F'/endA1 hsd17 (rK- mK+) supE44 thi-1 recA1 gyrA (Nalr) relA1 _ (lacZYA-argF) U169 deoR (F80dlacD-(lacZ)M15)

- *Escherichia coli* BL21-CodonPlus(DE3)-RIPL strain B F- ompT hsdS(rB- mB-) dcm+ Tetr gal λ(DE3) endA Hte [argU proL/Camr] [argU ileY leuW Strep/Specr]

Oligonucleotides for general screenings

All primers were purchased from Biomers.

Oligo ID	Sequence (5'-3')
VHPT2 antisense	TGGTGATGGTGAGTACTATCCAGGCCAGCAGTGGGTTTG
VLPT2 sense	TACCTATTGCCTACGGCAGCCGCTGGATTGTTATTACTC
pHygro sense	CTGCTTACTGGCTTATCG
pHygro anti	CAGATGGCTGGCAACTAG
PDIA1 sense	CCCAAGAGTGTGTCTGACTAT
PDIA1 anti	GTCGCTGTCGATGAAGATGAA
PDIh BamHI pTrc sense	AGCTGGATCCATGCATGCTGCGCCGCGCTCTG
PDI h EcoRIpTrc anti	AGCTGAATTCTTACAGTTCATCTTTCACAGCTTTCTG
Construct 1 sense	GAATCCGAAGCTTGGCTGTTTTGG
Construct 1 anti	AGCTGAATTCTTACCCTGCCCCATCCT
Construct 2 sense	GAATCCGAAGCTTGGCTGTTTTGG
Construct 2 anti	AAGCTGAATTCTTAGCCCTCCAGGAAGCG
Construct 3 sense	GAATCCGAAGCTTGGCTGTTTTGG
Construct 3 anti	AGCTGAATTCTTAGACAAGGGGCAGCTGG
Construct 4 sense	AGCTGGATCCCATCGAGTTCACCGAGC
Construct 4 anti	AGCTGAATTCTTACCCTGCCCCATCCT
Construct 5 sense	AGCTGGATCCGGACAAGCAGCCTGTC
Construct 5 anti	AGCTGAATTCTTACAGTTCATCTTTCACAGCTTTCTG
Construct 6 sense	AGCTGGATCCCATCGAGTTCACCGAGC
Construct 6 anti	AGCTGAATTCTTAGCCCTCCAGGAAGCG
Construct 7 sense	AGCTGGATCCGAAAATCAAGCCCCAC
Construct 7 anti	AGCTGAATTCTTACCCTGCCCCATCCT
Construct 8 sense	AGCTGGATCCGGACAGCGACC
Construct 8 anti	AGCTGAATTCTTACAGTTCATCTTTCACAGCTTTCTG
pDAN5 sense	TACCTATTGCCTACGGCAGCCGCTGGATTGTTATTACTC
pDAN5 anti	TGGTGATGGTGAGTACTATCCAGGCCAGCAGTGGGTTTG

11.3. Section 3: Standard protocols

Standard protocols used

PCR (Polymerase chain reaction)

Thermus aquaticus DNA polymerase (Finnzymes) was used.

Reaction mixture:

- Template DNA 0.01-1 ng (plasmidDNA)
- Sense primer 0.5 μ M
- Antisense primer 0.5 μ M
- Finnzymes Buffer 10x 2.0 μ L
- dNTPs (Promega) 0.25 mM
- MgCl₂ 1.5 mM
- Taq polymerase 0.025 units/ μ L
- H₂O to 20 μ L T

The following cycles were performed:

- Denaturation step, 5' at 94°C.
- 25 cycles of: denaturation, 45'' at 94°C; annealing, 45'' at 60°C; elongation, 1' every 1000bp at 72°C.
- Final elongation step: 10' at 72°C

Inverse PCR

Reaction was performed on plasmidpreparations as follows of the libraries subcloned in pTrcB vector:

- DNA (10 ng) 1 μ L
- Primer sense (0,5 uM) 1 μ L
- Primer anti (0,5 uM) 1 μ L
- Buffer HF (5x) 4 μ L
- dNTPs (0,4 mM) 0.4 μ L
- Fusion Pfu polymerase (Finnzymes) 0.2 μ L
- H₂O to 20 μ L

PCR amplification was performed as follows:

- Initial denaturation 30'' at 98°C

25 cycles as follows:

- 10'' at 98°C
- 10'' at 70°C
- 1'15'' at 72°C (15''/kb)
- Finale extension: 5' at 72°C

Amplicons were purified and 100 ng of the purified product were ligated O/N at 16°C. After transformation in *E.coli* competent cells, cultures were plated onto ampicillin containing agar plates. After O/N growth at 37°C, colonies were screened by PCR with specific primers.

DNA electrophoresis on agarose gels

Agarose (Sigma) gels with a concentration of 1.5 % in TAE buffer were used to separate PCR products; 0.8 % agarose gels were used to separate plasmidDNA preparations, before and after digestions. 1 µL of ethidium bromide (2mg/mL, Sigma) was added to 50 ml of agarose gel. 100 base-pairs plus and 1KB molecular weight markers were purchased from Fermentas.

PlasmidDNA extraction

The GeneJET Plasmid Miniprep Kit (Thermo Scientific) was used for plasmid DNA mini-preparations (1 to 5 ml of O/N bacterial culture), following the manufacturer instructions.

DNA digestion with restriction endonucleases

All restriction endonucleases were Fast Digest, purchased from Thermo Scientific.

Reaction mixture:

- DNA
- FD Buffer 10x
- Restriction endonuclease, 1 unit / µg of DNA
- H₂O to 20 µL

Incubation for 1 hour at the temperature required by the specific endonuclease.

Ligation

Plasmidvector DNA and insert DNA were mixed at a 1:3/1:5 ratio (number of molecules). T4 ligase was purchased from Thermo Scientific.

Reaction mixture:

- DNA (about 100 ng)
- T4 ligase Buffer 10x
- T4 ligase, 1 Unit/reaction
- H₂O to 10µL

Incubation O/N at 16°C.

Preparation of competent *E.coli*

50 mL of *E.coli* culture, DH5α or BL21(DE3)RIPL strains, were grown at 37°C in 2xTY liquid broth to OD₆₀₀ 0.5. Bacteria were chilled in ice for 10 min to stop growth, centrifuged at 4°C for 10 min at 3000 rpm and the supernatant was discarded. The bacterial pellet was resuspended in 8 mL of CCMB80 solution and put in ice for 20 min. After centrifuging for 10 min at 4°C, supernatant was discarded, bacterial pellet resuspended in 2 mL of CCMB80 and dispensed in 80 µL aliquotes. Competent cells were immediately used or stocked at -80°C up to four weeks.

To test the efficiency of the so prepared cells an electroporation of 10 pg of purified commercial pUC119 vector was performed. The efficiency was generally about 1010 transformed clones / μg DNA.

Bacterial transformation

5 μL of ligation reaction mixture or 10-50 ng of plasmid preparation were transferred into a tube containing 80 μL of competent cells. The mixture was incubated in ice for 20 min. Heat shock was applied at 42°C for 1 minute and bacteria were then chilled in ice for 2 minutes, resuspended in 1 ml of liquid broth and allowed to grow in absence of selective antibiotic for 1 hour. Bacteria were then plated on antibiotic-containing agar plates and grown O/N at 30°C.

DNA Sequencing

PCR products were purified with GeneJET Extraction and DNA Cleanup Micro kit of Thermo Scientific following manufacturer instructions. Reaction mixture for sequencing were composed as follows:

- 50-100 ng of purified PCR product
- 1 μL primer (3,2 μM)
- 2 μL Terminator Mix (Applied Biosystems, BigDye Terminator v1.1 Cycle Sequencing Kit)
- 2 μL buffer 5x
- H₂O to 10 μL

and the sequencing program was: 1 min at 96° ; 25 cycles: 15 min at 96°; 5 min at 50°; 4 min at 60°

Reactions were purified with CENTRI SEP Spin Columns, following manufacturer instructions. 5 μL of purified sequences were loaded on sequencing plates with 10 μL of formamide, denaturated for 2 min at 96° and analyzed with 3100 Genetic Analyzer sequencer (ABI PRISM-HITACHI).

11.4. Section 4: Methods

11.4.1. Patient samples and cell line

Samples preparation

Ascites were collected from 153 patients representing various disease conditions which include ascites from patients diagnosed with ovarian cancer (69), other cancers (34) and non-cancerous control ascitic fluid (50) from female patients with no known history of cancer. Numbers in brackets indicate the number of patients for each group. Ascitic fluid samples were obtained from i) the Department of Clinical and Experimental Medicine, University of Eastern Piedmont, ii) Department of Life Science, University of Trieste, iii) Istituto Nazionale Tumori, Milan and iv) University of Turin. All ascites samples were centrifuged at 11000 rpm at 4°C for 5 minutes and supernatants were stored at -80°C until processing. Immunoglobulins from all ascitic fluid were affinity purified using Protein A Agarose (Roche). 50 μl of crude ascitic fluid was mixed with starting buffer containing 100mM TRIS-HCl pH 8, 1% IGEPAL CA630, 1mM EDTA, 1mM PMSF, 1:100 dilution of protease inhibitor, 40 μl Protein A agarose in a final volume of 1ml. Incubated overnight at 4°C on a rotating platform. Washed and eluted to an equal volume of sample used with 100mM glycine pH 2.5, later added 20% 1M TRIS-HCl pH 8 for stability.

Cell lines

The human ovarian adenocarcinoma cell line OVCAR-3 (ATCC® HTB-161™) and IGROV were grown in RPMI 1640 media (SIGMA) containing 10% foetal calf serum, 2 mM glutamine, and 1% penicillin/streptomycin. Chinese hamster ovary cell (CHO) was grown in CHO-S media (Gibco Lab Technology) containing 2 mM glutamine, and 1% penicillin/streptomycin. Cells were maintained at 37°C in a humidified atmosphere containing CO₂.

11.4.2. Identification of autoantibodies in ascites

OVCAR-3 cells surface antigens staining

OVCAR Cells Surface Staining: The confluent cells on the cover slips were washed once with plain RPMI and 1: 10 diluted primary antibody in blocking buffer (5% BSA in serum free RPMI medium) was added. Anti-Folate receptors antibody (cMOV18 and cMOV19; 2 µg/ml each) were added together with primary antibodies for membrane surface staining. Coverslips were incubated on ice at 4°C for 2 hrs. After primary incubation, the unbound antibodies were removed by washing 3 times with blocking buffer. The cells transferred to new well and were subsequently incubated for another 1 hr on ice at 4°C with secondary antibody (anti-human-CY5 and anti-mouse-CY3) diluted 1:200 in blocking buffer. Afterwards coverslips were washed twice and were transferred to new wells in which the cells were fixed with 200µl of 4% PFA + 4% Sucrose on ice for 15 min, and permeabilised for 23min 0.2% triton in PBS. The fixed and permeabilized cells were incubated with 1:2000 dilution of propidium iodide (PI: nuclear stain) in PBS. Cells were washed thrice with 1xPBS and once with dH₂O, mounted to a glass slide with a small drop of mountant and the cells on cover slip facing the mountant and sealed with nail polish. The cells were directly analyzed with a Leica TCS-SP confocal laser scanning microscope using sequential scan tool. Laser power and photomultiplier settings were kept identical for all the samples to be able to compare the results.

Ovarian Cancer Cell surface ELISA

1x 10⁴ OVCAR-3 cells were seeded in 100µl in each well of the 96-well microplates and incubated in 5% CO₂ at 37° C in a cell culture incubator for 36hrs. The culture medium was removed from every well and washed once with 100µl RPMI medium containing 10 % FBS (pre warmed at 37°C). Primary antibody (Purified and normalized ascitic IgG) were diluted 1:100 in RPMI medium with 10% FBS and ensured proper mixing at least 30 min at RT. 100 µl of this preblocked primary antibody along with 1:200 diluted anti folate receptor antibody (positive control for the assay) were transferred into their appropriate wells in triplicate and incubated 1h 30min at 37°C in presence of CO₂. The plates were washed thrice with pre warmed RPMI medium and incubated for 1hr at 37°C in presence of CO₂ with 1:2000 dilution of peroxidase-conjugated secondary antibody in RPMI medium (Polyclonal rabbit anti-human immunoglobulins/HRP; Dako). A triplicate negative control wells incubated with only secondary antibody was included thus to reduce the non specific signal from the final reading. 3 washes were performed with RPMI medium and once with PBS 1X. Pipette 70µl TMB/well (3,3',5,5'-Tetramethylbenzidine liquid substrate, Sigma) and dark incubate at RT until proper intensity was observed. This TMB was transferred into a new ELISA plate already containing 35µl 1N H₂SO₄ to stop the enzymatic reaction. The absorbance at 450 nm was measured with a microplate reader. The cutoff value was calculated as cumulative mean + 2 (standard deviation) of the absorbance from noncancerous control wells.

Role of Cell Surface Antigen Interacting Antibodies in Tumor Regulation by complement dependent cytotoxicity

1 × 10⁴ OVCAR cells were seeded into each wells of 96-well tissue culture plate (Euroclone) and incubated 36 hrs at 37 °C in presence of CO₂. Once the cells were grown to confluence, culture

medium was carefully removed and washed with 380µl/well DPBS/Ca²⁺/Mg²⁺ containing 2% BSA (Wash/blocking buffer). To measure complement activation by antibody, the cells were incubated with 50 µl/well of wash/blocking buffer containing individual antibodies purified from ascites (20 µg/ml each) for 10 minutes at 37°C. Two controls were included in this assay i) we used the mixture of the two antibodies cMOV18 and cMOV19 (2 µg/ml each) as well as ii) cell incubated without antibody. NHS (Normal Human Serum: pool of human AB Rh+ sera) was then added without washing to a final volume of 100 µL (ie, 1:2 solution of NHS in DPBS/Ca²⁺/Mg²⁺/2% BSA (25 µl NHS + 25 µl Wash/blocking buffer), and incubation was continued for further 60 minutes at 37°C. The residual viable cells were counted using the 3-(4,5dimethylthiazol-2-yl)-2,5-diphenyltetrazolium bromide (MTT) assay. 20 µl MTT solution (5mg/ml) in 200 µl fresh culture medium was added to each well and incubate 4 hours at 37°C. After careful removal of culture medium, MTT crystals were solubilized by adding 200µl DMSO and read at 570nm with a reference wavelength set to 650nm. The experiment was performed in quadruplicate.

11.4.3. PDI antigen identification

SERPA analysis

Protein lysates were loaded by in-gel rehydration into Immobiline Dry strips(pH 3-10 non linear ; 7 cm; GE Healthcare Bio-Sciences) for analytical (100µl lysate) and preparative (150µl lysate) gels. Isoelectric focusing was performed on an IPGphor isoelectric focusing unit system (GE Healthcare Bio-Sciences) with a voltage gradient up to 5000V for a total of 16,000Vh. Before sodium dodecyl sulphate polyacrylamide gel electrophoresis (SDS-PAGE), IPG strips were equilibrated for 15 minutes with a solution of Tris-HCl buffer (5mM; pH8,8); urea (6M), 30% glycerol, 2% SDS, Bromophenol Bleu, and 2% DTT, and for a further 5 minutes in the same buffer containing 2,5% iodoacetamide in place of DTT. For the second dimension, strips were run on small NuPAGE Novex 4%-12% Bis-Tris Zoom precast gel (Invitrogen, Groningen, The Netherlands) using the Novex X-Cell II Mini-cell system (Invitrogen) at a constant voltage (200V) and then transferred into a Hybond enhanced chemiluminescence nitrocellulose membrane (GE Healthcare Bio-Sciences) using Novex X-cell II Blot Module (Invitrogen), or stained with Coomassie bleu for MS. The isoelectric point (PI) value of the protein spots were estimated from their position on the 2DE gel, using pH gradient graphs purchased from GE Healthcare Bio-Sciences. The molecular mass of the proteins was calculated by comparing with the migration of SeeBleu Plus2 Prestained standard (Invitrogen) of a known molecular mass. The 2DE gel images were acquired using “ProXPRESS 2D” (PerkinElmer Life Sciences, Boston, Massachusetts), with a 16-bit slow-scan CCD camera cooled to -35°C, and recorded in TIFF format. Blotted membranes were incubated for 15 hours at 4°C with blocking buffer consisting of 5% nonfat dry milk in tris buffered saline (TBS) and then incubated with horseradish peroxidase-conjugated rabbit anti-human IgG antibodies (Santa Cruz Biotechnology, Santa Cruz, California) at a 1:1000 working dilution for 90 min at 20°C. Immunodetection was carried out by Enhanced Chemiluminescence PLUS (GE Healthcare Bio-Sciences). The resulting chemiluminescence signals were scanned with ProXPRESS 2D(PerkinElmer) and for an exposure time of 12s. Images were recorded in TIFF format. Serum was tested 3 times on 3 replica blots. The 2DE WB image was compared with the 2DE map image using Progenesis PG240 (nonlinear dynamics) software to identify the probed spots.

Proteins identification by MS. Protein spots were excised from gel, reduced, alkylated, and in-gel digested for 18 hours at 37°C with bovine trypsin (10 ng/µl; Roche Diagnostic Corp). A volume of 5 µl of digested samples was desalted (Stage tips C18; ThermoScientific) and injected into a capillary chromatographic system (EasyL; Proxeon Biosystem). Peptide separations occurred on a 25 cm reverse phase silica capillary column, packed with 3µm ReproSil 100 Å C18 AQ. A gradient of

acetonitrile eluents was used to achieve separation (0,15µl/min flow rate). MS analysis was performed by nano-liquid chromatography (LC)-MS/MS using an linear trap quadrupole (LTQ)-Orbitrap XL Mass Spectrometer (ThermoScientific), equipped with a nanoelectrospray were acquired with the lock-mass option, resolution set to 60,000, and mass range from m/z 350 to 1700Da. The 10 most intense doubly and triply charged ions were selected and fragmented in the ion trap. All MS/MS samples were analyzed using the Mascot (c.2.2.07, Matrix Science) search engine to search the UniProt_Human Complete Proteome (UniProt_C-P_hum cp_hum_2015_03; 89909 sequences; 35686673 residues). Searched were performed allowing 2-missed cleavages, and N-terminus-acetylation, and methionine oxidation as variable modifications. Mass tolerance was set at 5ppm and 0,6Da for precursor and fragment ions, respectively.

ELISA assay PDI specificity of antibody in ascitic fluids.

96 well ELISA plate was pre coated (O/N at 4°C) with 1µg of purified full length HIS-PDI protein in 100 µL of PBS. Wells were saturated with blocking buffer (2% BSA in PBST0.05%) for 1 hr at 30°C. 1:50 diluted primary antibodies in blocking buffer were incubated at RT for 45 min enabled with proper mixing and were subsequently transferred into their appropriate well and incubated at 30°C for 90 min. Primary antibody used were affinity purified IgG from 153 ascites from patients which includes ovarian cancer, other cancer and non-cancerous control and normalized for concentration 1µg/µl. After incubation at 30°C, the unbound primary antibodies were removed by washing 3 times with PBST 0.05% and 1x PBS. Further, wells were incubation at 30°C for 1hr with 1:5000 dilution of peroxidase-conjugated secondary antibody in 2% blocking buffer. 70 µL of TMB was added to all well after final wash (3 times) with PBST0.05% and 1x PBS. The plate was incubated in dark until they have attained proper intensity of colour. The reaction was stopped by adding 35 µL/well of 1 N H₂SO₄. Plates were read spectrophotometrically at 450 nm. For each antigen validation, the cut-off value was independently calculated as 'sum of (cumulative mean + twice the standard deviation) of the absorbance from non-cancerous control wells.

Complement dependent cytotoxicity activation by anti-PDI antibodies.

1×10^4 OVCAR cells were seeded into each wells of 96-well tissue culture plate (Euroclone) and incubated 36 hrs at 37 °C in presence of CO₂. Once the cells were grown to confluence, culture medium was carefully removed and washed with 380µl/well DPBS/Ca²⁺/Mg²⁺ containing 2% BSA (Wash/blocking buffer). To measure complement activation by antibody, the cells were incubated with 50 µl/well of wash/blocking buffer containing anti-PDI antibodies affinity purified from ascites (20 µg/ml each) for 10 minutes at 37°C. Commercial anti-PDI antibodies (SIGMA) were tested in parallel with affinity purified antibodies. Affinity purified and commercial antibodies were also inhibited by incubating it with 20 times higher concentration of recombinant PDI protein. Two controls were included in this assay i) we used the mixture of the two antibodies cMOV18 and cMOV19 (2 µg/ml each) as well as ii) cell incubated without antibody. NHS (Normal Human Serum: pool of human AB Rh+ sera) was then added without washing to a final volume of 100 µL (ie, 1:2 solution of NHS in DPBS/Ca²⁺/Mg²⁺/2% BSA (25 µl NHS + 25 µl Wash/blocking buffer), and incubation was continued for further 60 minutes at 37°C. The residual viable cells were counted using the 3-(4,5dimethylthiazol-2-yl)-2,5-diphenyltetrazolium bromide (MTT) assay. 20 µl MTT solution (5mg/ml) in 200 µl fresh culture medium was added to each well and incubate 4 hours at 37°C. After careful removal of culture medium, MTT crystals were solubilized by adding 200µl DMSO and read at 570nm with a reference wavelength set to 650nm. The experiment was performed in quadruplicate.

11.4.4. Antibody selection

Phage Display antibody selection

Immuno-tube was coated with an antigen 10µg/ml in a volume of 0,5ml in 1xPBS at 4°C O/N. Immuno-tube and phages were blocked with 2% milk in 1xPBS in RT for 1h. (400µl for phages and 4ml for immune-tubes). After incubation phages were added to the immune-tube and incubated for 30min on rotator and 1h in static condition at RT. Then immune-tube was washed 10 times with 0,1% PBST and 10 times with 1xPBS. Afterwards, to elute bounded phages, 0,5ml of grown till OD 0,5 DH5aF' bacteria was added to the immune-tube and incubated for 45min on 37°C in static condition. Bacteria were plated and grown overnight on the agar plate. Phage in DH5aF' was titrated to determine the output.

Bacteria containing phagemids selected in phage display were grown till 0,5 OD. T helper phage in 10-20 times higher concentration was added for 45 min at 37°C in static conditions. Tube was spin down on 4000rpm for 15 min at RT and pellet was resuspended with medium containing ampicillin and kanamycin. It was left O/N at 28°C on shaking. The day after bacteria was centrifuged on 5000rpm at 10°C for 20min. Supernatant was collected and added to 10ml of 20% PEG in NaCl 2,5M filtered 0,2. It was left on ice for 45min. Phages collected after first selection were used to perform second selection round.

Finger printing

PCR on different phage colonies was performed by preparing mix of 20x VLPT2 and 20x VHPT2 primers, 2x Kapa mix (SIGMA), 1µl DNA and water to have total of 15µl per reaction. PCR product that showed amplification was used to perform a finger print. Mix containing 1µl of enzyme (BstN1 or HaeIII), 10x buffer 3.1 (for BstN1) or catsmart (for HaeIII) from NEB and 6-9µl of PCR reaction was prepared. Restriction reaction was performed at the temperature as required by enzyme and cutting patron was analyzed in agarose gel.

Phage ELISA

96 well "master plate" with 130 µl of 2xTY containing ampicillin and 1% glucose per well was prepared. Using a pipet tip colonies one by one were picked up from the plate and put inside each well. Plate was on shake for 2h on 37°C. 110µl of medium was put in a new 96 well "copy plate" and 10µl of bacteria from the "master plate" was added. Bacteria grown in "copy plate" till approximately 0,5 OD. Helper phage in concentration 10-20 times higher was added and left 45 min at 37°C in static condition. "Copy plate" was spin down on 2500rpm for 25 min at RT. Pellet was resuspended in 120µl of medium containing ampicillin and kanamycin and left ON at 28°C on shaking.

96 wells ELISA plate was coated with antigen of interest in concentration 5µg/ml O/N. Each well was blocked with 120µl of 2% milk in 1xPBS for 1h at RT. Phages grown in the "copy plate" were spin down at 2500 rpm for 20-30 min. 50µl of 4% milk was put in each well and 50µl of phage supernatant was added. Plate was incubated for 1,5h at RT in static conditions and washed 3 time with 0,1% PBST and 3 times with 1xPBS. 100µl of secondary antibodies diluted 1:5000 in 2% milk in 1x PBS was added in each well and incubated for 1h at RT. Plate was washed three time with 0,1% PBST and 1xPBS. 70 µL of TMB (SIGMA) was added to all wells and was incubated in dark until they have attained proper intensity of colour. The reaction was stopped by adding 30 µL/well of 1 N H₂SO₄. Plates were read spectrophotometrically at 450 nm.

11.4.5. Clones sequencing analysis

Identification scFv 's by sequencing

Those phages that showed binding to PDI processed to decode their sequence. As the first step, these screened clones were PCR amplified using pDAN5 sense and pDAN5 anti primers. The PCR amplified products were purified using GeneJET Extraction and DNA Cleanup Micro kit (Thermo Scientific) and the DNA fragment of varying size (150-800bp) were sequenced. Under optimised condition, a fluorescence based cycle sequencing reaction was performed with the purified PCR amplified fragments/template along with its sequence specific primer (pDAN5 sense or anti sense) and ABI BigDye Terminator v1.1 (Applied Biosystems). The extension products were purified using Centri-Sep Columns (Princeton separations) based on gel filtration. The reaction mixture was added directly on top of the hydrated illustra Sephadex fine DNA grade (GE healthcare) gel bed and spin down at 3600rpm. This was done to remove all free labelled dNTP's and unwanted buffer salts. The sequencing was carried out using ABI 3100 sequencer.

Cloning scFv in pcDNA3.1/Hygro(+) vector

scFv fragments were amplified by PCR using the VHPT2 and VLPT2 primers. Amplified sequences were restricted by enzymes BssH2 and Nhe I and subcloned into pcDNA3.1/Hygro(+) vector that contained cloned inside Human Fc sequence. Plasmid was transformed into DH5 α F (Gibco BRL) cells and plated to grow overnight. Single colonies were picked up from plates and were sequenced to detect possible mutation occurred during the cloning.

11.4.6. Recombinant antibodies production

CHO transfection and cell growing

The day before transfection CHO cells were seed in 2×10^4 in 24 well plate. 100 μ l of transfecting medium was prepared with 2 μ g of plasmid DNA. 100 μ l of transfecting media was prepared with 2 μ l of FreeStyle Max Reagent (SIGMA). Tube with DNA and a tube with FreeStyle Max Reagent were mixed together and left for 15-20 min at RT. Mixture was slowly added to the well and incubated at 37°C humid atmosphere, 5% CO₂. Supernatant was checked for antibody production after 48-72 hours.

ELISA check for transfection

Supernatant from transfected cells was coated on the ELISA wells in concentration 1:10 and 1:50 O/N at 4°C. Wells were blocked with 200 μ l of 2% milk in PBST0,01%. Wells were incubated with 100 μ l of anti-SV5 antibody in concentration 1:5000 for 1h at RT. Wells were washed three times with PBST0,1% and three times with 1xPBS. Wells were incubated with secondary anti-mouse (Novex) antibodies in concentration 1:5000 for 1h at RT. Wells were washed three times with PBST0,1% and three times with 1xPBS. 70 μ L of TMB (SIGMA) was added to all wells and was incubated in dark until they have attained proper intensity of colour. The reaction was stopped by adding 30 μ L/well of 1 N H₂SO₄. Plates were read spectrophotometrically at 450 nm.

Monoclonal selection

After transfection cells were replaces in 25cm² cell culture flesk in CHO-S medium containing 250 μ g/ml Hygromycin (Invitrogen) for selection. After two days cells were plated in 96 well plate in 200 μ l of medium containing Hygromycin one cell per each well. Cell grow was followed and antibody production was detected by ELISA assay. The best growing and antibody producing cells were expanded in big culture flasks.

Antibody purification from supernatant and quantification

Supernatant pH was adjusted with Tris/HCl 1M pH8 in the ratio 1:10. Supernatant was incubated with 100 µl slurry of Protein A (Genescript) for each 50 ml of supernatant at 4°C ON. Resin was prepared by washing it three times with Tris/HCl 100mM pH8 and centrifuging at 800 rpm at 10°C for 5 min. Resin was added to supernatant and incubated ON at 4°C. Supernatant was transferred to a column and flow-through was collected. Resin on the column was washed with 10-20 ml 1xPBS. Antibodies were eluted by adding 5ml of 100mM Glycine pH3 to the resin and elution fractions of 100-200µl were collected in ependorf tube that contained 10 µl 1M Tris/HCl pH8.

11.4.7. Antibodies characterization by standard laboratory assays

ELISA assay

PDI specificity of recombinant antibodies was tested performing indirect ELISA. 96 well ELISA plate was pre-coated (O/N at 4°C) with 1µg of purified full length PDI protein in 100 µL of 1xPBS. Wells were saturated with blocking buffer (2% BSA in PBST(0.01%)) for 1 hr at RT. Recombinant antibodies in different concentration were used as primary antibodies in blocking buffer and were incubated at RT for 1hr. Unbound primary antibodies were removed by washing 3 times with PBST0.01% and 1xPBS. Wells were incubated with 1:5000 dilution of peroxidase-conjugated secondary antibody in 2% blocking buffer at RT for 1hr. Wells were washed 3 times with PBST 0.01% and 1xPBS. 70 µL of TMB was added to all wells and was incubated in dark until they have attained proper intensity of colour. The reaction was stopped by adding 30 µL/well of 1 N H₂SO₄. Plates were read spectrophotometrically at 450 nm.

Western Blotting

Recombinant antibodies samples with 2x Sample buffer were loaded on SDS-PAGE gel and transferred on cellulose membrane (GE Healthcare). Membrane was blocked by 4% milk diluted in PBST0,1%. Later membrane was incubated by primary antibodies anti-SV5 (Thermo Fisher Scientific) or anti-human (Thermo Fisher Scientific) in concentration 1:5000 diluted in 2% BSA in PBST0,1% for 1 hour at RT. Afterwards membrane was washed three times by PBST0,1% and incubated by peroxidase-conjugated secondary antibody in concentration 1:5000 diluted in 2% BSA in PBST0,1%. Membrane was validated by Chemidoc Touch (Biorad).

Competition ELISA

96 well ELISA plate was pre-coated (O/N at 4°C) with 1µg of purified full length PDI protein in 100 µL of 1xPBS. Wells were saturated with blocking buffer (2% BSA in PBST(0.01%)) for 1 hr at RT. Recombinant antibodies in concentration 0,6ng/µl of H12, 2ng/µl of B10 and 0,04ng/µl of H7 were incubated with 0µg, 0,5 µg or 1 µg of HIS-PDI or HIS-TG2 for 1h on rotation at RT. These recombinant antibodies were used as primary antibodies in blocking buffer were incubated at RT for 1 hour. Unbound primary antibodies were removed by washing 3 times with PBST 0.01% and 1xPBS. Wells were incubated at RT for 1hr with 1:5000 dilution of peroxidase-conjugated secondary antibody in 2% blocking buffer. Wells were washed 3 times with PBST 0.01% and 1xPBS. 70 µL of TMB was added to all well and was incubated in dark until they have attained proper intensity of colour. The reaction was stopped by adding 30 µL/well of 1 N H₂SO₄. Plates were read spectrophotometrically at 450 nm.

Immunofluorescent assay

5 x 10⁴ OVCAR cells were plated onto coverslips in 24 well plate. The culture was incubated at 37°C in presence of CO₂ until they attained 80% confluence. This culture plate was washed once and the cover slips were transferred individually to new wells of 24 well culture plate.

OVCAR Cells Surface Staining: The confluent cells on the cover slips were washed once with plain RPMI and primary recombinant antibody in blocking buffer (5% BSA in serum free RPMI medium) was added. In the same blocking buffer was added Lectine from triticum vulgaris labeled by FITC (SIGMA) in concentration 1:500 for membrane staining. Primary antibodies and membrane staining was incubated on ice at 4°C for 2 hrs. After primary incubation, the unbound antibodies were removed by washing 3 times with blocking buffer. The coverslips were transferred to new well and were subsequently incubated for another 1 hour on ice at 4°C with secondary antibody (anti-human- CY5) diluted 1:200 in blocking buffer. 2 washes were performed and coverslips were transferred to new wells in which cells were fixed with 200µl of 4% PFA + 4% Sucrose on ice for 15 min, and permeabilised for 2-3min with 0.2% triton in 1xPBS. Cells were washed thrice with 1xPBS and once with dH₂O and were mounted to a glass slide with a small drop of mountant. Glass was sealed with nail polish. The cells were directly analyzed with a Leica TCS-SP confocal laser scanning microscope using sequential scan tool. Laser power and photomultiplier settings were kept identical for all the samples to be able to compare the results.

OVCAR Cells Surface Staining in competition assay: The confluent cells on the cover slips were washed once with plain RPMI. Recombinant antibodies in concentration 200ng for H12 and H7 and 500ng for B10 were incubated with 40 times higher concentration of HIS-PDI or HIS-TG2 protein on rotation for 2 hour at RT. Afterwards these recombinant antibodies were used as primary antibodies added to cells. In the same blocking buffer was added Lectine from triticum vulgaris labeled by FITC in concentration 1:500 (SIGMA) for membrane staining. Primary antibodies and membrane staining was incubated on ice at 4°C for 2 hrs. After primary incubation, the unbound antibodies were removed by washing 3 times with blocking buffer. The cells were transferred to new well and were subsequently incubated for another 1 hour on ice at 4°C with secondary antibody (anti-human- CY5) diluted 1:200 in blocking buffer. 2 washes were performed and cells were transferred to new wells in which cells were fixed with 200µl of 4% PFA + 4% Sucrose on ice for 15 min, and permeabilized for 2-3min with 0.2% triton in 1xPBS. Cells were washed thrice with 1xPBS and once with dH₂O and were mounted to a glass slide with a small drop of mountant. Glass was sealed with nail polish. The cells were directly analyzed with a Leica TCS-SP confocal laser scanning microscope using sequential scan tool. Laser power and photomultiplier settings were kept identical for all the samples to be able to compare the results.

Fixed and permeabilised OVCAR Cells for intracellular staining: The confluent cells on the cover slips were washed twice with prewarmed 1xPBS. The cells were fixed with 200µl of 4% PFA + 4% Sucrose on ice for 15 min, and permeabilized for 2-3min 0.2% triton in 1xPBS. The fixed and permeabilized cells were washed once with RPMI and primary antibody in blocking buffer (5% BSA in serum free RPMI medium) was added. After 2hr incubation at 37°C, the unbound antibodies were removed by washing 3 times with blocking buffer. The cells were transferred to new well and were subsequently incubated for another 1 hr at 37°C with secondary antibody (anti hIgG- cy5) diluted 1:200 in blocking buffer. 2 washes were performed and cells were transferred to new wells. Cells were washed thrice with 1xPBS and once with dH₂O and mounted to a glass slide with a small drop of mountant. Glass was sealed with nail polish. The cells were directly analyzed with a Leica TCSSP confocal laser scanning microscope using sequential scan tool. Laser power and photomultiplier settings were kept identical for all the samples to be able to compare the results.

Identification of surface PDI in OVCAR-3 cells by FACS

OVCAR-3 cells were used in concentration 5×10^5 cells/immunotube. Cells were spin down at 1500rpm for 5 min. Afterwards supernatant was removed and cells were resuspended in 100µl of staining buffer (1xPBS+10%FBS+0,01% sodium azide). Cells were spin down again on 1500rpm for 5min.

Supernatant was removed and cells were resuspended with 100µl of staining buffer. Primary antibodies were added to each tube in concentration 1µg/tube and cells were left for 20 min at 4°C in static conditions in dark. Afterwards 500µl of staining buffer was added to each tube. Cells were spin down at 1500 rpm for 5 min. Supernatant was removed and cells were resuspended with 100µl of staining buffer. Secondary antibodies anti-human CY5 were added to each tube (1µl/tube) preliminary being diluted 1:7 in staining buffer. Cells were left for 20 min at 4°C in static conditions in dark. Afterwards 500µl of staining buffer was added to each tube and cells were spin down at 1500 rpm for 5 min. Supernatant was removed and cells were fixed in 300µl of paraformaldehyde. Cells were stored at 4°C till its validation by FACS.

Immunoprecipitation

Medium from a confluent 10cm petri dish of OVCAR-3 cell was removed and cells were washed by 1xPBS. 1ml of cold RIPA buffer was added, cells were scratched from the plate and collected in ependorf tube. Cells were lysate by additional pipetting with syringe and spin down at 13000 rpm for 5 min. Supernatant was collected and incubated with 50 µl of Protein A slurry (Genescript) for 1h at 4°C. It was spin down at 4000rpm for 5 min and supernatant was transported to the other tube. 300 µl of supernatant was incubated with 500ng of recombinant antibodies and anti-PDI monoclonal commercial antibody for 1h at 4°C on rotation. 50 µl of Protein A slurry was added to each tube and incubated for 1h at 4°C. Negative control tube was incubated only with Protein A. Tubes were spin down at 4000rpm for 5 min at 4°C and supernatant was removed. Resin was washed with 500 µl of cold 1xPBS three times and resin resuspend in 2x sample buffer. Samples were denatured and used to perform SDS-PAGE. Proteins were transferred to nitrocellulose membrane and precipitated PDI protein was visualize using anti-PDI polyclonal commercial antibodies (SIGMA, #MFCD01094568).

11.4.8. Epitope mapping

Preparing of recombinant proteins

BL21 (CodonPlus(DE3)-RIPL) bacteria cells containing PDI sequence cloned into expression vector pTrc B (Invitrogen, #V360-20) using primers PDIh BamHI pTrc sense and PDIh BamHI pTrc anti and was plated on agar plate containing ampicillin and grown O/N at 37°C. Single colonies were picked up from plates and grown in 50ml of 2xTY medium at 37°C till 0,5OD. 0,2mM IPTG (Millipore) was added and incubated for 3h at 30°C. Bacteria was collected in 50ml tube and spin down at 7000 rpm for 15 min. Pellet was resuspend with 10ml/g/bacteria of lysis buffer (20mM Tris pH8, 500mM NaCl, 0,1% Triton X100, 5mM imidazole, 1mg/g/bacteria lysozyme, 1mM PMSF, 10-50µg/ml DNase). Lysate was incubated on ice for 30 min. Solution was sonicated for 1,5 min at lowest power and spin down at 11000rpm for 5 min. Supernatant was collected and incubated with 300µl of Ni-NTA (Thermo Scientific) resin beads for 1h at 4°C. Supernatant was loaded on a column and collected. Remained in the column resin was washed with 10ml of washing solution (20mM Tris pH8, 500mM NaCl). Protein was eluted adding 500µl of elution buffer (20mM Tris pH8, 500mM NaCl, 300mM imidazole) and collected in ependorf tube. Recombinant protein was dialyzed in 1xPBS O/N. Quantification of recombinant proteins was analyzed by SDS-PAGE.

Epitope fragments cloning

Different size fragments of PDI were amplified by PCR using specific primers. Amplified sequences were restricted by enzymes EcoRI (New England Biolabs) and BamHI (New England Biolabs) and subcloned into an expression vector pTrcHIS-B (Invitrogen, #V360-20). Plasmid has been transformed into DH5α (Gibco BRL), cells and plated to grow overnight. Single colonies were picked up from plates and were sequenced to detect possible mutation occurred during the cloning. Bacteria that contained correctly cloned vector was grown and vectors were purified using the Perfectprep Plasmid kit (Eppendorf). Vector was transformed into BL21 (CodonPlus(DE3)-RIPL). Purification of

recombinant proteins was done using Ni-NTA beads. The production and purification of recombinant proteins were analyzed by SDS-PAGE.

11.4.9. CDC assay

1×10^4 OVCAR-3 cells were seeded into each wells of 96-well tissue culture plate (Euroclone) and incubated 36 hrs at 37°C in presence of CO₂. Culture medium was carefully removed and washed with 380µl/well DPBS/Ca²⁺/Mg²⁺ containing 2% BSA (wash/blocking buffer). Cells were incubated with 50 µl/well of wash/blocking buffer containing 100ng/well individual antibodies for 10 minutes at 37°C. Positive control was included with mixture of the two antibodies (*Anti-Folate antibodies) cMOV18 and cMOV19 (2 µg/ml each). Negative control wells were incubated only with wash/blocking buffer. 25 µl of NHS (Innovative) mixed with 25 µl Wash/blocking buffer was added without washing to a final volume of 100 µL and incubation was continued for further 60 minutes at 37°C. Wash/blocking buffer containing antibodies was removed and 200 µl fresh culture medium was added to each well. 20 µl of 1mg/ml MTT solution (SIGMA) was added and incubated for 4 hours at 37°C. Culture medium was carefully removed and MTT crystals were solubilized by adding 200µl DMSO. Plate was read at 570nm with a reference wavelength set to 650nm. The experiment was performed in quadruplicate. The percentage of dead cells was calculated as: % of dead cells = 100 – [100 x (average of cells +Abs)/ (Average of cells +NHS)].

12. References

1. R.Di Niro, F.Ziller, F.Florian, S.Crovella, M.Stebel, M.Bestagno, et al. Construction of miniantibodies for the in vivo study of human autoimmune diseases in animal models. *BMC Biotechnology*. 2007;7(46):1-10.
2. N.Scholler, N.Urban. CA-125 in Ovarian Cancer. *Biomark Med*. 2007;December 1(4):513–23.
3. S.Xua, N.Alexey, B.Butkevich, Y.Roppei. Discovery of an orally active small-molecule irreversible inhibitor of protein disulfide isomerase for ovarian cancer treatment. *PNAS*. 2012;109(40):16348–53.
4. American_Cancer_Society. Ovarian cancer. 2013.
5. [Available from: <https://www.aacrfoundation.org/Celebrity-Diagnosis/Pages/shannon-miller-ovarian-cancer.aspx>.
6. J.S.Bereka, C.Crumb, M.Friedlanderc. Cancer of the ovary, fallopian tube, and peritoneum. *International Journal of Gynecology & Obstetrics*. 2012;119(2):118-29.
7. A.Stephen, M.D.Cannistra. Cancer of the ovary. *N Engl J Med*. 2004;2004(351):2519-29.
8. G.H.Eltabbakh, P.R.Yadev, A.Morgan. Clinical picture of woman with early stage ovarian cancer. *Gynecol Oncol*. 1999;75(3):476-9.
9. R.C.Bast, B.Hennessy, G.B.Mills. The biology of ovarian cancer: new opportunities for translation. *Nature Reviews Cancer*. 2009;9:415-28.
10. N.DiSanto. Research perspective: potential role of Nitazoxanide in ovarian cancer treatment. old drug, new purpose? *Cancers* 2013;5:1163-76.
11. K.Webber, M.Friedlander. Chemotherapy for epithelial ovarian, fallopian tube and primary peritoneal cancer. *Best Practice & Research Clinical Obstetrics and Gynaecology*. 2017;41:126-38.
12. J.E.Ang, S.B.Kaye. Molecular targeted therapies in the treatment of ovarian cancer. *Global science book* 2007.
13. N.B.La Thangue, D.J.Kerr. Predictive biomarkers: a paradigm shift towards personalized cancer medicine. *Nature Reviews Clinical Oncology* 2011;8:587-96. .
14. A.M.Bailey, Y.Mao, J.Zeng, V.Holla, A.Johnson, L.Brusco, et al. Implementation of biomarker-driven cancer therapy: existing tools and remaining gaps. *Discov Med*. 2014;7(92):101–14.
15. R.Mayeux. Biomarkers: potential uses and limitations. *The American Society for Experimental NeuroTherapeutics*. 2004;1(Aprile):182–8.
16. U.L.Roberti Maggiore, F.Bellati, I.Ruscito, M.L.Gasparri, F.Alessandri, P.L.Venturini, et al. Monoclonal antibodies therapies for ovarian cancer. *Expert Opin Biol Ther*. 2013;13(5):739-64.
17. K.K.Jain. *The Handbook of Biomarkers*. New York, Springer. 2010.
18. M.Kalia. Biomarkers for personalized oncology: recent advances and future challenges. *Metabolism* 2015;64(3):16-21.
19. F.A.Raja, J.M.Hook, J.A.Ledermann. Biomarkers in the development of anti-angiogenic therapies for ovarian cancer. *Cancer Treat Rev*. 2012;38:662-72.
20. R.A.Adam, Y.G.Adam. Malignant ascites: past, present, and future. *J Am Coll Surg*. 2004;198(6):999-1011.
21. I.Matte, D.Lane, C.Laplante, C.Rancourt, A.Piche. Profiling of cytokines in human epithelial ovariancancerascite. *AmJCancer Res*. 2012;2(5):566-80.
22. B.Davidson. Ovarian carcinoma and serous effusions. Changing views regarding tumor progression and review of current literature. *Anal Cell Pathol*. 2001;23(3-4):107-28.
23. A.Nuzhat, K.L.Stenvers. Getting to know ovarian cancer ascites: opportunities for targeted therapy-based translational research. *Frontiers in oncology*. 2013;3(256).
24. C.Kuk, V.Kulasingam, C.G.Gunawardana, C.R.Smith, I.Batruch, E.P.Diamandis. Mining the ovarian cancer ascites proteome for potential ovarian cancer biomarkers. *Mol Cell Proteomics* 2009;8(4):661-9.

25. L.Gortzak-Uzan, A.Ignatchenko, A.I.Evangelou, M.Agochiya, K.A.Brown, P.St.Onge, et al. A proteome resource of ovarian cancer ascites: integrated proteomic and bioinformatic analyses to identify putative biomarkers. *Journal of Proteome Research* 2008;7:339–51.
26. A.N.Houghton, J.A.Guevara-Patiño. Immune recognition of self in immunity against cancer *J Clin Invest.* 2004;Aug 16(114(4)):468–71.
27. A.N.Houghton, J.S.Gold, N.E.Blachere. Immunity against cancer: lessons learned from melanoma. *Curr Opin Immunol.* 2001;13:134–40.
28. H.Tong Tan, J.Low, S.Gee Lim, M.C.M.Chung. Serum autoantibodies as biomarkers for early cancer detection *FEBS Journal* 2009;276:6880–904.
29. K.Martin, C.Ricciardelli, P.Hoffmann, M.K.Oehler. Exploring the immunoproteome for ovarian cancer biomarker discovery. *Int J Mol Sci.* 2011;12:410-28.
30. J. Rauch, O.Gires. SEREX, Proteomex, AMIDA, and beyond: Serological screening technologies for target identification. *Proteomics Clin Appl.* 2008;2:355-71.
31. M.M.Gubin, M.N.Artyomov, E.R.Mardis, R.D.Schreiber. Tumor neoantigens: building a framework for personalized cancer immunotherapy. *J Clin Invest.* 2015;125(9):3413-21.
32. J.P.Finnigan, A.Rubinsteyn, J.Hammerbacher, N.Bhardwaj. Mutation-derived tumor antigens: novel targets in cancer immunotherapy. *Oncology.* 2015;29(12):970-2, 4-5.
33. T.N.Schumacher, R.D.Schreiber. Neoantigens in cancer immunotherapy *Science.* 2015;348(6230):69-74.
34. O.Gires, B.Seliger. Tumor-associated antigens: identification, characterization, and clinical application. Weinheim: John Wiley & Sons. 2009.
35. J. Rauch, O.Gires. EREX, Proteomex, AMIDA, and beyond: Serological screening technologies for target identification. *Proteomics Clin Appl.* 2008;2:355-71.
36. T.Krüger, T.Luo, H.Schmidt, I.Shopova, O.Kniemeyer. Challenges and strategies for proteome analysis of the interaction of human pathogenic fungi with host immune cells. *Proteomes.* 2015;3:467-95.
37. M.Capello, P.Cappello, F.Caterina Linty, R.Chiarle, I.Sperduti, A.Novarino, et al. Autoantibodies to Ezrin are an early sign of pancreatic cancer in humans and in genetically engineered mouse models. *Journal of Hematology & Oncology.* 2013;6(67).
38. P.Zacchi, D.Sblattero, F.Florian, R.Marzari, A.Bradbury. Selecting Open Reading Frames From DNA. *Genome Res.* 2003;13(5): 980-90.
39. M.Li. Applications of display technology in protein analysis. *Nat Biotechnol.* 2000;18(12):1251-6.
40. J.Y.Zhang. Tumor-associated antigen arrays to enhance antibody detection for cancer diagnosis. *Cancer Detect Prev.* 2004;28(2):114-8.
41. R.Wellhausen, H.Seitz. Facing current quantification challenges in protein microarrays. *Journal of Biomedicine and Biotechnology* 2012;2(831347):1-8.
42. L.M.Rogers, S.Veeramani, G.J.Weiner. Complement in monoclonal antibody therapy of cancer. *Immunol Res* 2014;August(59(0)):203–10.
43. T.W.Speer. Complement-Dependent Cytotoxicity (CDC). In: L.W. Brady, T.E.Yaeger, editors. *Encyclopedia of Radiation Oncology: Springer Berlin Heidelberg*; 2013. p. 133.
44. P.Macor, F.Tedesco. Complement as effector system in cancer immunotherapy. *Immunology Letters.* 2007;111:6-13.
45. B.Sheid. Angiogenic effects of macrophages isolated from ascitic fluid aspirated from women with advanced ovarian cancer. *Cancer Lett* 1992;62:153-8.
46. L Bjørge, J.Hakulinen, O.K.Vintermyr, H.Jarva, T.S.Jensen, O.E.Iversen, et al. Ascitic complement system in ovarian cancer. *British Journal of Cancer.* 2005;92:895-905.
47. [Available from: https://en.wikipedia.org/wiki/C3_convertase.
48. W.Wang, A.K.Erbe, J.A.Hank, Z.S.Morris, P.M.Sondel. NK cell-mediated antibody-dependent cellular cytotoxicity in cancer immunotherapy. *Front Immunol.* 2015;July 27.

49. T. Van Meerten, R.S. Van Rijn, S. Hol, A. Hagenbeek, S.B. Ebeling. Complement-induced cell death by rituximab depends on CD20 expression level and acts complementary to antibody-dependent cellular cytotoxicity. *Clinical cancer research* 2006;12(13):4027-35.
50. P.R. Pohlmann, I.A. Mayer, R. Mernaugh. Resistance to Trastuzumab in breast cancer. *Clinical cancer research*. 2009;15(24):7479–91.
51. M.C. Carroll. The complement system in regulation of adaptive immunity. *Nature immunology*. 2004;5(10):981-6.
52. M.C. Carroll. The complement system in B cell regulation. *Molecular immunology*. 2004;41(2-3):141-6.
53. D. Sblattero, A. Bradbury. Exploiting recombination in single bacteria to make large phage antibody libraries. *Nature biotechnology* 2000;18:75-80.
54. R. Di Niro, F. Ferrara, T. Not, A. Bradbury, F. Chirido, R. Marzari, et al. Characterizing monoclonal antibody epitopes by filtered gene fragment phage display. *BiochemJ*. 2005;388:889-94.
55. P. Macor, D. Mezzananza, C. Cossetti, P. Alberti, M. Figini, S. Canevari, et al. Complement activated by chimeric anti-Folate receptor antibodies is an efficient effector system to control ovarian carcinoma. *Cancer Res* 2006;66(7).
56. M.P. Lefranc, V. Giudicelli, P. Duroux, J. Jabado-Michaloud, G. Folch, S. Aouinti, et al. IMGT(R), the international ImMunoGeneTics information system(R) 25 years on. *Nucleic Acids Res*. 2015;43:413-22.
57. C.W. Gruber, M. Čemazár, B. Heras, J.L. Martin, Craik. DJ. Protein disulfide isomerase: the structure of oxidative folding. *TRENDS in Biochemical Sciences*. 2006;31(8):455-64.
58. C.S. Klade, T. Voss, E. Krystek, H. Ahorn, K. Zatloukal, K. Pummer, et al. Identification of tumor antigens in renal cell carcinoma by serological proteome analysis. *Proteomics* 2001;1:890–8.
59. R. Kellner, R. Lichtenfels, D. Atkins, J. Bukur, A. Ackermann, J. Beck, et al. Targeting of tumor associated antigens in renal cell carcinoma using proteome-based analysis and their clinical significance. *Proteomics* 2001;2:1743–51.
60. S.H. Hong, D.E. Misek, H. Wang, E. Puravs, T.J. Giordano, J.K. Greenson, et al. An autoantibody-mediated immune response to calreticulin isoforms in pancreatic cancer. *Cancer Res* 2004;64:5504–10.
61. H. Tong Tan, J. Low, S. Gee Lim, M. Chung. Serum autoantibodies as biomarkers for early cancer detection. *FEBS Journal*. 2009;276:6880–904.
62. C.M. Osowski, F. Urano. Measuring ER stress and the unfolded protein response using mammalian tissue culture system. *Methods Enzymol*. 2011;490:71–92.
63. S. Donnelly, W. Roake, S. Brown, P. Young, H. Naik, P. Wordsworth. Impaired recognition of apoptotic neutrophils by the C1q/calreticulin and CD91 pathway in systemic lupus erythematosus. *Arthritis Rheum* 2006;54:1543–56.
64. Y. Tamura, Y. Hirohashi, G. Kutomi, K. Nakanishi, K. Kamiguchi, T. Torigoe. Tumor-produced secreted form of binding of immunoglobulin protein elicits antigen-specific tumor immunity. *J Immunol* 2011;186:4325–30.
65. H. Udono, D.L. Levey, P.K. Srivastava. Cellular requirements for tumor-specific immunity elicited by heat shock proteins: tumor rejection antigen gp96 primes CD8+ T cells in vivo. *Proc Natl Acad Sci U S A* 1994;91:3077–81.
66. J. Nangalia, C.E. Massie, E.J. Baxter, F.L. Nice, G. Gundem, D. CWedge. Somatic CALR mutations in myeloproliferative neoplasms with non mutated JAK2. *Engl J Med*. 2013;369:2391–405.
67. A.M. Vannucchi, G. Rotunno, N. Bartalucci, G. Raugei, V. Carrai, M. Balliu. Calreticulin mutation-specific immunostaining in myeloproliferative neoplasms: pathogenetic insight and diagnostic value. *Leukemia*. 2014;28:1811-8.
68. V.R. Wiersma, M. Michalak, T.M. Abdullah, E. Bremer, P. Eggleton. Mechanisms of translocation of ER chaperones to the cell surface and immunomodulatory roles in cancer and autoimmunity. *Frontiers in Oncology*. 2015;5(7):1-14.

69. C.G.Gunawardana, C.Kuk, C.R.Smith, I.Batruch, A.Soosaipillai, E.P.Diamandis. Comprehensive analysis of conditioned media from ovarian cancer cell lines identifies novel candidate markers of epithelial ovarian cancer. *Journal of Proteome*. 2009;8:4705-13.
70. B.Lianga, P.Penga, S.Chenb, L.Lib, M.Zhangb, D.Caoa, et al. Characterization and proteomic analysis of ovarian cancer-derived exosomes. *Journal of Proteomics*. 2013;80:171-82.
71. C.Turano, S.Coppiari, F.Altieri, A.Ferraro. Proteins of the PDI family: unpredicted non-ER locations and functions. *Journal of cellular physiology* 2002;193:154-63.
72. C.N.Chen, C.C.Chang, T.E.Su, W.M.Hsu, Y.M.Jeng, M.C.Ho. Identification of calreticulin as a prognosis marker and angiogenic regulator in human gastric cancer. *Ann Surg Oncol* 2009;16:524-33.
73. H.A.Khanand, B.Mutus. Protein disulfide isomerase a multifunctional protein with multiple physiological roles. *Frontiers in Chemistry*. 2014;2(70).
74. J.J.Galligan, D.R.Petersen. The human protein disulfide isomerase gene family. *Human Genomics*. 2012;6(6).
75. G.Kozlov, P.Maattanen, D.Y.Thomas, K.Gehring. A structural overview of the PDI family of proteins *FEBS Journal* 2010;277(3924–3936).
76. Y.Honjo, H.Ito, T.Horibe, R.Takahashi, K.Kawakami. Protein disulfide isomerase-immunopositive inclusions in patients with Alzheimer disease. *Brain Res*. 2010;19(1349):90-6.
77. N.Di Santo JE. Potential role of nitazoxanide in ovarian cancer treatment. Old drug, new purpose? *Cancers* 2013;5:1163-76.
78. S.Xua, A.N.Butkevich, R.Yamadaa, Y.Zhouc, B.Debnatha, R.Duncana, et al. Discovery of an orally active small-molecule irreversible inhibitor of protein disulfide isomerase for ovarian cancer treatment. *PNAS*. 2012;109(40):16348–53.
79. A.K.Lappi, M.F.Lensink, H.I.Alanen, K.E.Salo, M.Lobell, A.H.Juffer, et al. A conserved arginine plays a role in the catalytic cycle of the protein disulphide isomerases. *J Mol Biol* 2004;335:283–95.
80. S.Vatolin, J.G.Phillips, B.K.Jha, S.Govindgari, J.Hu, D.Grabowski, et al. Novel Protein Disulfide Isomerase inhibitor with anticancer activity in multiple myeloma. *Cancer research*. 2016;Jun 1(76(11)):3340-50.
81. J.Ge, C.Zhang, L.Li, L.M.Chong, X.Wu, P.Hao, et al. Small molecule probe suitable for In situ profiling and inhibition of Protein Disulfide Isomerase. *ACS Chem Biol*. 2003;8:2577–85.
82. G.P.Prevoost, M.Garrido, M.Serova, J.François Briand, M.Gutmann, P.Ladam, et al. XCE853 is a promising protein disulfide isomerase (PDI) inhibitor exhibiting a strong inhibitory activity in preclinical tumor models. *American Association for Cancer Research* 2016;76(14):3760.
83. D.P.Goplen, J.Wang, B.B.Tysnes, A.J.Terzis, R.Bjerkvig, O.D.Laerum. Extracellular matrix and cell adhesion. Bacitracin inhibits glioma cell migration and invasion in vitro. *Cancer research*. 2005;46.
84. T.Hashida, Y.Kotake, S.Ohta. Protein disulfide isomerase knockdown-induced cell death is cell-line-dependent and involves apoptosis in MCF-7 cells. *J Toxicol Sci* 2011;36:1-7.
85. P.E. Lovat, M.Corazzari, J.L. Armstrong, S.Martin, V.Pagliarini, D.Hill, et al. Increasing melanoma cell death using inhibitors of Protein Disulphide Isomerases to abrogate survival responses to endoplasmic reticulum stress. *Cancer Res* 2008;July 1(68(13)):5363–9.
86. K.Steger, J.Brady, W. Wang, M.Duskin, K.Donato, M.Peshwa. CHO-S antibody titers >1 Gram/Liter using flow electroporation-mediated transient gene expression followed by rapid migration to high-yield stable cell lines. *J Biomol Screen*. 2015;20(4):545-51.
87. D.Goplen, J.Wang, P.Enger, B.B.Tysnes, A.J.A.Terzis, O.D.Laerum, et al. Protein Disulfide Isomerase expression is related to the invasive properties of malignant glioma. *Cancer Res*. 2006;66(20).
88. E.Lee, D.H.Lee. Emerging roles of protein disulfide isomerase in cancer. *BMB Rep*. 2017;50(8):401-10.
89. M.Popielarski, H.Ponamarczuk, M.Stasiaka, L.Michaleca, R.Bednareka, M.Studzianb, et al. The role of Protein Disulfide Isomerase and thiol bonds modifications in activation of integrin subunit alpha11. *Biochemical and Biophysical Research Communications* 2018;495:1635-41.